

Construction of a new peptide insertion site in the top domain of major core protein VP7 of African horsesickness virus

BY

JOANNE ELIZABETH RILEY

**Submitted in partial fulfilment of the requirements for the degree MSc(Agric) in the
Faculty of Natural and Agricultural Sciences**

University of Pretoria

Pretoria

January 2003

ACKNOWLEDGEMENTS

I would sincerely like to thank the following people for their contributions:

My supervisor, Professor H. Huismans for his guidance in this study.

Dr. F. F. Maree for his initial input and direction in this study.

My colleagues, Quinton Meyer, Michelle Freeman, Karen de Lange and Ruan van Rensburg, for their input and support.

Alan Hall and Chris van der Merwe from the Laboratory for Microscopy and Microanalysis for their help in preparation and analysis of samples for microscopy analysis.

Mario Smuts from the Biomedical Research Institute for the preparation of antiserum.

My family and friends for their patience and good humour.

The Tiger-Dragon Muay Thai and Kickboxing School for providing me with an alternative focus and an outlet for my frustrations.

SUMMARY

Construction of a new peptide insertion site in the top domain of major core protein VP7 of African horsesickness virus.

BY

JOANNE ELIZABETH RILEY

Supervisor: Prof Henk Huisman
Department of Genetics
University of Pretoria

For the degree MSc(Agric)

VP7 is the major core protein of AHSV. It is a 38kDa protein composed of 349 amino acids. VP7 is a highly insoluble protein and when expressed in large quantities in AHSV-infected cells (Burroughs *et al.*, 1994) or by recombinant baculovirus in insect cells (Chuma *et al.*, 1992; Maree *et al.*, 1998a; Maree *et al.*, 1998b), it aggregates into large crystal structures that are visible under the light microscope. These crystals, with a large surface area for the display of multiple epitopes, show potential for use as a vaccine delivery system. Two requirements for this system would be the ability of VP7 to accommodate epitope sequences without affecting its structural characteristics and, secondly, to present the epitope sequences in an effective manner to the immune system to generate a protective immune response. These two conditions were investigated in this study.

Two sites for the insertion of epitope sequences had been created by Maree (2000). In this study, a third site was created between amino acids 144 and 145 of AHSV-9 VP7. Restriction enzyme sites *Sma*I, *Eco*R1 and *Xho*I were introduced by PCR amplification. The effect of the insertion was investigated in terms of its influence on VP7 structure, its association into trimers and further aggregation into VP7 crystalline structures. In the second stage of the investigation, a twenty-five amino acid sequence of a VP2 neutralising epitope (Venter *et al.*, 2000; Bentley *et al.*, 2000; Martínez-Torrecuadrada *et al.*, 2001) was chosen to insert into the created site at position 144. This was achieved by PCR-amplification of the VP2 epitope to introduce *Eco*R1 and *Xho*I sites for directional cloning into site 144. The appropriate presentation of the insert was investigated in terms of its effect on VP7 structure, its effect on trimer formation and further aggregation of trimers into

crystalline particulate structures. Furthermore, the presentation of the insert was investigated in terms of its ability to generate antibodies with the potential to provide a protective immune response.

The insertion of restriction enzyme sites and resulting six amino acids at position 144, as well as the further insertion of the twenty-five amino acid VP2 epitope, did not affect the ability of VP7 to form trimers. The subsequent association of trimers into particulate structures was affected by an increase in the proportion of smaller structures, in comparison to that observed for the wild-type VP7. This was concluded to be a consequence of an increase in solubility of the proteins, caused by weakened hydrophobic interactions between trimers. This resulted in a reduced stability of larger particulate structures. The efficient presentation of the VP2 epitope could not be determined. A poor immune response was generated against the VP7^{mt144}-VP2 trimer in comparison to other proteins. The result was an inability of the antiserum to recognise native AHSV-9 VP7 and VP2 protein by western blot analysis. More informative conclusions regarding the presentation of the VP2 epitope on the surface of the VP7 epitope display vehicle may be drawn from a future virus neutralisation assay.

ABBREVIATIONS

AHS	African horsesickness
AHSV	African horsesickness virus
AHSV-9	African horsesickness virus serotype 9
AmAc	Ammonium Acetate
amp	ampicillin
A. P.	ammonium persulphate
BHK	Baby hamster kidney
bp	base pairs
BTV	Bluetongue virus
°C	Degrees Celsius
cDNA	complementary DNA
CLP	Core-like particle
DMSO	dimethylsulphoxide
DNA	Deoxyribonucleic acid
dH ₂ O	distilled water
ddH ₂ O	deionized distilled water
dNTP	deoxyribonucleoside-triphosphate
ds	double-stranded
EDTA	ethylenediaminetetra-acetic acid
EEV	Equine encephalosis virus
e.g.	<i>exempli gratia</i> (for example)
EHDV	Epizootic hemorrhagic disease virus
<i>et al.</i>	<i>et alia</i> (and others)
FCA	Freund's complete adjuvant
FCS	Fetal calf serum
FIA	Freund's incomplete adjuvant
Fig.	Figure
g	gram
HBcAg	Hepatitis B core antigen
HBV	Hepatitis B virus
hr	hour

i.e.	<i>Id Est</i> (that is to say)
IPTG	isopropyl- β -D-thiogalactopyranoside
KAc	Potassium Acetate
kDa	kilodalton
kb	kilobase pairs
kV	kilovolts
l	litre
LB	Luria Bertani
log	logarithmic
M	molar
MCS	multiple cloning site
mg	milligram
min	minutes
ml	millilitre
mM	millimolar
MOI	Multiplicity of Infection
M_r	molecular weight
mRNA	messenger ribonucleic acid
NaAc	sodium acetate
ng	nanogram
NS	non-structural
OD	optical density
PAGE	polyacrylamide gel electrophoresis
PBS	phosphate buffered saline
PCR	polymerase chain reaction
pmol	picomol
polh	polyhedrin
PSB	protein solvent buffer
RNA	ribonucleic acid
RNase	ribonuclease
rpm	revolutions per minute
SDS	sodium dodecyl sulphate
S.E.M.	scanning electron microscopy

Sf	<i>Spodoptera frugiperda</i>
ss	single-stranded
TCA	trichloroacetic acid
TEMED	N,N,N',N'-tetramethylethylenediamine
tet	tetracycline hydrochloride
Tris	Tris-hydroxymethyl-aminomethane
TSB	Transformation suspension buffer
TSBG	Transformation suspension buffer with glucose
µg	microgram
µl	microlitre
U	units
UV	ultraviolet
v	volume
V	volts
VIB	viral inclusion body
VLP	virus-like particles
VP	viral protein
w	weight
X-gal	5-bromo-4-chloro-3-indolyl-β-D-galactopyranoside

TABLE OF CONTENTS

Chapter One: Literature Review

1.1.	Introduction.	1
1.2.	Classification.	1
1.3.	Transmission, Epidemiology and Hosts of AHSV.	2
1.4.	AHSV Structure.	3
	1.4.1. Virus Genetics.	3
	1.4.2. Virus Proteins.	3
	1.4.2.1. Non-Structural Proteins.	4
	1.4.2.2. Inner Core Proteins.	4
	1.4.2.3. Outer Capsid Proteins.	9
1.5.	Vaccination.	11
1.6.	Epitope Vaccines.	14
1.7.	Particulate Structures as Vaccine Delivery Systems.	14
1.8.	Aims of this Study.	18

Chapter 2: The Construction of Cloning Site 144 and Its Effect on the Characteristic VP7 Structural Features

2.1.	Introduction.	20
2.2.	Materials and Methods.	22
	2.2.1. Materials.	22
	2.2.2. Site-Directed Mutagenesis of VP7 Gene by PCR.	22
	2.2.3. Construction of Modified VP7 Genes.	24
	2.2.3.1. Restriction Endonuclease Digestion.	24
	2.2.3.2. Analysis of DNA by Agarose Gel Electrophoresis.	24
	2.2.3.3. Purification of DNA Fragments from Agarose.	25
	2.2.3.4. Ligation and Transformation.	25
	2.2.3.5. DNA Isolation and Purification.	26
	2.2.3.6. Filling of Sticky Ends by Klenow.	26
	2.2.4. Cycle Sequencing Reactions.	27
	2.2.5. ABI Prism™ Sequencing.	27
	2.2.6. Hydropathy Predictions and Structural Modelling.	27

2.2.7.	Baculovirus Expression of Modified Proteins.	28
2.2.7.1.	Cell Culture.	28
2.2.7.2.	Transposition of Bacmid DNA.	28
2.2.7.3.	Transfection of Sf9 Cells for the Production of Recombinant Baculovirus.	29
2.2.7.4.	Expression of Recombinant VP7 Proteins.	29
2.2.8.	Harvesting Cells.	30
2.2.9.	Protein Analysis by SDS-PAGE.	30
2.2.10.	Plaque Purification.	31
2.2.11.	Sedimentation Analysis and Sucrose Gradients.	32
2.2.12.	Light Microscope Analysis.	32
2.2.13.	Scanning Electron Microscopy (S.E.M.).	33
2.3.	Results.	34
2.3.1.	Construction of Cloning Site 144.	34
2.3.2.	Sequence Verification of VP7mt144 and VP7mt144/200.	36
2.3.3.	Physicochemical Properties and Structural Modelling of the Modified Proteins.	41
2.3.4.	Expression of the Modified VP7mt144 and VP7mt144/200 Proteins.	44
2.3.5.	Light Microscope Observations.	46
2.3.6.	Solubility Studies of the Modified Proteins.	48
2.3.7.	Scanning Electron Microscopy (S.E.M.).	53
2.4.	Discussion.	55

Chapter 3: Insertion of AHSV VP2 Neutralising Epitope in the Modified VP7, VP7mt144, Its Effect on VP7 Structural Features and Immunogenicity

3.1.	Introduction.	59
3.2.	Materials and Methods.	61
3.2.1.	Materials.	61
3.2.2.	PCR Amplification of a Small Antigenic Region of VP2.	61
3.2.3.	Cloning of VP2 Epitope into the Modified VP7mt144 Gene.	62
3.2.3.1.	General.	62
3.2.3.2.	pMOS Blue Cloning.	62
3.2.3.3.	Isolation of VP2 Epitope by β -Agarase Digestion of Agarose.	62
3.2.4.	Immune Response Investigations.	63
3.2.4.1.	Preparation of Protein for Inoculation into Mice.	63
3.2.4.2.	Inoculation of Mice with VP7mt144-VP2.	63
3.2.4.3.	Western Blot Analysis of Immune Response.	64
3.2.4.3.1.	Sample Preparation.	64
3.2.4.3.2.	Western Blot.	64

CHAPTER ONE

LITERATURE REVIEW

1.1. Introduction.

African horsesickness (AHS) is an infectious, non-contagious disease affecting primarily equines, hence its descriptive name. Symptoms of the disease range from mild to severe with pulmonary or cardiac systems, or both, being affected. Symptoms include oedema of the lungs, subcutaneous, intermuscular and muscular tissues, and haemorrhaging of affected organs (reviewed by Burrage and Laegried, 1994; Laegried, 1994). The mildest form of the disease involves a low-grade fever. Mortality rates can reach higher than 95%, depending on the form of the disease. This has a significant economic impact on the horse industry, particularly the lucrative sport of horse-racing. In addition, the financial stakes and horse-trading value in the more traditionally recreational sports of show-jumping, dressage, eventing and polo are increasing and these sports also feel the economic impact of the disease. Increased knowledge of transmission of the disease has improved control methods. AHS is caused by African horsesickness virus (AHSV) and is spread primarily by biting midges (*Culicoides* species). The virus has the ability to replicate in both vertebrate and invertebrate hosts. Methods of control of AHS are therefore directed toward the vector (invertebrate) and the host (vertebrate) by control of the midges and quarantine of infected animals, as well as toward the virus itself by preventative vaccination.

1.2. Classification.

The aetiological agent of the disease is African horsesickness virus (AHSV), which is a member of the *Orbivirus* genus, of the family *Reoviridae* (Oellerman *et al.*, 1970; Bremer, 1976; Verwoerd *et al.*, 1979; Holmes, 1991; Murphy *et al.*, 1995). All viruses classified in the family *Reoviridae* have double-stranded RNA genomes of many segments (generally 10-12). These are encapsidated in a single virus particle with icosahedral symmetry. Members of the *Orbivirus* genus specifically have characteristic large doughnut-shaped structures on the surface of the virus particles which can be seen under the electron microscope, and hence the name given to that genus of *Orbivirus*. Various characteristics distinguish *Orbiviruses* in the *Reoviridae* family from other members such as *Reoviruses*. These include their smaller size and their transmission by insect vectors (Borden *et al.*, 1971; Murphy *et al.*, 1971; Gorman and Taylor, 1985; Murphy *et al.*, 1995). In addition to AHSV,

also included in the Orbivirus genus is Bluetongue virus (BTV), which is the prototype of the genus, equine encephalosis virus (EEV), epizootic hemorrhagic disease virus (EHDV) of deer and the recently identified St. Croix River virus (Attoui *et al.*, 2001). Nine distinct serotypes of AHSV have been identified which show little cross-neutralisation with each other (McIntosh, 1958; Howell, 1962; Calisher and Mertens, 1998).

1.3. Transmission, Epidemiology and Hosts of AHSV.

The principal vectors of AHSV are the *Culicoides* spp. Mosquitoes and ticks may also be involved in AHSV transmission (Mellor, 1994). AHS is enzootic to sub-Saharan Africa but outbreaks have occurred outside this niche on several occasions. These include outbreaks in North Africa, Southern Europe (specifically Spain and Portugal) and the Middle East (Pakistan, Afghanistan) (Mellor, 1993). The virus, however, does not seem able to persist outside enzootic areas for more than 2 to 3 years. This is probably due to climate conditions which provide a sufficient vector-free period, longer than the duration of viremia in the susceptible population (Mellor, 1994). Global climate changes may affect the distribution as well as abundance of the vectors and thus the disease may become a greater concern outside the current enzootic areas (Wittmann and Baylis, 2000). Within South Africa itself, there exists geographical variation in the transmission of the virus. A measure of the transmission of the virus, the force of infection, was found to be greatest in the northeastern part of the country and declined to the southwest, where an AHSV-free zone has been established (Lord *et al.*, 2002).

The natural host of AHS is *Equidae*. Horses are the most susceptible to the disease and are in general the only solipeds susceptible to the more severe forms of the disease. Mules are less susceptible than horses but more so than donkeys. Zebras are most resistant and show only minimal symptoms of the disease (reviewed in House, 1993). The more resistant animals, such as donkeys, may play an important role in the epidemiology of AHS, harbouring and providing a reservoir for the virus (Fassi-Fihri *et al.*, 1998; Hamblin *et al.*, 1998). AHSV has been found to infect other species such as dogs (Braverman and Chizov-Ginsburg, 1996). Antibodies against AHSV have also been found in other carnivores that ingest the meat of dead zebra or donkeys. These may act as natural reservoirs for the virus although their effect and role in the maintenance cycle of the disease is unknown (Alexander *et al.*, 1995).

1.4. AHSV Structure.

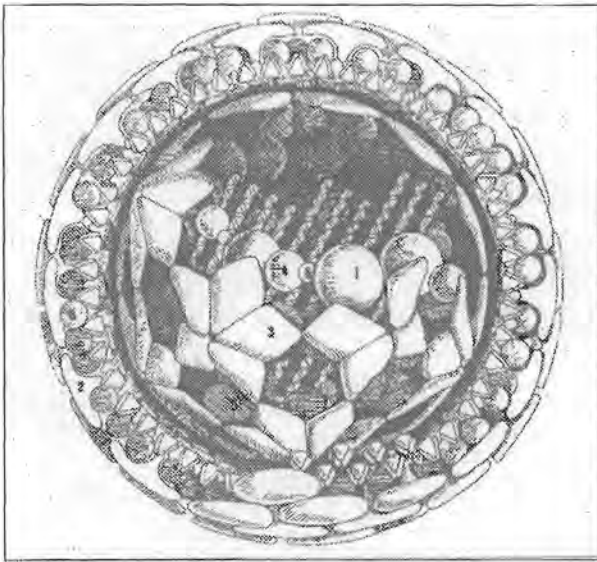


Figure 1.1. Schematic Representation of the BTV particle (Roy, 1992). Numbers indicate the corresponding viral proteins.

1.4.1. Virus Genetics.

AHSV has essentially identical morphology to that of BTV, the prototype of the genus. BTV has been studied in great detail and much of what is known of AHSV has been established and extended from knowledge of BTV. Orbiviruses are complex, non-enveloped viruses with a segmented genome of 10 double-stranded RNA segments. The segments have been designated L1-3, M4-6 and S7-10 according to their molecular weights (Verwoerd *et al.*, 1970; Bremer, 1976; Fukusho *et al.*, 1989; Roy, 1992; Vreede and Huismans, 1998). Each genome segment encodes one polypeptide with exception of S10, which encodes NS3 and NS3A depending on the in-frame initiation start codon used (Mertens *et al.*, 1984; Van Staden and Huismans, 1991; Van Staden *et al.*, 1995).

1.4.2. Virus Proteins.

Orbiviruses have seven structural proteins that are arranged in two shells, an inner core and an outer capsid layer. The outer capsid layer consists of two major proteins, VP2 and VP5. The inner core or nucleocapsid consists of two major proteins, VP3 and VP7, and three minor proteins, VP1, VP4 and VP6. The minor proteins are closely associated with the ten dsRNA segments also contained within the core. A schematic diagram of the BTV particle, the prototype of the Orbivirus

genus is shown in figure 1.1. In addition to these structural proteins, non-structural proteins are also found in virus-infected cells (Verwoerd *et al.*, 1972; Huismans and Van Dijk, 1990, Roy *et al.*, 1994).

1.4.2.1. Non-Structural Proteins.

The non-structural proteins are thought to be involved in various facets of viral morphogenesis, including virus assembly and release from infected cells. NS1, encoded by genome segment M5, is synthesised in large quantities and polymerises into NS1 tubules in AHSV-infected cells (Huismans, 1979; Urakawa and Roy, 1988) and when expressed by recombinant baculovirus (Maree and Huismans, 1997; Van Staden *et al.*, 1998). These tubules are attached to intermediate filaments of the cytoskeleton and may be involved in virus transportation within the cell (Eaton and Hyatt, 1989).

NS2, encoded by genome segment S8, is also synthesised in large quantities. It is the major component of viral inclusion bodies (VIB's), which are thought to be involved in early virion assembly (Thomas *et al.*, 1990). NS2 is the only virus-specific phosphoprotein, possessing nucleotidyl phosphatase activity (Taraporewala *et al.*, 2001) which supports its association with viral mRNA species. It may play a role in the selection of the ten ssRNA segments into subviral particles prior to the synthesis of dsRNA (Huismans *et al.*, 1987a), although ssRNA-binding by NS2 has been shown to be non-specific (Uitenweerde *et al.*, 1995).

NS3 and NS3A are both synthesised from genome segment S10, using different initiation codons. Both are involved in virus release from infected cells (Hyatt *et al.*, 1993) and are related to the virulence of the virus. This is likely to be determined by membrane association, causing an alteration in permeability of the membrane and cell death (Van Staden *et al.*, 1995; O'Hara *et al.*, 1998; Van Niekerk *et al.*, 2001a). NS3 and NS3A show high levels of variation, being the second most variable protein of AHSV (Martin *et al.*, 1998; Van Niekerk *et al.*, 2001b). Consequently, this leads to observed variations in virulence of AHSV.

1.4.2.2. Inner Core Proteins.

The BTV core is approximately 700 Å in diameter (Prasad *et al.*, 1992). The major components of core particles are VP3 and VP7, with VP1, VP4 and VP6 forming minor constituents. It is presumed that VP1, encoded by genome segment L1, has RNA polymerase activity (Roy *et al.*, 1988). VP4, encoded by genome segment M4, is a capping enzyme with characteristic features of a guanylyltransferase enzyme (Martinez-Costas *et al.*, 1998; Ramadevi *et al.*, 1998). It is thought that there is a cooperative enzyme role of VP1 and VP4 in the transcription and replication of viral RNA

(Huismans and Van Dijk, 1990; Martinez-Costas *et al.*, 1998). VP6, encoded by genome segment S9, binds ssRNA and dsRNA and may act as a chaperone in the incorporation of viral RNA into virus particles (Roy *et al.*, 1990; Turnbull *et al.*, 1996).

VP3 and VP7 are the major proteins exposed on bluetongue virus cores (Lewis and Grubman, 1990). VP3 is encoded by genome segment L3. It forms a scaffold in the core particle on which the characteristically shaped capsomeres are arranged (Huismans *et al.*, 1987b). VP7, encoded by genome segment S7, is the main component of the capsomeres on the surface of the cores. Capsomeres are constituted by arrangements of 260 trimers of VP7 forming a T=13 lattice on the VP3 inner layer of the core (Grimes *et al.*, 1997). Both BTV and AHSV corelike particles (CLP's) have been synthesised by recombinant baculovirus expressing the two major core proteins (French and Roy, 1990; Maree *et al.*, 1998a and b). These CLP's resemble the authentic viral cores in terms of size, appearance and arrangements of VP3 and VP7 proteins. The successful synthesis of CLP's indicates that neither the minor core proteins nor the non-structural proteins are required for the construction of empty cores.

CLP's have provided a useful model to study the interaction of the two major proteins, VP3 and VP7, in the viral core. Studying the effects of various mutations and modifications to the constituent proteins of the core has provided valuable information regarding the structure of viral cores. Tanaka *et al.*, 1995, modified VP3 of BTV and investigated the effect on CLP formation. Sequences were inserted at three internal sites and at the carboxy terminal of VP3. All mutants with the exception of one at an internal site were able to form CLP's, indicating that VP3 can accommodate foreign sequences at certain positions without affecting the ability to form CLP's. Deletion, extension and point mutations of BTV VP7 were studied by Le Blois and Roy, 1993. Deletions and extensions at the carboxy-terminal of VP7 prevented the formation of CLP's, whereas an extension mutation at the amino terminal of VP7 allowed for the formation of CLP's. This indicates that an intact carboxy terminal is essential for the formation of cores, whereas the amino terminus can be modified without affecting the formation of cores. A specific substitution of lys225 for leu also prevented CLP formation, indicating a critical role for this amino acid. In a similar study, Belyaev and Roy, 1992, synthesised a chimeric VP7 protein containing 48 amino acids of the hepatitis B virus preS₂ region epitope. In this case CLP's were formed containing the chimeric protein when wild-type VP7 was also present. Protein sequences have also been inserted at internal sites of VP7 and not affected the synthesis of CLP's (Roy and Sutton, 1998). These studies have shown that the structure of VP7, its arrangement in trimers and association in the core seem to be robust.

VP7:

VP7 is the major core protein of the *Orbivirus* particle. In the core particle VP7 is arranged as trimers to form capsomeres on the surface of a VP3 scaffold. Investigation of the crystal structure of BTV VP7 (Grimes *et al.*, 1995) revealed that VP7 consists of two domains, an upper and lower domain. The upper domain is formed by the central part of the VP7 molecule (amino acid residues 121-249). It is exposed on the core and has an anti-parallel β sandwich arrangement common to many capsid proteins (Basak *et al.*, 1997). The lower domain is in contact with VP3 in the virus core and is composed of nine α helices. The N-terminal third of the molecule (amino acid residues 1-120) provides five of these helices and the C-terminal (amino acid residues 250-349) provides four. The crystal structure of the top domain of AHSV has been investigated (Basak *et al.*, 1996) and shows great similarity with that of BTV. Only small differences in hydrophilicity are evident at some areas on the molecular surface of the molecule, owing to the variation in amino acid sequence. The similarity of the two molecules has been emphasised by domain-switching between BTV-10 and AHSV-4 VP7. Chimeric constructs were made in which the central upper domain of BTV VP7 was replaced by that of AHSV and vice-versa. Both chimeric constructs were able to associate into trimers, indicating a strong similarity between BTV and AHSV VP7 domains. However, the chimeric constructs were unable to form CLP's when coexpressed with BTV VP3, suggesting that the folding or composition of the bottom domain is important in forming associations with VP3 in the core (Monastyrskaya *et al.*, 1997).

Sequencing of VP7 of BTV and AHSV has revealed a highly hydrophobic protein of 349 amino acids (Eaton *et al.*, 1991; Roy *et al.*, 1991; Maree *et al.*, 1998a), with an estimated molecular weight of 38 kDa (Roy *et al.*, 1991). There is a high degree of conservation of VP7 between serotypes as well as serogroups (Bremer *et al.*, 1990; Roy *et al.*, 1991; Iwata *et al.*, 1992). Tracts of conserved amino acids are especially found in the amino and carboxyl-terminal regions, which are involved in interactions with VP3 in the viral core. The lower domain of VP7 in contact with VP3 is more hydrophobic, while the upper domain, which is in contact with the outer capsid layer, is slightly more hydrophilic (Basak *et al.*, 1996). VP7 consists of a large number of alanine, methionine and proline residues. It contains a single lysine residue that has been shown to play a critical role in the structure of VP7 and in the formation of core particles (Le Blois and Roy, 1993). Two conserved cysteine residues are found at the same positions in the amino acid sequence (positions 15 and 165). This may impose a structural constraint, with cysteine residues playing an important role in the secondary structure of proteins.

BTV and EHDV VP7 both contain an RGD (arginine-glycine-aspartate) motif at positions 168-170. The RGD motif may be a determining sequence for attachment of the virus to a cell surface receptor (Grimes *et al.*, 1995; Xu *et al.*, 1997), and has been shown to be responsible for *Culicoides* cell-binding activity (Tan *et al.*, 2001). AHSV has an AGQ sequence at the corresponding position, which is unlikely to fulfil the same role as the RGD sequence in BTV. There is an RGD sequence in AHSV at position 178-180. This is situated on a flexible loop (175-180) located in the lower part of the top domain. Although this is likely to be less accessible than position 168-170, structural modelling has shown that the structure should allow for docking to a cell surface receptor (Basak *et al.*, 1996). This supports the theory that RGD-integrin recognition may be a feature in the early stages of infection by orbiviruses, at least in insect cells. Another finding supporting this theory, that VP7 may be involved in cell recognition and infection, is that BTV core particles are just as infectious to insect vectors as the intact virus particle also containing the VP2 and VP5 outer capsid proteins (Mertens *et al.*, 1996). In mammalian cells, the core particles show a reduced infectivity compared to intact virions but VP7 may be an important factor in the infection of the insect vector.

VP7 of AHSV is highly insoluble compared to BTV. A unique feature of AHSV virus is the presence of disc-shaped, hexagonal crystals in the cytoplasm and nucleus of AHSV-infected and VP7-recombinant baculovirus-infected cells (Burroughs *et al.*, 1994; Chuma *et al.*, 1992, Maree *et al.*, 1998a and b). VP7 expressed by recombinant baculovirus produces these disc-shaped crystals which vary in size and number. Infected cells have been found to contain between one and three crystals per cell. These structures were shown to have a maximum diameter of approximately 25µm and a maximum length of 250µm (Chuma *et al.*, 1992). The average diameter is 6µm. VP7 crystals also form in BHK 21 cells infected with AHSV-9. These flat, usually hexagonal crystals have a highly ordered lattice that is consistent with a trimeric subunit structure. This appears to have a direct structural similarity to the ring-shaped VP7 capsomeres on the outer surface of the viral core (Burroughs *et al.*, 1994; Basak *et al.*, 1997; Grimes *et al.*, 1997).

Another distinct result of the reduced solubility of VP7 of AHSV is the fact that the yield of CLP's obtained by co-expression of VP3 and VP7 is much lower than that of BTV (Maree, personal communication; Zheng *et al.*, 1999). This can be explained in the following way. VP7 exists as a trimer in the virus particle. The trimer is also the state of oligomerisation of VP7 in solution (Basak *et al.*, 1992) and VP7 exists as a trimer in the cytosol of infected cells prior to incorporation into a viral structure (Eaton *et al.*, 1991). An equilibrium will exist between the trimer state and the structural particle. In the case of AHSV the insolubility of the protein will drive the formation of the crystals visible in infected cells. This will leave fewer trimers available for the incorporation into CLP's.

Because BTV VP7 is more soluble and does not form crystals, a greater proportion of trimers are available for incorporation into CLP's, producing higher yields (Maree, 2000).

Amino acids have been identified that may be responsible for the increased insolubility of AHSV VP7 compared to that of BTV. Assuming that hydrophobic residues contribute to the tendency for the protein to aggregate into crystal structures, Basak *et al.*, 1996, have identified two amino acids Ala-167 and Phe-209 that may affect the aggregation of the protein. These replace Arg-168 and Thr-209 respectively in the structure of BTV VP7 and increase the hydrophobicity of AHSV VP7 compared to that of BTV. In fact, in domain-switching experiments conducted by Monastyrskaya *et al.*, 1997, the chimeric construct composed of the upper domain of AHSV VP7 and lower domain of BTV VP7 displayed the same insolubility as the wild-type AHSV VP7. The selected amino acids, Ala-167 and Phe-209 were replaced by the corresponding amino acids of BTV, Arg and Thr respectively and this successfully improved the solubility of the chimeric VP7 protein. However, the replacement of the same amino acids in the wild-type AHSV VP7 did not significantly alter the solubility of the protein. This led to the identification of another amino acid, leu345, as playing a role in the increased insolubility of AHSV VP7 (Meyer, personal communication).

VP7 is the major group-specific antigen (Oldfield *et al.*, 1990) and can be used as a group-specific diagnostic reagent (Chuma *et al.*, 1992; Bremer *et al.*, 1994). However VP7 has been shown not to be strictly group-specific in all immunoassays (Cloete *et al.*, 1994; Bremer *et al.*, 1994). Some degree of cross-reactivity between VP7 of different orbiviruses may be expected if one considers the conserved nature of the sequence, with tracts of conserved amino acids occurring at the amino- and carboxy-terminal ends of the molecule.

The reactive epitopes of VP7 have been broadly mapped. Lewis and Grubman, 1990, suggested that BTV VP7 has at least two epitopes exposed on the virus surface. Eaton *et al.*, 1991, confirmed an epitope occurring at the amino-terminal of VP7 is accessible on the surface of BTV particles. This indicates that the N-terminal of VP7 may be exposed on the surface of the BTV particles and not located inside the core. Wang *et al.*, 1996, identified at least six different epitopes of VP7. They also found that one of the epitopes located near the N-terminal of the molecule is accessible on the surface of the intact virion, as well as the core particle. The other epitopes were detected weakly only in core particles.

VP7 is not the major neutralisation antigen of AHSV. It seems that in terms of an immune response, VP7 plays a more specific role in a non-humoral response. This has been shown by Wade-Evans *et*

et al., 1997, who demonstrated that a VP7 subunit vaccine was effective in providing immunity against a heterologous serotype challenge. Antibody was not solely responsible for protection as passive transfer of antibody did not protect mice against a virus challenge.

1.4.2.3. Outer Capsid Proteins.

The outer capsid layer is composed of capsid proteins, VP2 and VP5, which are encoded by genome segments L2 and M6 respectively. These two proteins show the largest variation among the structural proteins of BTV. VP5 shows less variation than VP2, indicating a greater restraint on the structural variability of VP5 (Huisman and Van Dijk, 1987). Purified VP5 has been shown to be able to permeabilise mammalian and *Culicoides* cells and to induce cytotoxicity (Hassan *et al.*, 2001), although VP2 is solely able to facilitate virus entry into cells (Hassan and Roy, 1999). VP5 has at least three strong hydrophobic domains. Consequently, VP5 is probably less exposed on the virus surface than VP2 (Roy *et al.*, 1994). It follows that although VP5 has been shown to contain neutralising epitopes (Martínez-Torrecuadrada *et al.*, 1999), VP2 is the major neutralising antigen (Roy *et al.*, 1996; De Maula *et al.*, 2000).

VP2:

VP2 sequences among different serotypes of BTV and AHSV display the highest levels of variation of all the viral-encoded proteins. At the same time, the VP2 proteins maintain strong structural similarities. When VP2 of BTV serotype 13 was sequenced and compared to serotypes 10, 11 and 17, it showed only an overall 40% homology to the other three species (Fukusho *et al.*, 1987). When VP2 of AHSV serotype 9 was sequenced and compared to serotypes 3, 4 and 6, multiple sequence alignment showed an overall identity of 33.4%. When comparing individual sequences, identities ranged from 48-50% with the exception of AHSV-6 and AHSV-9, which showed a 60% identity in VP2 sequence (Venter *et al.*, 2000).

A closer look at the VP2 sequence reveals areas with greater variability and regions of greater conservation. This is expected from a surface protein, which should present a unique structure to give an evolutionary advantage (corresponding to greater variation), while still maintaining the structural properties of the protein (corresponding to lesser variation). The 3' non-coding region of BTV-13 VP2 showed greater homology than the average (60-61%), whereas the 5' non-coding region showed greater sequence divergence except for the 6 terminal nucleotides which were identical. A number of clusters of variable amino acids in the 956 amino acid sequence were

identified, including amino acids 14-66, 155-178, 430-451, 585-608 and 632-663. The most homologous portion in the BTV VP2 sequence occurs near the carboxy terminal and therefore possibly fulfils some structural requirement (Fukusho *et al.*, 1987). In the VP2 sequence of AHSV, two regions of amino acids 120-420 and 540-840 were found to be highly variable. The N-terminal and C-terminal regions are much more conserved and the two non-coding regions are highly conserved. A high conservation of cysteine, proline and glycine residues is evident (Venter *et al.*, 2000). The high conservation of cysteine residues suggests that VP2 has a highly ordered structure that is maintained by disulphide bonds (Roy, 1989). The C-terminal is the most conserved region as well as being the least immunogenic region of VP2 (Martínez-Torrecuadrada and Casal, 1995) and may play a role in interaction with other capsid proteins such as VP5. The highly variable regions of VP2 contain mainly hydrophilic amino acids, with a prominent hydrophilic domain occurring at amino acids 369-403. This suggests that these regions are found exposed at the surface of the protein. The hydrophilic nature and high variability both indicate these regions are exposed to immunological pressure and may contain epitopes that are serotype-specific (Venter *et al.*, 2000).

VP2 is the virus hemagglutinin protein (Cowley and Gorman, 1987; Hassan and Roy, 1999) and is the serotype-specific antigen (Huismans and Erasmus, 1981; Kahlon *et al.*, 1983; Burrage *et al.*, 1993; Vreede and Huismans, 1994). VP2 has been shown to induce a protective immune response. Huismans *et al.*, 1987c, used purified BTV VP2 to induce neutralising antibodies in sheep that fully protected the animals when challenged with a virulent virus. Subsequently, it has been confirmed that VP2 is the main determinant of the neutralisation-specific immune response. VP2 of AHSV-4 in a crude protein extract, at doses as low as 5µg, was able to elicit a protective immune response against AHSV-4 (Roy *et al.*, 1996). Roy and Laegreid, 1996, showed that presentation of AHSV-4 VP2 as a vaccinia virus construct was also sufficient to induce a protective immune response in horses. Soluble baculovirus-expressed VP2 of AHSV-5 can also induce complete protection when delivered with appropriate adjuvants (Scanlen *et al.*, 2002).

The neutralisation domains and epitopes of VP2 have been the subject of investigation due to their role in protective immunity. From sequence data, the regions of possible neutralisation epitopes can be predicted from areas of high variability and hydrophilicity. A neutralisation epitope of BTV was identified to lie between amino acids 325 and 335 (Gould *et al.*, 1988). This was supported by the sequence data which showed that although the flanking regions of this variable region contained variable and conserved sequences, the regions flanking that (amino acids 279-293 and 354-372) contained highly conserved sequences, each containing a conserved cysteine residue. These two conserved regions may play an important role in the presentation of a neutralisation epitope in providing a suitable structure for display, possibly involving a disulphide bond.

The major antigenic domain of AHSV-4 VP2 was localised to a central region between amino acids 200 and 413 (Martínez-Torrecuadrada and Casal, 1995). This region could be subdivided into smaller fragments eliciting neutralising antibodies, which indicates the presence of several smaller sites within the large antigenic domain. Venter *et al.*, 2000, found a strong linear epitope located in a large hydrophilic domain between amino acids 369 and 407 of AHSV-9 VP2. Bentley *et al.*, 2000, identified several epitopes on AHSV-3 VP2 by filamentous phage display of random VP2 peptides. Several continuous epitopes were identified in the N-terminal region, and significant levels of antigenicity were found to occur in the region of amino acids 393-432. Neutralising activity was localised further to residues 283-379 and 379-413. Results have been supported by work by Martínez-Torrecuadrada *et al.*, 2001, which identified a major antigenic region between residues 223 and 400 of AHSV-4 VP2. Sequences between amino acids 321 and 339, and 377 and 400 were able to induce neutralising antibodies. The identification of neutralising epitopes is important in understanding the protective mechanisms by which immunity may be established. A greater understanding of the immune response to AHSV may lead to the development of a more effective vaccination programme for control of the virus.

1.5. Vaccination.

Vaccination is an important component in the control of AHS. One of the vaccines used in endemic areas contains eight live, attenuated serotypes of AHSV that are given as two separate quadrivalent inoculations (Taylor *et al.*, 1992). A particular complication in vaccination against AHSV is the multiple serotypes of the virus, which do not offer cross-protection and therefore animals must be vaccinated with all relevant serotypes of the virus. In epizootic areas, where vaccination is not implemented on an annual basis as a control, horses can be vaccinated with the single relevant serotype in the event of an outbreak. Outbreaks in epizootic areas have always been due to one AHSV serotype.

Various problems may be encountered with the use of live, attenuated, multivalent vaccines. A particular concern is that the attenuated form may revert to a virulent form and cause disease in horses. Also, the simultaneous administration of multiple strains of a vaccine can result in interference during replication and thereby cause incomplete immunity. Another potential problem is that during replication, genetic reassortment of the ten dsRNA segments may occur between the different serotypes present in the multivalent vaccine and result in progeny virus with novel characteristics, including new virulence characteristics (Cowley and Gorman, 1989; Nuttall *et al.*,

1992). Replication of the attenuated AHSV generates virus-specific antibodies and this complicates distinction between vaccinated horses and naturally-infected horses and thereby complicates export control measures (Laviada *et al.*, 1995). An additional problem in the use of live vaccine is the potential hazards to humans during the production of the vaccine. There have been reported cases of laboratory workers being infected during the large-scale production of live, attenuated vaccines and this has resulted in the withdrawal of neurotropic vaccine strains from preparations (Van der Meyden *et al.*, 1992). There is therefore substantial reason to investigate and develop alternative and safer forms of vaccination against AHSV.

The efficacy of inactivated AHSV vaccines has been investigated. Advantages of inactivated vaccines compared to live, attenuated vaccines include the fact that inactivated vaccines cannot revert to virulent forms and will not recombine with other viruses. They also do not have the potential to infect insect vectors. House *et al.*, 1994, showed that one dose of inactivated AHSV-4 vaccine given in an equine population during an outbreak of the disease prevented equine losses. Despite the advantages of inactivated vaccines, an important aspect concerning the safety of the vaccine is the possibility of incomplete inactivation of the virus during preparation and thus the possibility of causing disease in vaccinated horses.

To avoid problems associated with complete virus particles, whether inactivated or attenuated, focus has shifted to the possibility of subunit vaccines where immunity may be induced by a particular protein, protein sequence or combination of proteins. VP2 is the major neutralising antigen of AHSV and BTV. It has been shown that purified BTV VP2 is able to induce neutralising antibodies in sheep, which offers full protection against challenge by virulent virus (Huismans *et al.*, 1987c). However, it was noted that there was a significant loss in immunogenicity of VP2 when it was removed from the virion structure. Roy *et al.*, 1996, showed that baculovirus-expressed VP2 of AHSV-4 administered in two doses of 5µg was sufficient to provide protection against AHSV-4. However, Du Plessis *et al.*, 1998, found that problems associated with protein aggregation of baculovirus-expressed AHSV-5 VP2 affected the level of immunity provided by VP2. In crude cell extracts only 10% of the protein was in soluble form and this provided only partial protection against a virulent virus challenge. Only the soluble form of VP2 was able to induce neutralising antibodies. Recent work by Scanlen *et al.*, 2002, showed that soluble baculovirus-expressed VP2 of AHSV-5 is the biologically active form of the protein and induces complete protection when delivered with saponin adjuvants.

Avoiding the problems of protein insolubility and purification, the immune response elicited by the inoculation of the VP2 gene has also been investigated (Stone-Marschat *et al.*, 1996; Romito *et al.*,

1999). A cDNA copy of AHSV-3 VP2 was placed under the control of cytomegalovirus immediate-early enhancer/promoter in the pCI plasmid vector, and administered as a DNA vaccine. VP2-specific antibodies were found to be present, but neutralisation titres were low. A cytotoxic cellular reaction was observed against virus-infected target cells (Romito *et al.*, 1999). Stone-Marschat *et al.*, 1996, used a vaccinia construct containing cDNA of AHSV-4 VP2 to immunise horses. The immunisation was successful in inducing a protective immune response against challenge with a lethal dose of AHSV-4.

Despite showing that VP2 alone is sufficient to induce a protective immune response against virus challenge, there are various problems that complicate the use of a VP2 subunit vaccine. As discussed previously, the insolubility of VP2 may be a problem in preparation of the subunit vaccine. Another particularly evident factor that may limit the usefulness of a VP2 subunit vaccine is the fact that the neutralising antibodies elicited by VP2 are serotype-specific and do not offer cross-protection. Thus, any comprehensive vaccination programme would have to include VP2 from all relevant serotypes of AHSV. Results proving the effectiveness of VP2 as a subunit vaccine have also not been entirely consistent. Martinez-Torrecuadrada *et al.*, 1996, found that only mixtures of purified baculovirus-expressed VP2, VP5 and VP7 were able to confer protection against challenge with AHSV-4. This mixture produced the highest AHSV-4 specific antibodies compared to VP2 alone or mixtures of VP2 and VP5, showing the high immunogenicity conferred by purified VP7. It was suggested that when co-expressed with VP5 and VP7, the natural conformation of VP2 is better conserved than when expressed and purified alone. This would induce a more effective set of neutralising antibodies and thereby confer protection to immunised horses. Also, VP5 and VP7 may contain important T cell epitopes that would enhance the immune response. In a similar vein, later work showed that peptides of VP2, which were capable of inducing an immune response, produced low neutralisation titres (Martinez-Torrecuadrada *et al.*, 2001). It was suggested that a synthetic vaccine would require presentation of the VP2 peptides in the correct conformation and would possibly need the presence of sequences of VP5 and VP7.

The immunogenicity of VP7 has also been demonstrated by Wade-Evans *et al.*, 1996, who showed that VP7 of BTV-1 expressed as a recombinant capripox virus provided a significant level of cross-serotype protection against virus challenge. VP7 of AHSV has also been shown to confer protection to mice after inoculation with VP7 in its crystal form (Wade-Evans *et al.*, 1997; Wade-Evans *et al.*, 1998). It was found that at least 90% protection was obtained in mice after a single inoculation with VP7 crystals. Inoculation with AHSV-9 VP7 crystals was also able to provide protection against the heterologous serotype AHSV-7. Being the group-specific antigen and therefore being cross-reactive to serotypes, VP7 may potentially be effective itself as a subunit vaccine against all serotypes of

AHSV. With a passive transfer of antibody from immunised mice, recipient mice were not protected from AHSV-7 challenge, suggesting that the protective response is not due to antibody alone (Wade-Evans *et al.*, 1997). In vaccine development there is increased awareness that subunit vaccines should elicit both humoral and cell-mediated immunity. The role of VP7 in cell-mediated immunity is an important consideration in the development of new vaccines.

1.6. Epitope Vaccines.

With the development of the subunit approach to vaccination, a particular area of focus has been the development of methods for the presentation of single or multiple epitopes to the immune system. The idea of an epitope-based vaccine is compelling. A small, immunologically important sequence is capable of inducing a protective immune response. However, the simplicity of such a system is complicated by the limitations it incurs. Many epitopes are not linear or continuous and are rather formed by discontinuous scattered residues. They are thus not suitable for presentation in an epitope vaccine. The stability of an epitope vaccine is also an important consideration (Suhrieb, 1997). Being a short protein sequence, a naked epitope would easily be subjected to protein degradation and therefore a carrier system for the presentation of epitopes is a necessity. The presentation of an epitope outside its native protein and viral environment would likely reduce its immunogenicity and an additional vaccine adjuvant would be a necessity. Some new and improved adjuvants and vaccine delivery systems include iscoms or "immune stimulating complexes" (Sjolander *et al.*, 1996), liposomes (Guan *et al.*, 1998), and protein-based adjuvants. Adjuvants that generally stimulate innate cells of the immune system are also being improved (O'Hagan *et al.*, 2001). Adjuvants acting as vaccine delivery systems are largely particulate structures and target their associated antigens to antigen presenting cells, generating T cell responses (Jennings *et al.*, 1998; O'Hagan *et al.*, 2001). Potential tools in a vaccine delivery system are the particulate structures formed by AHSV proteins, namely the virus-like particles (VLP's), core-like particles (CLP's) and VP7 crystal structures.

1.7. Particulate Structures as Vaccine Delivery Systems.

The protein-based particulate vaccine delivery systems, such as non-infectious viral cores, provide a substantial and well-supported approach for the delivery of epitopes to the immune system. One such system is that of the highly immunogenic hepatitis B core antigen (HBcAg). It assembles to form subviral particles and has been used to present epitopes to the immune system (Yon *et al.*, 1992; Schodel *et al.*, 1994; Schodel *et al.*, 1996; Fehr *et al.*, 1998; Milich *et al.*, 2001). The high

immunogenicity of HBcAg can be attributed to its ability to directly activate B cells, to elicit a strong T cell response and to being efficiently processed and presented by antigen presenting cells (Milich *et al.*, 1995; Schodel *et al.*, 1996). HBcAg has also shown to be flexible as a carrier scaffold for the insertion of foreign amino acid sequences (Milich *et al.*, 1995; Schodel *et al.*, 1996; Milich *et al.*, 1997). These characteristics demonstrate that HBcAg may be an ideal carrier for B cell epitopes, particularly as it inherently generates a T cell response (Milich *et al.*, 1995; Milich *et al.*, 1997). A candidate malaria vaccine has been developed with B cell neutralising epitopes of the circumsporozoite protein of the malaria parasite as well as a universal T cell epitope contained within the HBcAg, and was shown to be a potent immunogen (Milich *et al.*, 2001).

Other particulate structures that have shown potential as vaccine carrier systems include Japanese encephalitis virus (Konishi *et al.*, 1997; Hunt *et al.*, 2001), the murine leukemia virus (Kayman *et al.*, 1999) and the cowpea mosaic virus (Brennan *et al.*, 2001). Filamentous phages displaying peptides (Grabowska *et al.*, 2000; Yip *et al.*, 2001) and flagella display systems also show promise (Westerlund-Wikstrom, 2000).

VLP's and CLP's of BTV have shown potential as a vaccine delivery system, and as a safe and effective vaccine against the virus itself. VLP's consists of the empty double-shell of the virus particle, therefore containing proteins VP7 and VP3 of the inner core and VP2 and VP5 of the outer capsid layer. They are biologically and immunologically similar to the native virions and induce high levels of neutralising antibodies. Low doses of VLP's (as low as 10µg) are able to induce complete protection against challenge with BTV (French *et al.*, 1990). They are non-infectious and lack any genetic material for replication and therefore do not replicate in host cells. This avoids some of the problems associated with the current live attenuated vaccines. VLP's are more immunogenic than subunit vaccines or inactivated viruses and are effective at eliciting both humoral and cell-mediated immunity (Roy, 1996). They are also safe to produce and, in the case of BTV, can be synthesised in large quantities.

Core-like particles (CLP's) and modifications of CLP's of BTV have been studied in terms of their ability to generate an immunological response. Foreign epitopes have been successfully inserted into CLP's and were able to induce an immune response, demonstrating the possible use of CLP's and even VLP's as epitope or antigen presentation systems. As discussed previously, chimeric VP7 molecules have been synthesised containing foreign antigenic sequences and were still successful in forming CLP's. A 48 amino acid sequence of Hepatitis B preS₂ region was inserted at the N-terminus of BTV VP7 and formed core-like particles in the presence of wild-type VP7 and VP3 (Belyaev and Roy, 1992). The foreign insert was exposed on the surface of the CLP's. Also, a ten

amino acid sequence of the rabies G protein was incorporated in the N-terminal of VP7 and led to the successful formation of CLP's (Belyaev and Roy, 1992). Internal sites of BTV VP7 have also been modified and restriction enzyme sites have been created for the insertion of foreign epitopes. A Hepatitis B surface antigen has been inserted at the RGD region, amino acid 168-170, and successfully produced CLP's. Immunogenic regions of a surface glycoprotein gp51 of bovine leukemia virus (BLV) have been inserted at Ala-145 and Gly-238 sites of VP7 and also produced CLP's (Roy and Sutton, 1998). A CD4+ T cell epitope (155 amino acids in length) of influenza virus matrix protein has also been inserted into site Ala-145 of VP7 of BTV. CLP's were produced and the inserted epitope was presented very efficiently to the specific T cell clone (Adler *et al.*, 1998). These results show that foreign epitopes can be successfully inserted into VP7 of BTV without affecting the structure and ability to form CLP's.

A particular advantage of CLP's as a possible antigen delivery system is that it is composed of an arrangement of 260 VP7 trimers and thus shows a great capacity for the presentation of multiple epitopes on the surface. A particular requirement of an epitope or antigen presentation system would be that it should include as many immunogenic sequences as possible to elicit maximum immunity. For BTV and AHSV which both consist of many serotypes, a multi-epitope presentation system including epitopes from all relevant serotypes would simplify the vaccination procedure. Although CLP's of AHSV have been synthesised by baculovirus expression of the relevant proteins (Maree *et al.*, 1998a and b), the yields of CLP's are low. Therefore focus has shifted to investigate the use of the other particulate structures associated with AHSV, namely the NS1 tubules and the unique crystal structures of VP7 that are synthesised in infected cells and which should provide similar advantages in terms of a multi-epitope presentation system as CLP's.

NS1 aggregates to form particulate tubular structures when expressed. NS1 is able to accommodate the insertion of foreign amino acid sequences, a primary requirement for use as an epitope display system. It can also be purified in large quantities and recombinant NS1 tubules have been shown to elicit an immune response (Mikhailov *et al.*, 1996; Ghosh *et al.*, 2002). Foreign sequences from 44 to 116 amino acids have been inserted at the C-terminus of BTV-10 NS1. The recombinant NS1 retained the ability to form tubular structures, with inserts being exposed on the surface of the tubules. NS1 tubules were also constructed containing different chimeric NS1 protein with different inserts (Mikhailov *et al.*, 1996). This demonstrates its potential for the display of multiple epitopes to the immune system. The ability of NS1 tubules to elicit an immune response was demonstrated by the insertion of a T cell epitope of the lymphocytic choriomeningitis virus into BTV NS1 resulting in the successful induction of a T cell response and providing protective

immunity (Ghosh *et al.*, 2002). The potential of AHSV NS1 for use as an epitope display system is under investigation (De Lange, personal communication).

Another characteristic particulate protein structure of AHSV, the VP7 crystal, also shows potential for the display of multiple epitopes to the immune system. The maintenance and stability of the CLP structure from modified VP7 of BTV shows that the trimer arrangement of VP7 is not easily disturbed by the introduction of foreign sequences (Belyaev and Roy, 1992; Le Blois and Roy, 1993; Adler *et al.*, 1998; Roy and Sutton, 1998). Thus it may be expected, similarly, that the trimer structure and then possibly the particulate crystal structure of VP7 of AHSV not be disturbed by the insertion of foreign epitopes. VP7 crystals alone have been shown to induce protection against heterologous serotype challenge, probably involving cell-mediated immunity (Wade-Evans *et al.*, 1997, Wade-Evans *et al.*, 1998). VP7 crystals with the insertion of additional epitopes would be expected to improve the protection offered. Similarly to CLP's, the VP7 crystal structures are composed of numerous VP7 trimers and would provide placement of numerous different epitopes inserted into VP7. This is particularly important as inoculation with a combination of proteins, such as VP2 and VP5, has provided most consistent protection (Martínez-Torrecuadrada *et al.*, 1996; Lobato *et al.*, 1997; Martínez-Torrecuadrada *et al.*, 2001). The VP7 crystals may also inherently offer adjuvant effects. It has been suggested that the use of cross-linked protein crystals improves the stability and enhances the immune response provided by protein subunit vaccines. It has been found that protein crystals have a profound self-adjuvanting effect comparable to that of Freund's incomplete adjuvant (St.Clair *et al.*, 1999). The VP7 crystal itself may produce similar effects, which would enhance the immune response elicited by epitopes on its surface.

Two sites of AHSV-9 VP7 have been modified for the insertion of foreign epitopes (Maree, 2000). Restriction enzyme sites, *HindIII*, *XbaI* and *SalI* have been inserted between amino acids 177 and 178 as well as 200 and 201, creating VP7mt177 and VP7mt200 respectively. Effects on the structure of VP7 in terms of trimer and crystal formation have been studied. It was found that the modification at site 200-201 did not affect the ability of the protein to form crystals. The modification at site 177-178 did affect the ability to form crystals. It was found that solubility of the protein was increased and there was significant increase in the proportion of unincorporated trimers in comparison to particulate structures. The 177-178 modification still produced a particulate structure, with a more rounded ball-like appearance than the regular hexagonal crystals of wild-type VP7 and VP7mt200 (Maree, 2000). Other sites have been identified on the surface of VP7 that may be suitable for the presentation of foreign epitopes.

1.8. Aims of this Study.

The potential for the use of VP7 particulate structures as an antigen or epitope presentation system has been introduced in this literature review. To highlight the main points, VP7 crystals alone elicit a protective immune response in mice, probably of a non-humoral nature (Wade-Evans *et al*, 1997; Wade-Evans *et al.*, 1998). The crystals themselves are composed of arrangements of VP7 trimers and provide a great possibility for the presentation of multiple epitopes on their surface. This should simplify the problems associated with vaccination against multiple serotypes of AHSV. The sites of amino acids 177/178 and 200/201 of AHSV-9 VP7 have been modified by the insertion of 6 amino acids and investigated in terms of its effect on VP7 solubility, trimer and crystal formation (Maree, 2000). This provided an initial idea of the potential of VP7 to carry additional epitopes. An essential requirement of VP7 for the purpose of epitope display would be to maintain its main structural characteristics when its sequence is altered by the insertion of additional epitope sequences. One might expect any such major modification might interfere with the appropriate folding of the protein and hence affect its structural display. A further requirement would be to present the epitope effectively to the immune system.

The broad purpose of this study was to further investigate the potential of VP7 structures as an epitope presentation system and to provide a greater understanding of the prospective limitations of such a proposed system. The identification and investigation of additional sites was of interest to broaden the potential for possible presentation of epitopes at different sites on the VP7 surface. One would expect that different sites on the surface of VP7 would have varying capabilities for epitope presentation depending on their accessibility in the larger composite structures of VP7 such as the trimer and crystals. The insertion of an identified epitope of AHSV at a proposed site could provide a further indication to the potential or limitations of VP7 in carrying additional sequences. Also, directed investigations could provide an indication of the capability of the site in displaying the epitope to the immune system.

This study was divided into two main parts:

- The modification of an additional site on VP7 by the insertion of three restriction enzyme sites to provide a cloning site for the later insertion of selected epitopes. The effects of this insertion, corresponding to a six amino acid insertion, on VP7 structure and solubility was investigated in relation to its potential as an antigen delivery system.

The second phase was to insert a selected neutralising epitope of AHSV into the chosen site and, similarly, investigate the effects on the structure and solubility of the protein. Furthermore, the

CHAPTER 2

The Construction of Cloning Site 144 and its Effect on Characteristic VP7 Structural Features

2.1. INTRODUCTION.

VP7 is a 38kDa protein composed of 349 amino acids. VP7 of AHSV is highly insoluble and forms crystal structures when expressed by a recombinant baculovirus in insect cells (Chuma *et al.*, 1992; Burroughs *et al.*, 1994; Maree *et al.*, 1998a and b). The highly ordered lattice of the crystal is composed of trimers of VP7 and thereby shows a structural similarity to the VP7 capsomers exposed on the surface of the AHSV viral core (Burroughs *et al.*, 1994; Basak *et al.*, 1997; Grimes *et al.*, 1997).

The crystalline particulate structure may provide a scaffold for the presentation of antigenic peptides on its surface and, in this way, may be useful as a vaccine delivery system. Unmodified VP7 crystals have been shown to elicit a protective immune response in mice (Wade-Evans *et al.*, 1997; Wade-Evans *et al.*, 1998). This appears to be non-humoral in nature and, in combination with exposed neutralising epitopes eliciting a humoral immune response, a more effective cumulative response may be produced. The presentation of antigenic peptides requires modification at suitable sites of the VP7 gene. The insertion of restriction enzyme sites at such sites facilitates the subsequent insertion of the antigenic peptides themselves.

When looking at the effects of such modifications on VP7 structures, and thereby assessing the potential of VP7 as a vaccine delivery system, the effects of the modification must be considered on various levels. Firstly, the effect of the modification on the VP7 protein as a single monomer unit must be considered. Any modification that notably affects the structure of VP7, particularly in terms of the folding of the protein, will affect its aggregation into trimers and ultimately crystals. More subtle changes may affect the associations and interactions between individual proteins and therefore the effect of modifications must also

be considered in terms of the effect on trimer formation. The final level would be to consider the effect of the modifications on crystal formation as the insertion of foreign peptide sequences may affect the interactions between trimers and their associations to form crystals.

The choice of the site itself is an influential factor in determining the effect of modifications on VP7 structure and its associations into larger particulate structures. The crystalline structure of the top domain of AHSV has been investigated (Basak *et al.*, 1996). This has revealed a number of hydrophilic regions, some of which may be exposed as loops on the surface of VP7. These loops may provide suitable sites for the insertion and presentation of antigenic peptides. Due to their positions on the protein, these sites would be less likely to affect the overall folding and structure of the protein if modified by the additional insertion of sequences. Two sites, amino acids 177/178 and amino acids 200/201, have been modified by the insertion of three restriction enzyme sites, *HindIII*, *XbaI* and *SalI*, providing cloning sites for the insertion of antigenic peptides (Maree, 2000). A third hydrophilic site, at amino acids 144-145, was modified in this study by the insertion of three different restriction enzyme sites.

The insertion of the three restriction enzyme recognition sites at sites 177/178 and 200/201 resulted in the introduction of six amino acids. Four of these six amino acids are hydrophilic. The modification was not expected to significantly alter the overall hydrophilicity of the region nor affect its exposure on the surface of VP7. A more non-polar, hydrophobic combination of amino acids encoded by restriction enzyme recognition sites was chosen for insertion at site 144/145. The effect of a more hydrophobic insert on the loop and structure of the protein could then be investigated. The recognition sequences of restriction enzyme sites *SmaI*, *EcoRI* and *XhoI* encode the amino acid sequence pro-gly-glu-phe-leu-glu. The effects of this insert on the structure, solubility and crystal formation of VP7 was investigated, as this would influence its potential as a vaccine delivery system.

2.2. MATERIALS AND METHODS.

2.2.1. Materials.

Primers used were obtained from GIBCO BRL (Bethesda Research Laboratories) and resuspended to a concentration of 100pmol/ μ l. TaKaRa Ex TaqTM polymerase was also obtained from GIBCO BRL (Life Technologies). The thermal cycler used for PCR and automated DNA sequencing cycling reactions was the Perkin Elmer Gene Amp PCR system 9600. Restriction endonucleases, RNase A, T4 DNA ligase, Klenow polymerase, dNTP's and DNA molecular marker II (MWII) were obtained from Roche Diagnostics. *HaeIII*-digested Φ X174 DNA was obtained from Promega. The GeneCleanTM DNA purification kit was obtained from Bio101 Incorporated. ABI PRISMTM Big Dye Terminator Cycle Sequencing Ready Reaction kit was purchased from Perkin Elmer Biosystems. The BAC-TO-BACTM baculovirus expression system was obtained from Life Technologies, Inc. RainbowTM protein molecular weight marker (14 300- 200 000 Da) was purchased from Amersham. CellfectinTM was obtained from GIBCO BRL. Grace's insect medium and foetal calf serum were obtained from Highveld Biological. Sf9 cells were supplied by the NERC Institute of Virology and Environmental Microbiology, Oxford, U.K.

2.2.2. Site-Directed Mutagenesis of VP7 gene by PCR.

A pBS clone of the wild-type S7 gene was obtained from Dr F. F. Maree and was used as a template in PCR, in which two separate sets of primers were used to amplify the gene in two segments. When combined, this introduced an 18 nucleotide insertion of restriction endonuclease sites *Sma*1, *Eco*R1 and *Xho*1. In the first reaction, a forward primer complementary to the 5' end of VP7, containing a *Bgl*II recognition site overhang (Son2a), and a reverse primer with reverse complementarity to the nucleotides 432-449 of VP7, containing an overhang of *Sma*1 and *Eco*R1 recognition sites (mt144R), was used to amplify the 5' end of VP7 up to and including nucleotide 449 (codon 144) (table 2.1). In the second step, two separate reactions were carried out to generate different 3' segments of VP7mt144 and VP7mt144/200. To generate the 3' sequence of VP7mt144, wild-type S7 (in pBS) was used as a template in PCR. To generate the 3' end of VP7mt144/200, a previously constructed mutant, S7mt200 in pFastBac (Maree, 2000), was used as a template. The same set of primers was used in both reactions. The forward primer was complementary to nucleotides 450-466, containing an overhang of *Eco*R1 and *Xho*1 recognition sites (mt144F), and the reverse primer showed reverse complementarity to the 3' end of VP7, containing a *Bgl*II recognition site (Son2b) (table 2.1). T_m values were calculated according to two formulas. For the

initial five amplification cycles, the formula used to calculate T_m values for primers less than 18 nucleotides long was used, that is $T_{m1} = 2(AXT) + 4(GXC)$. For the later phase of amplification, a second formula was used for primers of greater than 18 nucleotides in length, that is $T_{m2} = 81.5 + 16.6X\log[Na^+] + 0.41(\%G+C) - 675/n$. The annealing temperatures were calculated at 5°C less than the average T_m of the two primers and adjusted appropriately to fit both primers used in the amplification reactions.

Table 2.1: Primer sequences used in PCR site-directed mutagenesis of VP7.

<u>Primer Name</u>	<u>Directed Position (VP7)</u>	<u>Sequence</u>	<u>T_m values (°C)</u>
<u>Amplification of VP7 5' segment:</u>			
Son2a	Nucleotides 8-25	5' CACAGATCITTCGGTTAGGATGGACGC 3' <i>Bgl</i> II	$T_{m1}=56$ $T_{m2}=56$
Mt144R	Nucleotides 450-466	5' GCGAATTC CCCCGGG CGGTACGTAATATCTGCC 3' <i>Eco</i> RI <i>Sma</i> I	$T_{m1}=54$ $T_{m2}=63$
<u>Amplification of VP7 or VP7mt200 3' segment:</u>			
Son2b	Nucleotides 1148-1167	5' CACAGATCTGTAAGTGTATTCGGTATTGA 3' <i>Bgl</i> II	$T_{m1}=54$ $T_{m2}=52$
Mt144F	Nucleotides 432-449	5' GCGAATTCCTCGAGCAAGGTCGAACGCGTGG 3' <i>Eco</i> RI <i>Xho</i> I	$T_{m1}=58$ $T_{m2}=63$

All PCR reactions were carried out using TaKaRa EX-Taq™ DNA polymerase, with reagents and recipes provided by manufacturer. Reactions were set up to a final volume of 100µl as follows: 100pmol of each of the primers, 5ng template DNA, 0.5µl of a 2.5mM stock dNTP's, 6µl of a 25mM stock MgCl₂, one tenth final volume of provided buffer, 2.5U of the enzyme TaKaRa Ex-Taq™ and ddH₂O to make up to the final volume. A negative control of an identical reaction without template DNA was also set up. The amplification of the 5' segment of S7 involved a 5-phase program including:

- A 2 minute initial denaturation at 94°C,
- 5 cycles of denaturation, annealing at 50°C and elongation,
- 15 cycles of denaturation, annealing at 54°C and elongation,
- 15 cycles of denaturation, annealing at 54°C with an increase of 0.5°C per cycle, and elongation,
- A final elongation step at 72°C for 7 minutes.

The amplification of the 3' end of S7 and S7mt200 involved a similar 5-phase program including:

- A 2 minute denaturation step at 94°C
- 5 cycles of denaturation, annealing at 51°C and elongation,
- 15 cycles of denaturation, annealing at 52°C and elongation,
- 15 cycles of denaturation, annealing at 52°C with an increase of 0.5°C per cycle, and elongation,
- A final elongation at 72°C for 7 minutes.

Samples of the PCR products were analysed by agarose gel electrophoresis using a 1% agarose gel (as described in section 2.2.3.2). Size was estimated by comparison against size marker Φ X174. PCR products were concentrated and washed by simple ethanol precipitation: adding 0.1X the volume 3M NaAc pH4.8 and 2.5X the volume of absolute ethanol. Samples were incubated at -20°C for between 2 to 24 hours and collected by centrifugation at 12000rpm for 30 minutes. Pellets were washed with 70% ethanol and resuspended in ddH₂O.

2.2.3. Construction of Modified VP7 genes.

2.2.3.1. Restriction Endonuclease Digestion.

Preparations of DNA fragments for cloning, as well as screening for recombinant colonies at various stages during the construction of modified VP7 genes required digestion by restriction endonucleases. Restriction enzyme digestions were performed according to manufacturer's recommendation for the specific enzymes (Roche Diagnostics). Reaction volumes included appropriate buffers for the enzyme at 0.1X the final volume of the reaction. At various stages digestion by two enzymes was required. This was either carried out in a single step or as a two-step double digestion. In the single step, two enzymes were simultaneously used in the same suitable buffer. In the two-step method, the first enzyme was allowed to digest for an appropriate time, in its appropriate buffer. This was followed by an increase in the reaction volume, the addition of the second enzyme and adjustment by the appropriate buffer when necessary.

2.2.3.2. Analysis of DNA by Agarose Gel Electrophoresis.

Analysis and separation of DNA was required at various stages during the construction of VP7 mutant genes. This included analysis of PCR products, analysis and separation of restriction

enzyme digestions for the preparation of fragments for cloning, as well as the screening of recombinant DNA at various stages of construction of the mutant genes. DNA was separated by agarose gel electrophoresis on a standard 1% agarose gel (w/v) in 1xTAE buffer (40mMTris-HCl, 20mM Na-Acetate, 1mMEDTA (pH=8.0)). DNA fragments were visualised under UV light by ethidium bromide staining (0.5µg/ml contained in the gel). Included as controls in each gel were size markers ΦX174 (Promega) and/or MWII (Roche Diagnostics).

2.2.3.3. Purification of DNA fragments from Agarose.

Selected DNA fragments were excised from the gel and purified by the GeneClean™ purification kit (Bio101), according to protocol provided by the manufacturer. In this method, the gel slice was melted at 45°C-55°C in 2.5 volumes of 3M NaI. 5µl of the ice-cold glassmilk solution was added and incubated at 4°C for 5 to 15 minutes to allow binding of the DNA to the glassmilk particles. The glassmilk with the bound DNA was pelleted by high-speed pulse centrifugation. The pellet was washed three times with 500µl NewWash solution, provided by the manufacturer (Bio101). DNA was eluted from the glassmilk in ddH₂O by incubation at 45°C-55°C for 10 minutes, centrifugation and recovery of the DNA in the supernatant. Elution was performed twice for maximum yield of DNA. Recovery of the required fragments was confirmed again by agarose gel electrophoresis.

2.2.3.4. Ligation and Transformation.

Sticky-end ligation was performed at 16°C overnight using T₄ DNA ligase (Roche Diagnostics). The reaction volume comprised an approximate ratio of 3:1 of insert to vector, 0.1X the final volume of provided ligation buffer and 1U T₄ DNA ligase. Where blunt-ended ligation was necessary, the reaction volume was increased to 20µl and ligation was performed at 20°C for 16 hours.

E. coli XL1Blue cells were made competent for transformation by the calcium chloride method (Mandell and Higa, 1970). In this method, cells were grown in LB-broth to log phase ($OD_{450} = 0.45-0.5$), harvested by centrifugation and resuspended in 10ml ice-cold 50mM CaCl₂. Cells were incubated at 4°C for 1hour prior to use in transformation. Competent cells were transformed by the heat-shock method, as described by Sambrook *et al.*, 1989. The ligation reaction was incubated with 100µl competent cells at 4°C for 30 minutes, thereafter incubated at 42°C for 90 seconds and then chilled on ice for 2 minutes. 1ml preheated LB-broth was added and cells were incubated at 37°C with shaking for 1 hour and then plated onto LB-agar plates supplemented with ampicillin (amp) (100 µg/ml) and tetracycline hydrochloride (tet) (12.5 µg/ml). These antibiotics are

appropriate for selection of both pFastBac- and pBS-transformed *E. coli* XL1Blue cells. pBS has blue/white selection due to the occurrence of the MCS in the lacZ gene, therefore plates used in pBS screening were supplemented with 50 µl of a 2% X-gal solution and 10 µl of a 2% IPTG.

2.2.3.5. DNA Isolation and Purification.

DNA preparations were required at various stages during the construction of the mutant VP7 genes, including screening for recombinant colonies. Selected colonies were picked and grown up in a 4ml overnight culture of LB-broth, supplemented with amp (100µg/ml) and tet (12.5µg/ml). In the case of screening during pBS cloning, white recombinant colonies were selected. Plasmid was isolated by a standard alkaline-lysis method (Sambrook *et al.*, 1989), first described by Birnboim and Doly (1979). In this method, cells were harvested by centrifugation at 5000rpm for 3 minutes. Cell pellets were resuspended in 100µl of Solution 1 (50mM glucose; 10mM EDTA; 25mM Tris (pH 8.0)). 200µl solution 2 (0.2M NaOH; 1%SDS) was added to complete cell lysis and denature DNA. This was incubated on ice for 5 minutes. 150µl solution 3 (3M NaAC pH 4.8) was added and after incubation on ice for 10 min, genomic DNA, high molecular weight RNA and protein was pelleted by centrifugation at 15000rpm for 10 minutes to leave plasmid DNA in the supernatant. The plasmid DNA was precipitated by ethanol precipitation and washed free of salt by 70% ethanol. The DNA pellet was dried and resuspended in ddH₂O. DNA samples were analysed by agarose gel electrophoresis as described in section 2.2.3.2.

Where necessary, for example for purposes of sequencing, DNA samples were purified by the High Pure PCR Product Purification kit or the High Pure Plasmid Isolation kit (Roche Diagnostics). The methods followed were those provided by the manufacturer, with the exception of elution. DNA was eluted in ddH₂O rather than the provided elution buffer.

2.2.3.6. Filling of Sticky Ends by Klenow.

For specific requirements in the manipulation of the modified VP7 genes, Klenow fragment was used to add dNTP's to fill in the sticky ends created by restriction enzyme digestion. A restriction endonuclease buffer was included in the reaction at 0.1X the final volume, 1µl of 2.5mM stock of dNTP's and 2U Klenow were added and the reaction was incubated at 37°C for 3 hours. The reaction products were purified by the High Pure PCR Purification kit (Roche Diagnostics).

2.2.4. Cycle Sequencing Reactions.

Automated DNA sequencing was used to confirm insert orientation and sequence authenticity. Reactions were set up with 3.2 pmol primer, 250-500 ng double-stranded plasmid template and 8µl Terminator ready reaction mix (Perkin Elmer). The reaction was made up to a final volume of 20µl with ddH₂O. Half-reactions were also used, in which 4 µl ready reaction mix was used and which were made up to a total volume of 10µl. The cycle sequencing reactions were carried out in the Perkin Elmer GeneAmp PCR system 9600 with a heated lid, thus omitting the need for a mineral oil overlay. The cycle sequencing reaction itself involved the following: a rapid thermal ramp to 96°C followed by incubation for 10 seconds at 96°C, a rapid cooling ramp to 50°C for annealing, a rapid thermal ramp to 60°C, followed by incubation at 60°C for 4 minutes for primer extension. This method was cycled 25 times, followed by a rapid cooling to 4°C. The excess dye terminators were removed by a basic ethanol precipitation step: half-reactions were made up to the final volume of 20µl and 2µl of 3M NaAc pH 4.8 was added to the 20µl reaction volume. The reaction was transferred to 50µl absolute ethanol and incubated at 4°C for ten minutes, followed by centrifugation at 15000rpm in a standard tabletop microfuge for 30 minutes. The pellet was washed twice with 70% ethanol to remove any traces of salt.

2.2.5. ABI PRISM™ Sequencing.

Samples were resuspended in 30µl sequence loading buffer, composed of a 5:1 ratio of deionised formamide to 25mM EDTA pH 8.0 containing 50mg/ml dextran blue. Samples were denatured by heating to 95°C for 2 minutes and then placed on ice before loading. 1,5µl sample was loaded on a 4% denaturing polyacrylamide gel and run for 7 hours at 1.6kV in the ABI PRISM 377 sequencer. Sequences were analysed by using the ABI PRISM Sequencing Analysis™ program, as well as the ABI PRISM Sequence Navigator™ program.

2.2.6. Hydropathy Predictions and Structural Modelling.

Hydropathy plots of the VP7 mutants were prepared using the ANTHEPROT package (Geourjon *et al.*, 1991; Geourjon and Deleage, 1995) and the Hopp and Woods predictive method (Hopp and Woods, 1981; Hopp and Woods, 1983). The structural protein modelling was done using the SWISS-MODEL Version 36.0002 program available through the SWISS-PROT database (Peitsch, 1995; Guex and Peitsch, 1997, Guex *et al.*, 1999). Modelling data was analysed and viewed through the Swiss PDB Viewer (DeepView) Version 3.7b1.

2.2.7. Baculovirus Expression of Modified Protein.

2.2.7.1. Cell culture.

Spodoptera frugiperda cell clone Sf9 was used to propagate the wild-type or recombinant baculovirus. Cells were maintained in a shaking culture in Grace's medium (Summers and Smith, 1987) supplemented with 10% (v/v) fetal calf serum, an antimycotic solution (Highveld Biological) and 10% Pluronic-F68 (Sigma Cell Culture). The antimycotic solution gave final concentrations of 0.12mg/ml Penicillin G, 0.12mg/ml Streptomycin sulphate and 0.0325µg/ml Fungizone. Cultures were incubated at 27°C. Cells were counted under a light microscope (Nikon model TMS) using a haemocytometer after staining cells with an equal volume of 0.4% trypan blue solution (in 1 X PBS).

2.2.7.2. Transposition of Bacmid DNA.

E. coli DH₁₀BAC cells were grown to log phase ($OD_{550} = 0.45-0.5$) in LB-medium supplemented with kanamycin (50µg/ml) and tetracycline hydrochloride (12.5µg/ml) and were made competent by the DMSO method (Chung and Miller, 1988). In this method, cells were collected by centrifugation and resuspended in 0.1X the original volume TSB medium (LB-medium supplemented with 10% w/v PEG, 5% v/v DMSO, 10mM MgCl₂ and 10mM MgSO₄). Cells were incubated on ice for 20 minutes, then mixed with the recombinant pFastBac DNA and incubated a further 30 minutes on ice. TSBG medium (TSB with 10% glucose) was added and cells were incubated with shaking at 37°C for 4 hours. Cells were plated out on agar plates supplemented with tetracycline hydrochloride (12.5 µg/ml), kanamycin (50µg/ml) and gentamycin (7µg/ml), as well as X-gal (50µl of a 2% solution) and IPTG (10µl of a 2% solution) for blue/white colour distinction. Plates were incubated at 37°C for 24 hours, followed by overnight incubation at 4°C to improve blue/white colour distinction. White recombinant DH₁₀BAC colonies were selected and grown up overnight in a small-scale culture in LB-medium supplemented with tet, kanamycin and gentamycin. Recombinant bacmid DNA was isolated by a modified alkaline lysis method, specifically for the isolation of high molecular weight DNA (Luckow *et al.*, 1993). In this method, cell pellets were resuspended in 300µl Solution 1, then lysed by the addition of 300µl Solution 2. After incubation at room temperature for 5 minutes, 300µl 3M KAc pH=5.5 was added and incubated further on ice for 10 minutes. After centrifugation, DNA was precipitated from the supernatants by isopropanol. The DNA was collected by centrifugation and washed with 70% ethanol, before resuspending in 40µl sterile ddH₂O in a sterile environment. Care was taken during resuspension to avoid shearing the high molecular weight DNA.

2.2.7.3. Transfection of Sf9 cells for the Production of Recombinant Baculovirus.

Sf9 insect cells were seeded at $0.9-1 \times 10^6$ per well in a 6-well cell culture plate. The recombinant or wild-type bacmid DNA was prepared for transfection by allowing it to associate with the lipid complex reagent, CELLFECTIN™ in clean Grace's medium. 6µl DNA was added to 100µl Grace medium lacking the antibiotic/antimycotic solution, and 5µl CELLFECTIN™ was added to 100µl Grace medium also lacking antibiotic/antimycotic solution. The two solutions were combined and left standing for 45 minutes; 800µl clean Grace medium was added before transferring to cells. Seeded cells were washed with 1ml clean Grace medium and the DNA-CELLFECTIN™ complex was added to cells. The cells were incubated at 27°C for 5 hours before the transfection mix was removed and replaced by Grace medium with the full complement of antibiotics, fetal calf serum and pluronic acid. Incubation at 27°C continued for 4 days, after which the supernatant was removed and stored at 4°C. The presence of recombinant baculovirus in the transfection supernatant was tested by infection of cells on a 24-well plate.

2.2.7.4. Expression of Recombinant VP7 Proteins.

Various levels and quantities of expression of proteins were obtained by infection of sf9 cells on small- or large-scale. Small-scale expression was achieved by infection of sf9 cells on a 24-well or 6-well plate. On a 24-well plate, cells were seeded at $0.2-0.3 \times 10^6$ per well in a total of 500µl Grace medium supplemented with the full complement of FCS, antibiotics/antimycotics and pluronic acid. After 1 hour the medium was removed and 150µl of the baculovirus with 350µl fully complemented Grace medium was added. Cells were incubated at 27°C for 3 days. On a 6-well plate, cells were seeded at 1×10^6 cells per well in 2ml Grace medium with the complete set of supplements described above. Similarly, cells were seeded for 1 hr, after which the medium was removed. Cells were infected with 200µl of baculovirus in 1.8ml fully complemented Grace medium. Infections were incubated at 27°C for three days. Expression of the mutant VP7 proteins was obtained by infection with the corresponding recombinant baculovirus. Expression of the wild-type baculovirus proteins was obtained by infection with wild-type baculovirus.

For large-scale expression, monolayers of sf9 cells were seeded at 1×10^7 cells in 75 cm³ tissue culture flasks. The medium was removed when cells had sufficiently adhered, after approximately 1 hour, to remove any unattached cells. Cells were infected at a M.O.I. of 5 –10 pfu/cell with the appropriate baculovirus in 6ml Grace medium with full complement of additives. Infections were

incubated for 2 hours at 27°C thereafter 9ml of complete Grace medium was added and incubation was continued at 27°C for 4 days.

2.2.8. Harvesting Cells.

Cells were harvested from 6-well or 24-well plates by removing the virus supernatant and washing the cells from the plates with 1ml or 500µl 1X PBS solution (137mM NaCl, 2.7mM KCl, 4.3 mMNa₂HPO₄·2H₂O, 1.4mMKHPO₄; pH=7.4). Cells were then pelleted by centrifugation at 3000rpm for 5 minutes and washed with 500µl 1XPBS. A second centrifugation at 3000rpm for 5 minutes was used to pellet the cells, which were resuspended in 30-50µl 1XPBS. Cells were harvested from the large 75cm³ flasks similarly to the small-scale infections, except virus supernatant was not removed. Cells were removed from the flask surface by agitation and resuspended in the supernatant. Cells were pelleted by centrifugation in the Beckman J2-21 centrifuge using the JS7-5 rotor at 3000 rpm for 5 minutes, and washed with 10 ml 1XPBS. The centrifugation was repeated and the cell pellet was resuspended in 1ml 1XPBS or other appropriate buffer.

2.2.9. Protein Analysis by SDS-PAGE.

For protein analysis, a sample of cells were added to an equal volume of 2XPSB (125mM Tris-HCl pH=6.8; 4%SDS; 20% glycerol; 10% 2-mercaptoethanol; 0.002% bromophenol blue) and denatured by boiling for 5 minutes, followed by sonication for 5 minutes. Samples were analysed by electrophoresis on a 12% denaturing separating SDS-PAGE minigel (7X10 cm Hoefer Mighty Small™ electrophoresis units) in 1XTGS running buffer (0.025M Tris-HCl, pH 8.3; 0.192M glycine; 0.1% SDS), run at 120V for 1hr30min to 2 hours. Separating gels were prepared from 30% acrylamide, 0.8% biscrylamide stocks, and contained 0.375M Tris-HCL pH=8.8 and 0.1% SDS. The 5% stacking gels contained 0.125M Tris-HCl pH=6.8 and 0.1% SDS. Gels were polymerised by the addition of 0.008% (v/v) tetra-methyl-ethylene-diamine (TEMED) and 0.08% (w/v) ammonium peroxyulphate (AP). For improved resolution of samples, electrophoresis was carried out on a 10% denaturing polyacrylamide gel in the larger 16X18cm Hoefer Sturdier slab gel apparatus. This was run at 60V overnight.

Gels were stained by Coomassie blue staining (0.125% Coomassie blue; 50% methanol; 10% acetic acid) and destained in a 5% acetic acid and 5% ethanol solution. Rainbow Marker™ (Amersham) was run on gels as a protein size marker.

2.2.10. Plaque Purification

To obtain homogenous virus stocks, plaque purifications were carried out. Cells were seeded in complete Grace medium at 1.5×10^6 cells per well on 6-well plates. Serial dilutions were prepared from the transfection supernatants. 10 μ l of the transfection supernatant was made up to 1ml (dilution 10^{-2}). Thereafter serial dilutions were made of 10^{-4} , 10^{-5} , 10^{-6} , 10^{-7} , 10^{-8} , 10^{-9} and 10^{-10} transfection supernatant in a total volume of 1ml. Medium was removed from seeded cells and the 1ml serial dilutions were each added to a well and incubated at 27°C for 2 hours. A 3% Low Melting Point agarose solution was made and sterilised in the autoclave. When cooled, a 1:1 dilution of the 3% agarose and complete Grace medium was made. The virus dilutions were removed from the cells and 2 ml of the agarose/Grace medium solution was carefully overlaid. The plates were incubated at 27°C for 4 days. The plates were then overlaid with 1ml of neutral red solution. The neutral red solution was prepared in the following way: a 1mg/ml neutral red solution was made with water and then filter sterilised. A 10X dilution was then made with complete Grace medium. After 5 hours, the neutral red solution was removed and incubation was continued overnight. Virus plaques were visible from 10^{-4} , 10^{-5} and 10^{-6} dilutions. Plaques were plucked using the tip of sterile Pasteur pipettes and added to 1ml complete Grace Medium. This was then vortexed to release the virus into the medium.

Plaque-purified virus was amplified by infection of 1×10^6 cells on a 6-well plate. 250 μ l of the 1ml virus inoculums from the titrations and 250 μ l complete Grace medium was added to seeded cells and incubated for 1 hour at 27°C. A further 1.5 ml of complete Grace medium was added and incubation was continued for 4 days at 27°C. The supernatant – the first passage virus stock – was used to infect cells on a 24-well plate to test protein expression. Cells were seeded at 0.2×10^6 and infected with 200 μ l of the first passage virus stock, using complete Grace medium to make up a final volume of 500 μ l. Cells were incubated at 27°C for 3 days before harvesting. Levels of protein expression from different plaques was tested by SDS-PAGE analysis of cell lysate from the 24-well infections, as described in section 2.2.9.

The first passage virus stock that showed good levels of protein expression was used to generate large-scale virus stocks. Monolayers of 1×10^7 cells were infected with 200 μ l of first passage virus stock in a total of 6 ml. Cells were incubated at 27°C for 1 hour. A further 9 ml was added and infections were incubated at 27°C for 3 days. The supernatant containing the virus was centrifuged at 3000 rpm for 5 min to collect any detached cells. The supernatant was filter sterilised and stored at 4°C.

2.2.11. Sedimentation Analysis and Sucrose Gradients.

Recombinant VP7 proteins were expressed on large-scale (section 2.2.8.4) and harvested according to the method described in section 2.2.9. The collected cell pellet from each monolayer was resuspended in 1 ml lysis buffer (50mM Tris-HCl pH=8, 50mM NaCl; 0.5% Nonidet p40). Cells were lysed by incubation on ice for 30 minutes. One fifth the total volume (200µl) of cell lysate was loaded on a discontinuous 30–50% (w/v) sucrose gradient. The 30% and 50% sucrose solutions were made up in sterile 100 mM Tris-HCl pH=8, 50mM NaCl. The 40% sucrose solution was made by combining equal proportions of 30% and 50% sucrose solutions. The 35% and 45% solutions were made by mixing equal proportions of 30% and 40%, and 40% and 50% solutions respectively. The gradient was created by layering 800 µl of each sucrose solution in increasing concentrations with 50% at the bottom and 30% at the top in the 5ml Beckman polyallomer ultracentrifuge tubes. The gradient was centrifuged in the SW50.1 Sorvall rotor at 14000rpm for 1 hour and 15 minutes or at increased conditions of 40 000rpm for 20 hours. Fractions were tapped as 20 drops per fraction, giving 10 –11 fractions. The pellet from the gradient was resuspended in 100 µl 100mM Tris-HCl pH=8, 50mM NaCl buffer. Fractions were stored at 4°C until further use.

Protein content of the fractions was analysed by SDS-PAGE after precipitation out of the sucrose gradient. 100µl of each fraction was diluted with an equal volume of ddH₂O and 40 µl of 50% TCA solution was added. Samples were incubated on ice for 1 hour and centrifuged for 25 minutes at 15000 rpm at 4°C. Pellets were resuspended in 15 µl 2XPSB and analysed on a 10% denaturing polyacrylamide gel, as described in section 2.2.10. The specified protein content of the fractions was quantified by the Sigma Gel™ software program (Jandel Scientific) which measures the relative band intensities on an SDS-PAGE gel.

2.2.12. Light Microscope Analysis.

Cells were seeded on sterilised cover-slips at a density of 1×10^6 cells per well of a 6-well plate. Cells were infected as described in 2.2.7.4. When crystals were visible in infected cells, cover-slips with adhered infected cells were examined under the Light microscope (the Zeiss Axiovert 200 model). Photographs of the infected cells were taken with the Nikon Digital Camera DXM1200 model at a magnification of 63 times.

2.2.13. Scanning Electron Microscopy (S. E. M.).

Fractions from the sucrose gradient containing suspected particulate structures of the mutant proteins were pooled and protein was pelleted by dilution of the sucrose solution to 3ml with buffer (100 mM Tris-HCl pH=8, 50mM NaCl) followed by centrifugation at 20 000rpm for 2 hours. The pellet was resuspended in 300µl 1XPBS. Preparation for the scanning electron microscopy involved fixation in a 0.15M Na phosphate buffer with 0.1% glutaraldehyde content for 15 minutes, followed by a washing for 15 minutes in the Na phosphate buffer and then each consecutively in 30%, 50%, 70%, 90% and three times in 100% ethanol. Samples were then dried, mounted onto a stub and then spatter coated with gold beladium particles in a S.E.M. autocoating unit E5200 (Polaron equipment ltd.). Samples were viewed in the Jeol 840 S.E.M.

2.3. RESULTS.

A site between amino acids 144 and 145 of AHSV-9 VP7 was chosen as a target for the insertion of restriction endonuclease sites, *Sma*I, *Eco*RI and *Xho*I. This area occurs as an exposed loop on the surface of the VP7 protein, determined by protein modelling and predicted by hydrophobicity and antigenicity plots (Maree, 2000). It should therefore be a suitable site for the display of inserted, foreign epitopes. The restriction enzyme sites, *Sma*I, *Eco*RI and *Xho*I encode amino acids proline, glycine, glutamate, phenylalanine, leucine and glutamate respectively. Of these six amino acids, only the two glutamate residues are hydrophilic. The addition of a majority of hydrophobic amino acids at an exposed hydrophilic site would be expected to increase the overall hydrophobicity at the site and could thus influence protein structure in that area.

2.3.1. Construction of Cloning Site 144.

The cloning site was inserted in both the wild type VP7 gene and the previously modified VP7mt200 gene, which had been modified by the insertion of a cloning site between amino acids 200 and 201 (Maree, 2000). The construction of the two modified genes, designated VP7mt144 and VP7mt144/200, involved a two-step cloning procedure using PCR to generate two segments of the gene. The construction strategy is summarised in figure 2.1. Primers were designed to incorporate the required restriction endonuclease sites as overhangs (section 2.2.2.; table 2.1.). In the first step, PCR was used to amplify the 5' end of the VP7 gene (S7). The PCR product obtained (figure 2.2(a)) corresponded to the expected size of 465bp. This was cloned directly into pFastBac between *Bam*HI and *Eco*RI sites. This amplified 5' end of the S7 gene contained a *Bgl*II site at its 5' end and *Sma*I and *Eco*RI sites at its 3' end. When digested by *Eco*RI and *Bgl*II in a single step, sticky ends were created that were complementary to *Eco*RI and *Bam*HI sticky ends of the pFastBac vector. Directional cloning of the fragment was thus possible. The appropriate pFastBac-5' intermediates were screened by digestion with *Bam*HI and *Eco*RI which released a fragment of 369bp (figure 2.2(c)). The original *Bam*HI site in the MCS of the vector was abolished by the ligation with the *Bgl*II sticky end. The smaller fragment of 369bp compared to the 465bp of the PCR product was released due to the presence of an internal *Bam*HI site in the 5' end of the VP7 gene.

A second PCR was used to amplify the 3' end of both the VP7 and VP7mt200 genes. Fragments corresponding to the expected sizes of 741bp for the VP7 amplification and 759bp for the VP7mt200 amplification were obtained as shown in figure 2.2(b). The size difference between the two amplified fragments is evident in the agarose gel photograph. These PCR products, containing *EcoR*I and *Xho*I sites at the 5' end and a *Bgl*II site at the 3' end, were first cloned between *EcoR*I and *Bam*HI sites of pBS. Again, in the preparation of the PCR fragments and pBS vector, the double digestions were performed in a single step. The use of two different restriction enzymes again allowed for simple directional cloning of the fragment. Recombinant clones were selected by digestion of extracted DNA with *EcoR*I and *Pst*I, which confirmed the presence of the appropriate segments. Due to the tendency of *Pst*I to require a longer time period to effectively cut at its recognition site, this double digest was carried out in a two-step manner. The digestion was first carried out with *Pst*I for an appropriate time, followed by *EcoR*I, which was directly added to complete the double digestion. The fragment released by the *EcoR*I/*Pst*I digestion was then transferred to the pFastbac-5'VP7 intermediate between *EcoR*I and *Pst*I sites. This step removed most of the restriction endonuclease sites from the multiple cloning site of pFastBac, but also introduced sites from the pBS multiple cloning site. This is also indicated in figure 2.1.

The justification for the two-step cloning procedure used for the 3' segment of the gene is as follows: some difficulty was observed attempting to clone the 3' segment directly into the pFastBac-5' intermediate. pBS, on the other hand, is a smaller vector and more easily manipulated than pFastBac and therefore more efficient as a simple cloning vector. Cloning first into pBS provided an unlimited supply of the 3' segment. Excision from pBS by restriction enzyme digestion also ensured sticky ends at both ends of the segment. The correct recombinant clones were selected by *Sac*I digestion of isolated DNA samples, which released a fragment of 765bp for pFastBac-VP7mt144 and 783bp for pFastBac-VP7mt144/200. This is shown in figure 2.2(d).

To facilitate the use of the created site at position 144/145, the *Xho*I recognition site occurring in the MCS of pFastBac was removed. Restriction enzyme digestion using *Pst*I and *Kpn*I removed a small segment from the MCS of the plasmid, including the *Xho*I recognition site. A two-step double digest was performed. Digestion was first carried out

with *Kpn1*. The reaction was then adjusted with the appropriate buffer for further digestion by *Pst1*. The sticky ends were filled with Klenow fragment (2.2.3.6.) and the resulting blunt ends ligated (2.2.3.3.). This is also indicated in figure 2.1. Sequence verification of pFastBac-VP7mt144 and pFastBac-VP7mt144/200 was deemed necessary to confirm insertion of correct restriction enzyme sites as well as to control the fidelity of the PCR reaction.

2.3.2. Sequence Verification of VP7mt144 and VP7mt144/200.

The colonies selected by restriction endonuclease digestion were sequenced by automated DNA sequencing (section 2.2.4 and 2.2.5). This confirmed the insertion of the restriction endonuclease sites *SmaI*, *EcoRI* and *XhoI* between amino acids 144 and 145 of VP7 and VP7mt200 genes (nucleotides 449-450). A mutation from the wild-type AHSV-9 sequence at nucleotide position 30/31 was found in which CG sequence had been switched to GC. This could be explained by infidelity of the PCR reaction. Due to the strategy used in construction of the two mutants, this mutation was evident in both VP7mt144 and VP7mt144/200. The nucleotide change resulted in a change in amino acid 5 from wild-type arginine to alanine. It was assumed that this change would not influence the structural tendencies of the protein since AHSV serotype 4 also contains an alanine at amino acid position 5 (Roy *et al.*, 1991) and has been shown to form crystals when expressed by the baculovirus system in insect cells (Chuma *et al.*, 1992). A mutation from the wild-type was also found at nucleotide position 1086 of VP7mt144/200 in which a G was substituted with a C. This resulted in a missense mutation with substitution of valine to leucine at amino acid 357. Valine and leucine are both non-polar amino acids, with similar chemical and physical properties. It was assumed therefore that this mutation would not influence the structure of the protein. The sequences were compared and aligned using ClustalX version 1.81 (Higgins and Sharp, 1988; Higgins *et al.*, 1996), shown in figure 2.3. After confirming a complete intact modified VP7 sequence, which should encode a full-length protein, the influence of the insertion on the hydrophilicity profile as well as predicted protein structure was investigated.

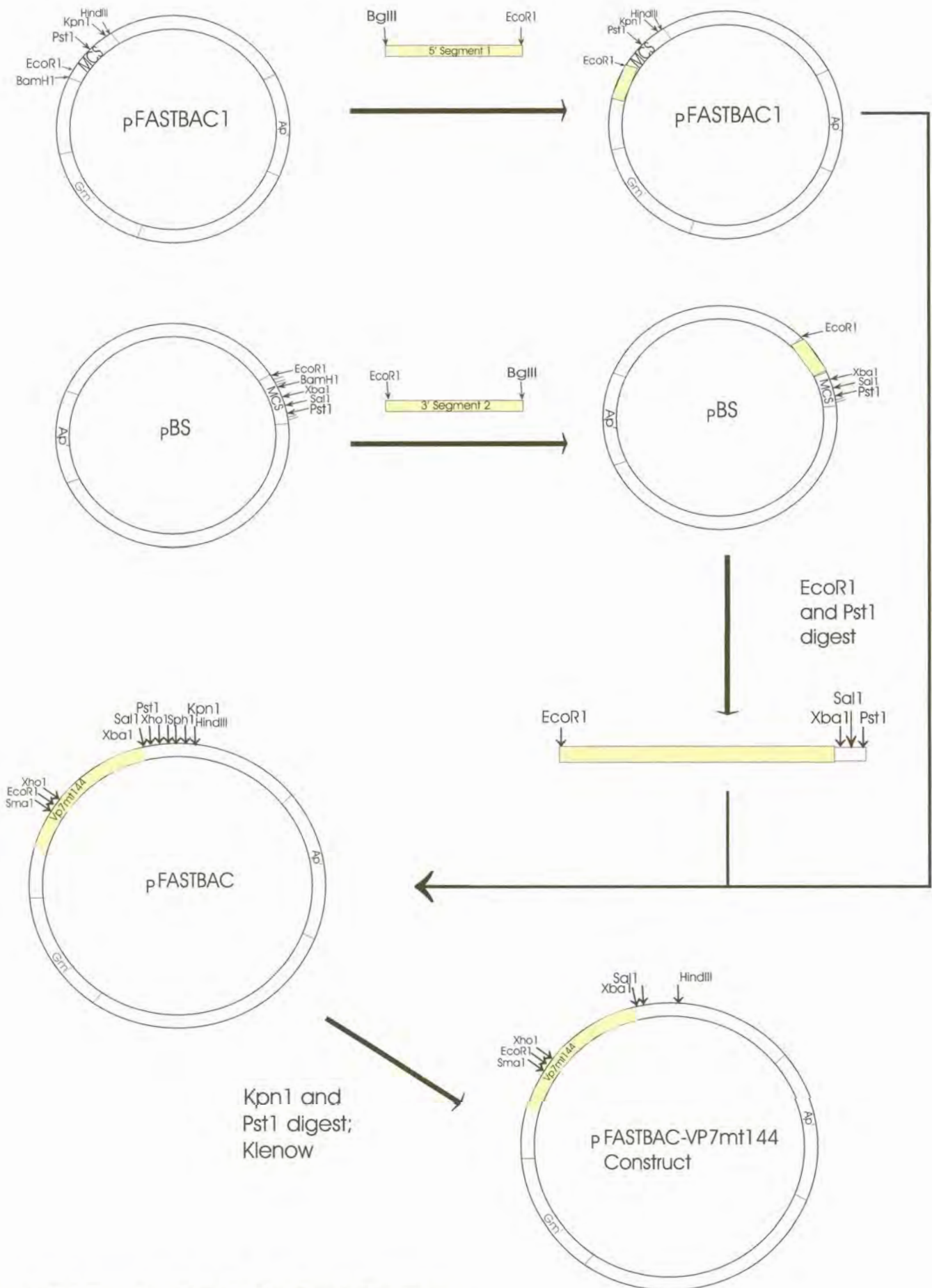


Figure 2.1 Construction of pFastBac-VP7mt144.

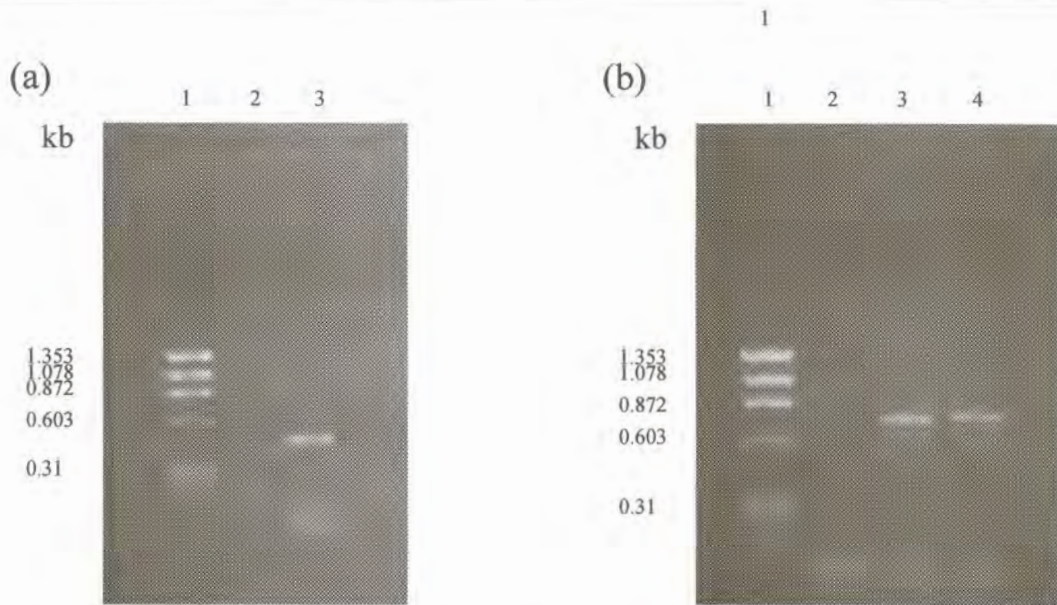


Figure 2.2(a) and (b). Agarose gel electrophoresis of the PCR products of the amplification of the 5' segment of VP7 (2.2(a), lane 3), 3' segment of VP7 (fig2.2(b) lane 3) and 3' segment of VP7mt200 (fig2.2(b) lane 4). In both (a) and (b) lanes 1 and 2 represent the size marker $\phi\chi 174$ and negative controls of the PCR reactions lacking template, respectively.

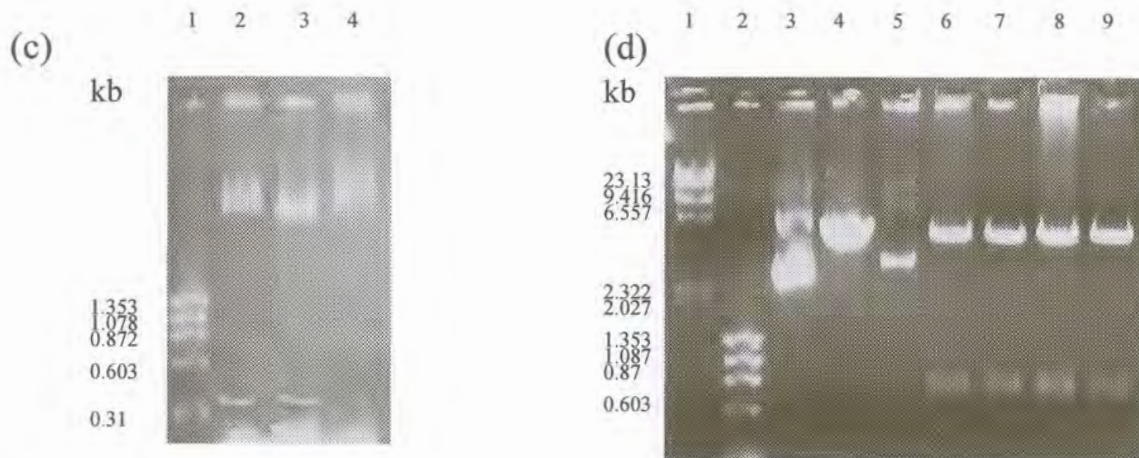


Figure 2.2(c) Agarose gel electrophoresis analysis of *Bam*HI and *Eco*R1 digestions of pFastBac-VP7 5' intermediates. Lane 1 represents the size marker $\phi\chi 174$. Lanes 2 and 3 represents two positive samples, releasing fragments of expected size of 367bp. Lane 4 represents a negative sample not containing the VP7 5' insert.

Figure 2.2 (d) Agarose gel electrophoresis of *Sac*I digestion of VP7mt144 (lanes 6 and 7) and VP7mt144/200 (lanes 8 and 9). Lanes 1 and 2 represent size markers MWII and $\phi\chi 174$ respectively. Lanes 3 and 4 represent uncut and *Sac*I digested pFastBac-5' intermediates respectively. Lane 5 represents an undigested VP7mt144/200 sample.

Figure 2.3.

CLUSTAL X (1.81) Multiple Sequence Alignment (VP7mt144 and VP7mt144/200 to VP7).

```

VP7          GTTTAAATTCGGTTAGGATGGACGCGATACGAGCAAGAGCCTTGTCGGTTGTACGGGCAT 60
mt144       GTTTAAATTCGGTTAGGATGGACGCGATAGCAGCAAGAGCCTTGTCGGTTGTACGGGCAT
mt144/200   GTTTAAATTCGGTTAGGATGGACGCGATAGCAGCAAGAGCCTTGTCGGTTGTACGGGCAT
*****

VP7          GTGTCACAGTGACAGATGCGAGAGTTAGTTTGGATCCAGGAGTGATGGAGACGTTAGGGA 120
mt144       GTGTCACAGTGACAGATGCGAGAGTTAGTTTGGATCCAGGAGTGATGGAGACGTTAGGGA
mt144/200   GTGTCACAGTGACAGATGCGAGAGTTAGTTTGGATCCAGGAGTGATGGAGACGTTAGGGA
*****

VP7          TTGCAATCAATAGGTATAATGGTTTAAACAAATCATTTCGGTATCGATGAGGCCACAAACCC 180
mt144       TTGCAATCAATAGGTATAATGGTTTAAACAAATCATTTCGGTATCGATGAGGCCACAAACCC
mt144/200   TTGCAATCAATAGGTATAATGGTTTAAACAAATCATTTCGGTATCGATGAGGCCACAAACCC
*****

VP7          AAGCAGAACGAAATGAAATGTTTTTATGTGTACTGATATGGTTTTAGCGGCGCTGAACG 240
mt144       AAGCAGAACGAAATGAAATGTTTTTATGTGTACTGATATGGTTTTAGCGGCGCTGAACG
mt144/200   AAGCAGAACGAAATGAAATGTTTTTATGTGTACTGATATGGTTTTAGCGGCGCTGAACG
*****

VP7          TCCAAATTGGAATATTTACCAGATTATGATCAAGCGTTGGCAACTGTGGGAGCTCTCG 300
mt144       TCCAAATTGGAATATTTACCAGATTATGATCAAGCGTTGGCAACTGTGGGAGCTCTCG
mt144/200   TCCAAATTGGAATATTTACCAGATTATGATCAAGCGTTGGCAACTGTGGGAGCTCTCG
*****

VP7          CAACGACTGAAATTCATATAATGTTTCAGGCCATGAATGACATCGTTAGAATAACGGGTC 360
mt144       CAACGACTGAAATTCATATAATGTTTCAGGCCATGAATGACATCGTTAGAATAACGGGTC
mt144/200   CAACGACTGAAATTCATATAATGTTTCAGGCCATGAATGACATCGTTAGAATAACGGGTC
*****

VP7          AGATGCAAAACATTCGGACCAAGCAAAGTGCAAACGGGGCCTTATGCAGGAGCGGTTGAGG 420
mt144       AGATGCAAAACATTCGGACCAAGCAAAGTGCAAACGGGGCCTTATGCAGGAGCGGTTGAGG
mt144/200   AGATGCAAAACATTCGGACCAAGCAAAGTGCAAACGGGGCCTTATGCAGGAGCGGTTGAGG
*****

VP7          TGCAACAATCTGGCAGATATTACGTACCGC-----AAGGTCGAACGC 480
mt144       TGCAACAATCTGGCAGATATTACGTACCGCCCGGGGAATTCCTCGAGCAAAGGTCGAACGC
mt144/200   TGCAACAATCTGGCAGATATTACGTACCGCCCGGGGAATTCCTCGAGCAAAGGTCGAACGC
*****

VP7          GTGGTGGGTACATCAATTCAAATATTGCAGAAGTGTGTATGGATGCAGGTGCTGCGGGAC 560
mt144       GTGGTGGGTACATCAATTCAAATATTGCAGAAGTGTGTATGGATGCAGGTGCTGCGGGAC
mt144/200   GTGGTGGGTACATCAATTCAAATATTGCAGAAGTGTGTATGGATGCAGGTGCTGCGGGAC
*****

VP7          AGGTCAATGCGCTGCTAGCCCCAAGGAGGGGGGACGCAGTCATGATCTATTTGTTGGA 620
mt144       AGGTCAATGCGCTGCTAGCCCCAAGGAGGGGGGACGCAGTCATGATCTATTTGTTGGA
mt144/200   AGGTCAATGCGCTGCTAGCCCCAAGGAGGGGGGACGCAGTCATGATCTATTTGTTGGA
*****
  
```

VP7 GACCGTTGCGTATATTTTGTGATCCTCAAGGTGCG-----TCACTTG
 mt144 GACCGTTGCGTATATTTTGTGATCCTCAAGGTGCG-----TCACTTG
 mt144/200 GACCGTTGCGTATATTTTGTGATCCTCAAGGTGCGAAGCTTTCTAGAGTCGACTCACTTG 680

VP7 AGAGCGCTCCAGGAACTTTTGTACCCGTTGATGGAGTAAATGTTGCAGCTGGAGATGTTCG
 mt144 AGAGCGCTCCAGGAACTTTTGTACCCGTTGATGGAGTAAATGTTGCAGCTGGAGATGTTCG
 mt144/200 AGAGCGCTCCAGGAACTTTTGTACCCGTTGATGGAGTAAATGTTGCAGCTGGAGATGTTCG 740

VP7 TCGCATGGAATACTATTGCACCAGTGAATGTTGGAAATCCTGGGGCACGCAGATCAATTT
 mt144 TCGCATGGAATACTATTGCACCAGTGAATGTTGGAAATCCTGGGGCACGCAGATCAATTT
 mt144/200 TCGCATGGAATACTATTGCACCAGTGAATGTTGGAAATCCTGGGGCACGCAGATCAATTT 800

VP7 TACAGTTTGAAGTGTATGGTATACGTCCTTGGATAGATCGCTAGACACGGTTCCGGAAT
 mt144 TACAGTTTGAAGTGTATGGTATACGTCCTTGGATAGATCGCTAGACACGGTTCCGGAAT
 mt144/200 TACAGTTTGAAGTGTATGGTATACGTCCTTGGATAGATCGCTAGACACGGTTCCGGAAT 860

VP7 TGGCTCCAACGCTCACAAGATGTTATGCGTATGTCTCTCCCACTTGGCACGCATTACGCG
 mt144 TGGCTCCAACGCTCACAAGATGTTATGCGTATGTCTCTCCCACTTGGCACGCATTACGCG
 mt144/200 TGGCTCCAACGCTCACAAGATGTTATGCGTATGTCTCTCCCACTTGGCACGCATTACGCG 920

VP7 CTGTCATTTTTCAGCAGATGAATATGCAGCCTATTAATCCGCCGATTTTTCCACCGACTG
 mt144 CTGTCATTTTTCAGCAGATGAATATGCAGCCTATTAATCCGCCGATTTTTCCACCGACTG
 mt144/200 CTGTCATTTTTCAGCAGATGAATATGCAGCCTATTAATCCGCCGATTTTTCCACCGACTG 980

VP7 AAAGGAATGAAATGTTGCGTATCTATTAGTAGCTTCTTTAGCTGATGTGTATGCGGCTT
 mt144 AAAGGAATGAAATGTTGCGTATCTATTAGTAGCTTCTTTAGCTGATGTGTATGCGGCTT
 mt144/200 AAAGGAATGAAATGTTGCGTATCTATTAGTAGCTTCTTTAGCTGATGTGTATGCGGCTT1040

VP7 TGAGACCAGATTTTCAGAAATGAATGGTGTGTCGCGCCAGTAGGCCAGATTAACAGAGCTC
 mt144 TGAGACCAGATTTTCAGAAATGAATGGTGTGTCGCGCCAGTAGGCCAGATTAACAGAGCTC
 mt144/200 TGAGACCAGATTTTCAGAAATGAATGGTGTGTCGCGCCAGTAGGCCAGATTAACAGAGCTC1100

VP7 TTGTGCTAGCAGCCTACCACTAGTGGCTGCGGTGTTGCACGGTCACCGCTTTCATTAGTG
 mt144 TTGTGCTAGCAGCCTACCACTAGTGGCTGCGGTGTTGCACGGTCACCGCTTTCATTAGTG
 mt144/200 TTGTGCTAGCAGCCTACCACTAGTGGCTGCGGTGTTGCACGGTCACCGCTTTCATTAGTG1160

VP7 TCGCGTCGGTTCCTTATGCTGATAAAGTACGCATAAGTAATACGTCAATACCGAATACACT
 mt144 TCGCGTCGGTTCCTTATGCTGATAAAGTACGCATAAGTAATACGTCAATACCGAATACACT
 mt144/200 TCGCGTCGGTTCCTTATGCTGATAAAGTACGCATAAGTAATACGTCAATACCGAATACACT1220

VP7 TACAGA
 mt144 TACAGA
 mt144/200 TACAGA 1280

2.3.3. Physicochemical Properties and Structural Modelling of the Modified Proteins.

VP7 is a highly hydrophobic protein. This can be seen in figure 2.4(a) showing the hydrophilicity plot of VP7 calculated according to the method by Hopp and Woods (Hopp and Woods, 1981; Hopp and Woods, 1983) (section 2.2.6). Very few small regions of VP7 show a net hydrophilicity, with the majority of the protein having negative values for hydrophilicity. A peak of net hydrophilicity occurs in the region of amino acids 144 and 145, which is expected of a sequence exposed on the surface of the protein. The effect of the insertion of six amino acids on the hydrophilicity of that area may affect its exposure to the surface. Of the six amino acids inserted (pro-gly-glu-phe-leu-glu), only the two glutamate residues are charged and hydrophilic. Some increase in hydrophobicity of that region would be expected with contributions from four of the six amino acids inserted. As shown in figure 2.4(b), there is significant decrease in hydrophilicity toward the N-terminal end of this region. The proline and glycine residues at the N-terminal end of the insert would contribute to this drop. A significant increase in hydrophilicity, with a value greater than 5, is shown toward the C-terminal end of the foreign insert. The glutamate at the C-terminal end of the insert would be the main contributory factor to this hydrophilicity peak. The hydrophilicity plot of the double mutant, mt144/200, is also shown. This indicates the same effect at site 144 and also shows the increase in hydrophilicity caused by the inserted amino acids at site 200, where four of the six amino acids are hydrophilic.

The effect of the predicted change in hydrophilicity on the structure of the protein, particularly in terms of the exposure of the foreign insert on the surface, was investigated further. Structural modelling of the modified protein was done using the top domain (amino acids 121 to 249) of AHSV-4 VP7 sequence as a template (section 2.2.6). Thus, the results in figure 2.5 show only the top domain of the modified proteins. The anti-parallel β sandwich structure of the upper domain of VP7 is clearly visible. The results indicate that the insert of six amino acids at site 144 appears to loop out of the surface of the protein. This looping would provide excellent exposure for an epitope on the surface of the protein. No other major changes in the protein folding and structure are visible, however it is impossible to predict the effect of the insert on inter-protein interactions based on this structural modelling. Thus, one cannot predict the effect of the insert on crystal formation.

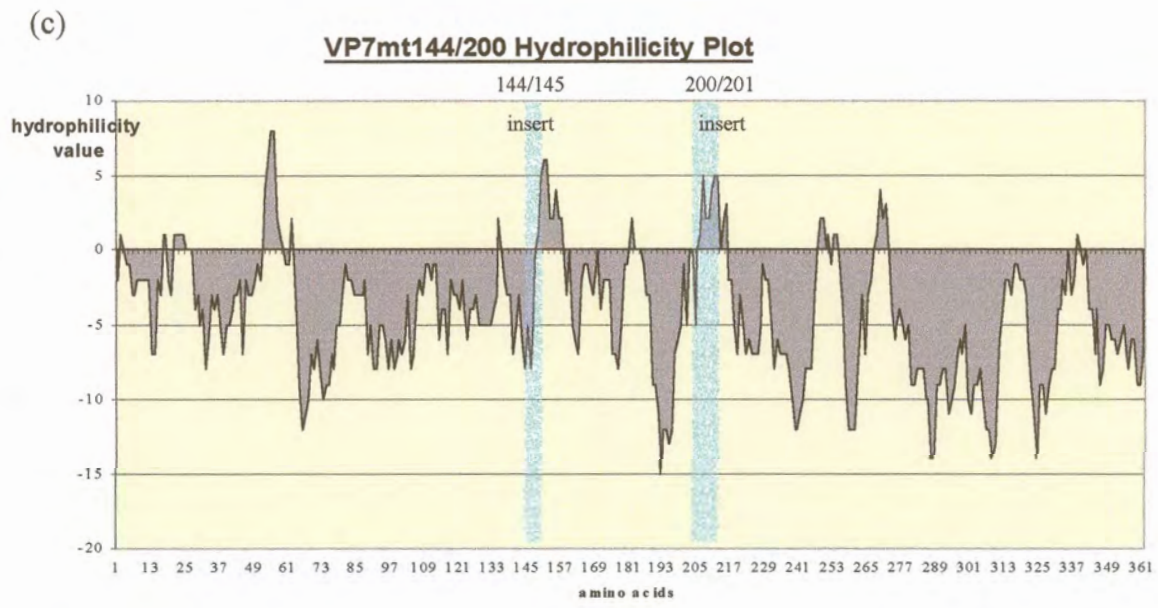
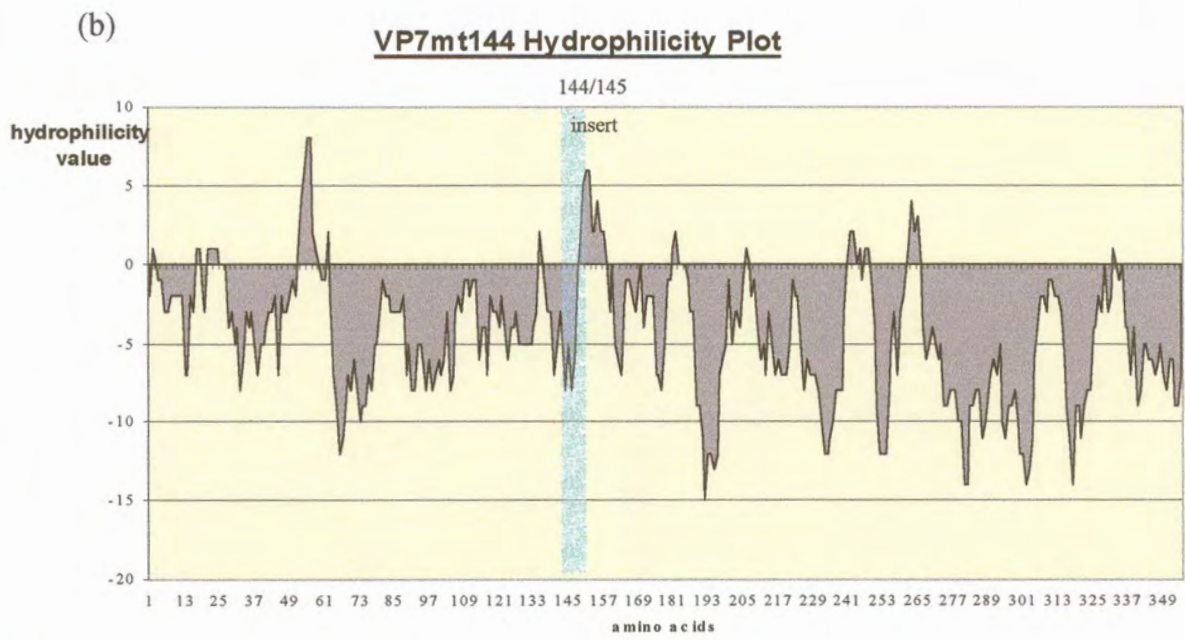
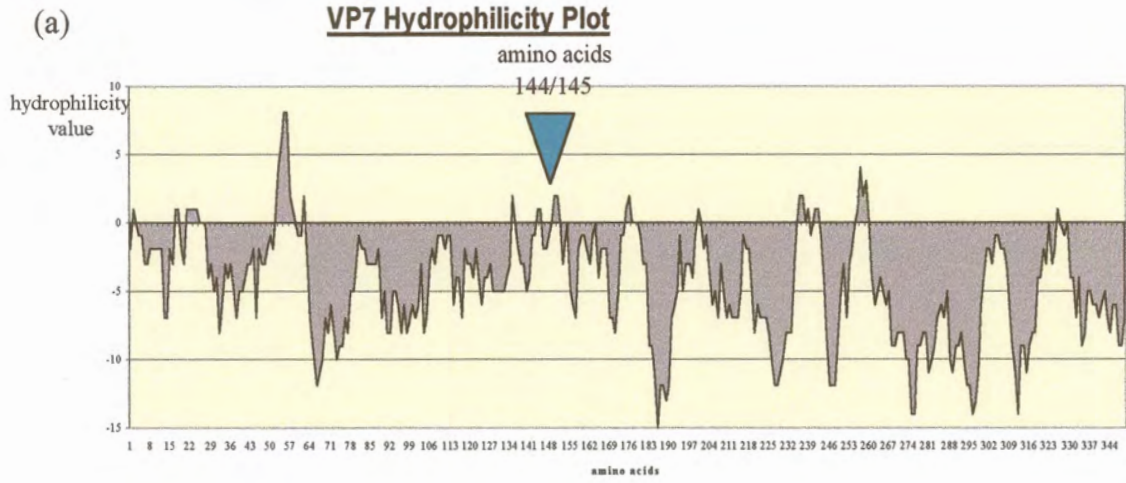


Figure 2.4. Hydrophilicity Plots of VP7 (a), VP7mt144 (b) and VP7mt144/200 (c) according to the Hopp and Woods Predictive Method (Hopp and Woods, 1981;Hopp and Woods, 1983).

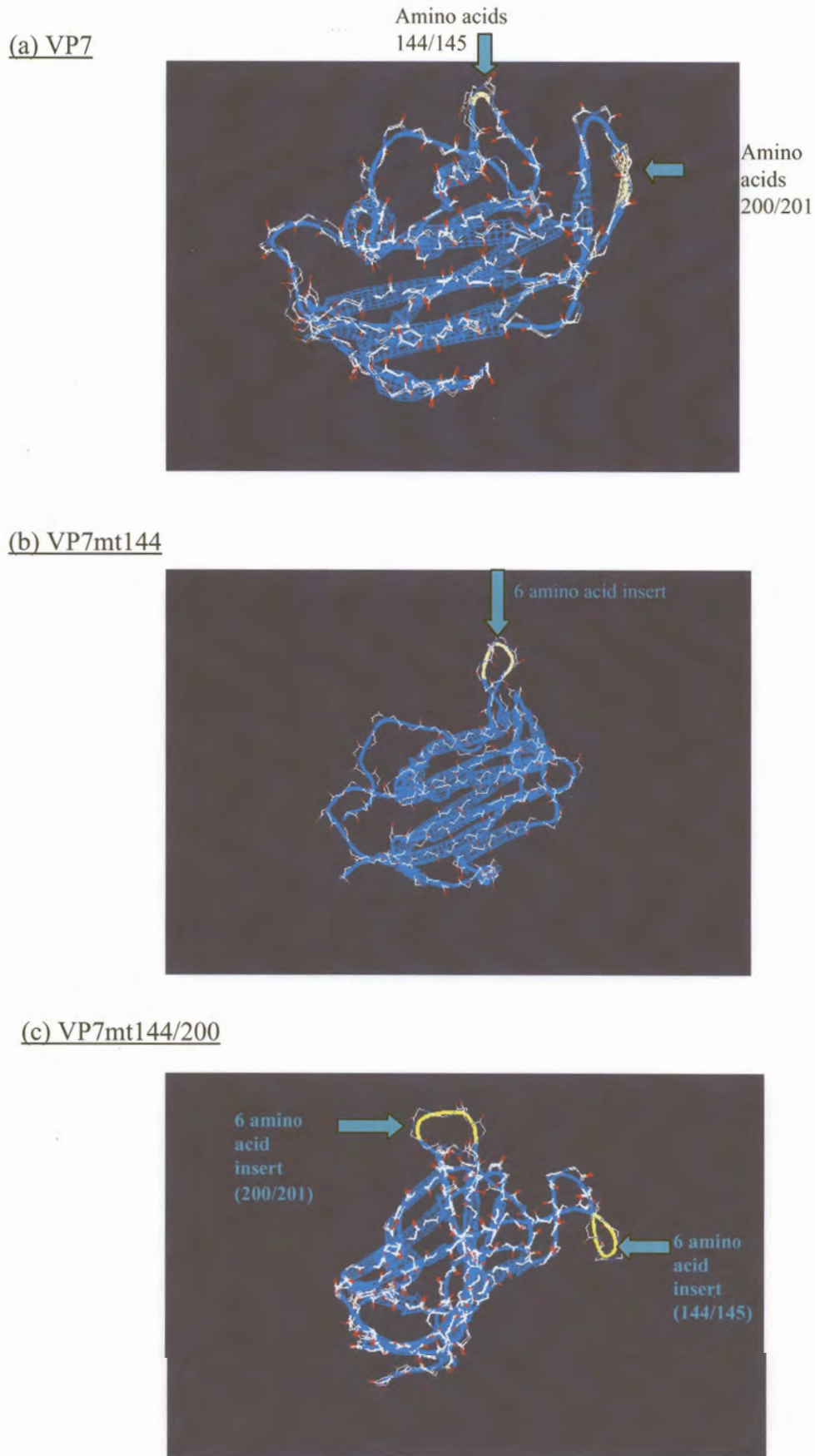


Figure 2.5. Structural Modeling of VP7mt144 (b) and VP7mt144/200 (c) in comparison to VP7 (a) shows the inserted amino acids to loop out of the surface of the protein. The loops are indicated in yellow.

2.3.4. Expression of the Modified VP7mt144 and VP7mt144/200 Proteins.

The modified VP7 genes were expressed using the baculovirus expression system. The recombinant pFastBac transfer plasmids containing the modified VP7 genes were used to transform competent *E. coli* DH₁₀BAC cells (2.2.7.2). Transposition (by homologous recombination) of the wild-type bacmid DNA in successfully transformed DH₁₀BAC cells produced recombinant bacmid DNA, which was isolated and used to transfect sf9 insect cells (2.2.7.3). Recombinant baculovirus was recovered in the supernatant after four days. This was designated Bacmt144 and Bacmt144/200. The expression of the modified proteins was tested by SDS-PAGE analysis of the infected cell lysates from 24-well infection (2.2.9 and 2.2.7.4). Homogenous virus with high-level expression was obtained by plaque purification and was amplified by low titre infection of sf9 monolayers seeded at 1×10^7 cells per flask. To study the expression of the modified VP7 proteins, VP7mt144 and VP7mt144/200, monolayers seeded at 1×10^7 cells were infected at a MOI of approximately 10^8 with the recombinant baculoviruses Bacmt144 and Bacmt144/200 respectively. Infected cell lysate was analysed by SDS-PAGE and Coomassie blue staining and is shown in figure 2.6. The VP7mt144 and VP7mt144/200 proteins were clearly visible as distinct bands not visible in the mock- or wild-type baculovirus- infected cells. A size increase from the wild-type VP7 was just visible on a 12% polyacrylamide gel, which has a resolution of approximately 1kDa. This is shown in figure 2.6(a). Figure 2.6(b) shows the same samples run on a 15% SDS-PAGE gel. The size difference is more clearly visible, with VP7mt144 being slightly larger than VP7 due to the insertion of 6 amino acids and VP7mt144/200 being slightly larger than VP7mt144 due to the additional six amino acids at position 200. The level of expression for both modified proteins is high, estimating from an SDS-PAGE gel of about 30–40 μg per 1×10^7 infected cells. The level of expression of the protein does not seem to be significantly affected by the mutation at site 144. The level of expression of VP7mt144 is comparable to that of VP7.

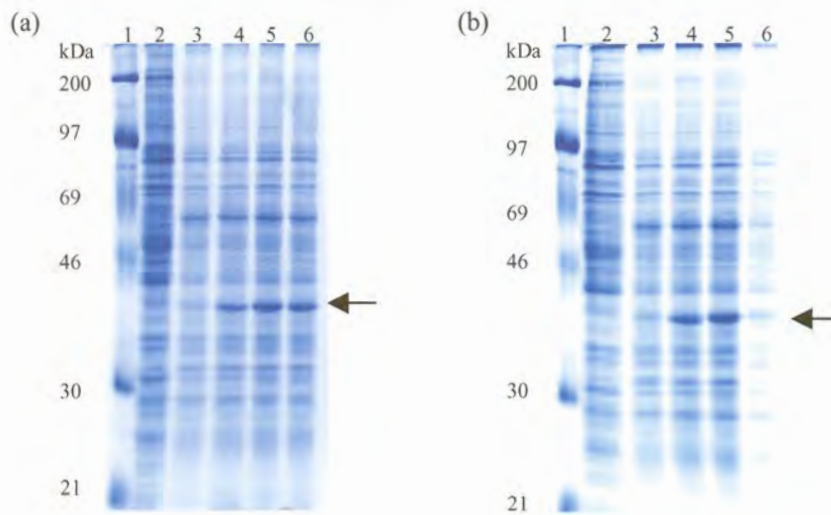
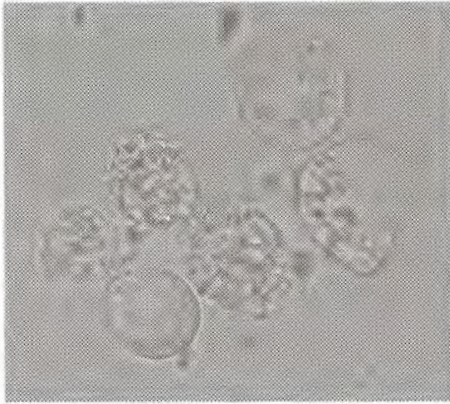


Figure 2.6. SDS-PAGE analysis of Modified Proteins VP7mt144 (fig (a), (b) lane 5) and VP7mt144/200 (fig (a), (b) lane 6) on a 12% (fig (a)) and 15% (fig (b)) polyacrylamide gels. In both (a) and (b), lane 1 represents the protein size marker. Lanes 2 and 3 contain cell lysate from mock- and wild-type baculovirus-infected cells respectively. Lane 4 contains cell lysate from recombinant baculovirus BacVP7-infected cells. The arrows in (a) and (b) indicate the position of VP7 and modified VP7 proteins on the gel.

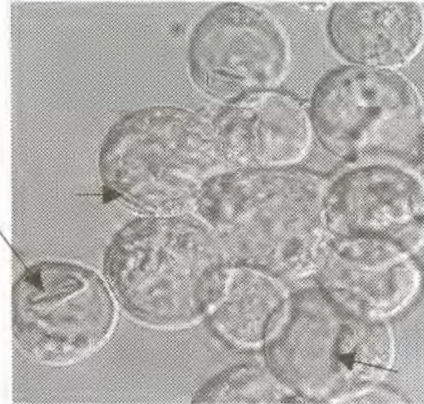
2.3.5. Light Microscope Observations.

The crystal structures formed by VP7 are visible in the recombinant VP7 baculovirus-infected cells. The distinct crystal structures appear as needle-shaped structures that refract the light similarly to the cellular membranous structures. The wild-type VP7 crystal is visible extensively across an infected monolayer, often up to 5 or 6 crystals occurring in one cell. Crystal structures are also visible in Bacmt144-infected cells. The same needle shape can be seen. However, a significant proportion of the crystals visible appeared to be smaller than those of wild-type VP7. Multiple crystals have also been observed in a single cell, although the distribution is clearly not as extensive as that seen for the wild-type VP7. The characteristic needle-shaped or rod-shaped structures are also visible in Bacmt144/200-infected cells, although in general do not appear as large or as abundant. Cells infected with wild-type baculovirus do not exhibit any crystal-like structures in their cytoplasm. The light microscope observations of crystal structures in BacVP7-, Bacmt144-, Bacmt144/200-infected cells as well as lack of structures in wild-type baculovirus-infected cells are shown in figure 2.7. Photographs were taken at a 63X magnification.

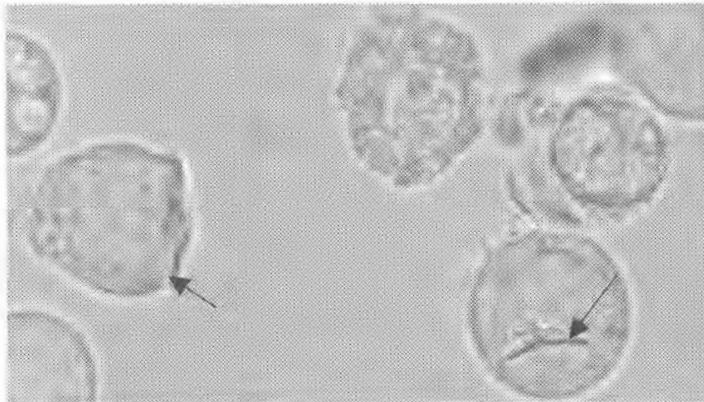
(a) Wild-type



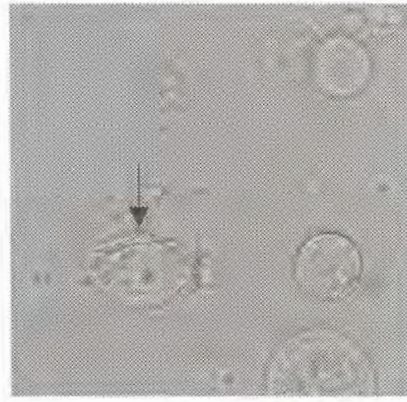
(b) VP7



(c) VP7mt144



(d) VP7mt144



(e) VP7mt144/200



(f) VP7mt144/200

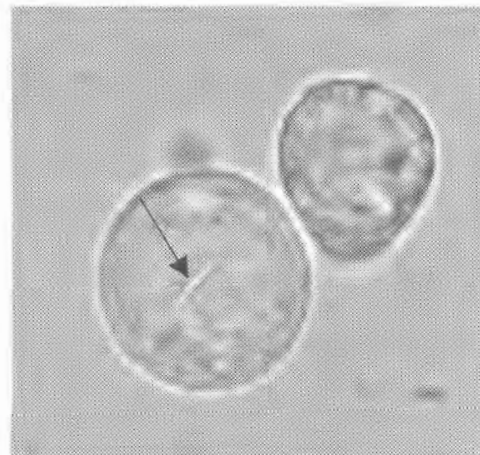


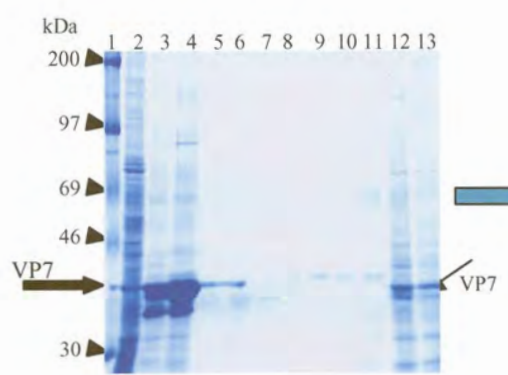
Figure 2.7. Light microscope observations of particulate structures present in sf9 insect cells infected with recombinant baculovirus expressing VP7 (b), VP7mt144 ((c) and (d)) and VP7mt144/200 ((e) and (f)). The control, (a), shows cells infected with wild-type baculovirus. The arrows indicate the particulate structures. Photographs were taken at 63X magnification.

2.3.6. Solubility Studies of the Modified Proteins.

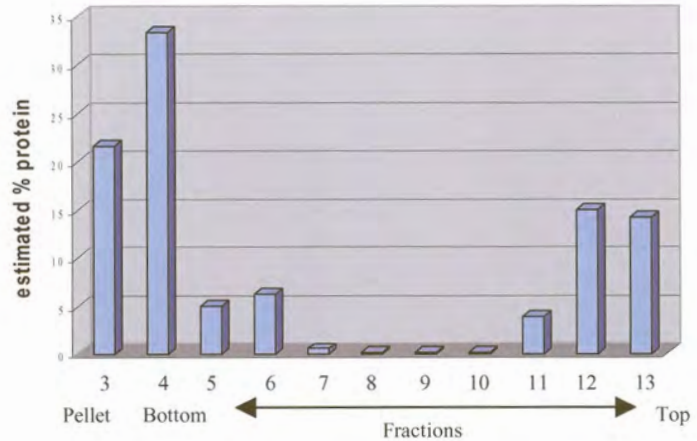
The influence of the six amino acid insertion on the solubility of the protein would give some insight into and offer some prediction of the structures formed by the protein. The solubility, as well as structure, is an important consideration in terms of vaccine delivery. To study the particulate structures formed by the modified proteins, samples of whole cell lysate harvested from recombinant bacmid-infected cells were loaded on discontinuous 30-50% (w/v) sucrose gradients. Fractions were collected per twenty drops and precipitated by TCA precipitation (methods described in 2.2.11). Fractions were analysed by SDS-PAGE. The distribution of the specified proteins visible on the SDS-PAGE gel was converted to a graphic form to provide a more informative visualisation of the distribution of the relevant protein. This was done using the SigmaGel™ software package in which the specified protein content of a fraction can be estimated by measurement of its band intensity in the SDS-PAGE gel. These values are not absolute values of protein concentrations and were thus converted to and interpreted as relative percentages of the total specified protein content across all fractions. Due to the inherent possibilities for variations in this experiment, it was repeated a minimum of three times and average values were calculated.

Under the centrifugation conditions used i.e. 14000rpm for 1hour 15 minutes, the majority of VP7 (in the form of crystals) pellets to the bottom of the sucrose gradients, with a small proportion being found in the top two fractions, presumably in the form of trimers (shown in figure 2.8(a)). In the modified protein, VP7mt200 (Maree, 2000), a proportion of the protein is distributed across all fractions of the gradient with greater proportions occurring in the top two fractions and in the pellet and bottom few fractions. This can be seen in figure 2.8(c) by two distinct peaks occurring at the bottom and top of the gradient. A greater proportion of VP7mt200 is found in the top two fractions when compared to VP7. In comparison to VP7mt200, a similar distribution is seen for the modified protein VP7mt144 (figure 2.8(b)). There are typically two peaks showing the greater proportions of protein occurring in the bottom and top fractions of the gradient. However, in comparison to VP7mt200, there is a significantly greater proportion of protein occurring in the middle fractions, indicating an increase in proportion of smaller particulate structures formed by VP7mt144 compared to VP7mt200. The distribution of the modified protein VP7mt144/200 corresponds similarly to that of VP7mt144 (figure 2.8(d)).

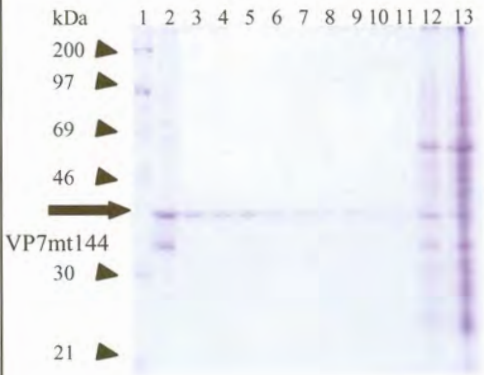
(a)



VP7 Particle Distribution



(b)



VP7mt144 Particle Distribution

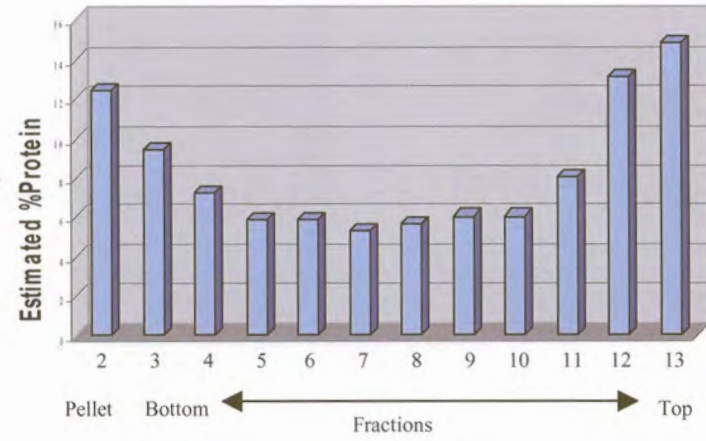


Figure 2.8 (a), (b). Distribution of VP7 (a) and VP7mt144(b) in 30 –50% Sucrose Gradient (centrifugation conditions of 14 000rpm 1hr 15min) shown by SDS-PAGE analysis and graphic representation. In (a) and (b) the band intensities on SDS-PAGE gels of VP7 or VP7mt144 in each fraction were quantitatively analyzed by the Sigma Gel™ analysis program and relative quantities were converted into the graphic form shown.

In figure (a) on the SDS-PAGE gel, lanes 1 and 2 respectively represent a protein size marker and the cell lysate of BacVP7-infected cells providing a VP7 marker. Lanes 3 represents the pellet of the gradient and lanes 4 to 13 represent the sequential fractions of the gradient from bottom to top. In figure (b) on the SDS-PAGE gel, lane 1 represents a protein marker, lane 2 represents the pellet of the gradient and lanes 3 to 13 represent the sequential fractions of the gradient. The graphs shows fractions containing an estimated percentage of the total protein.

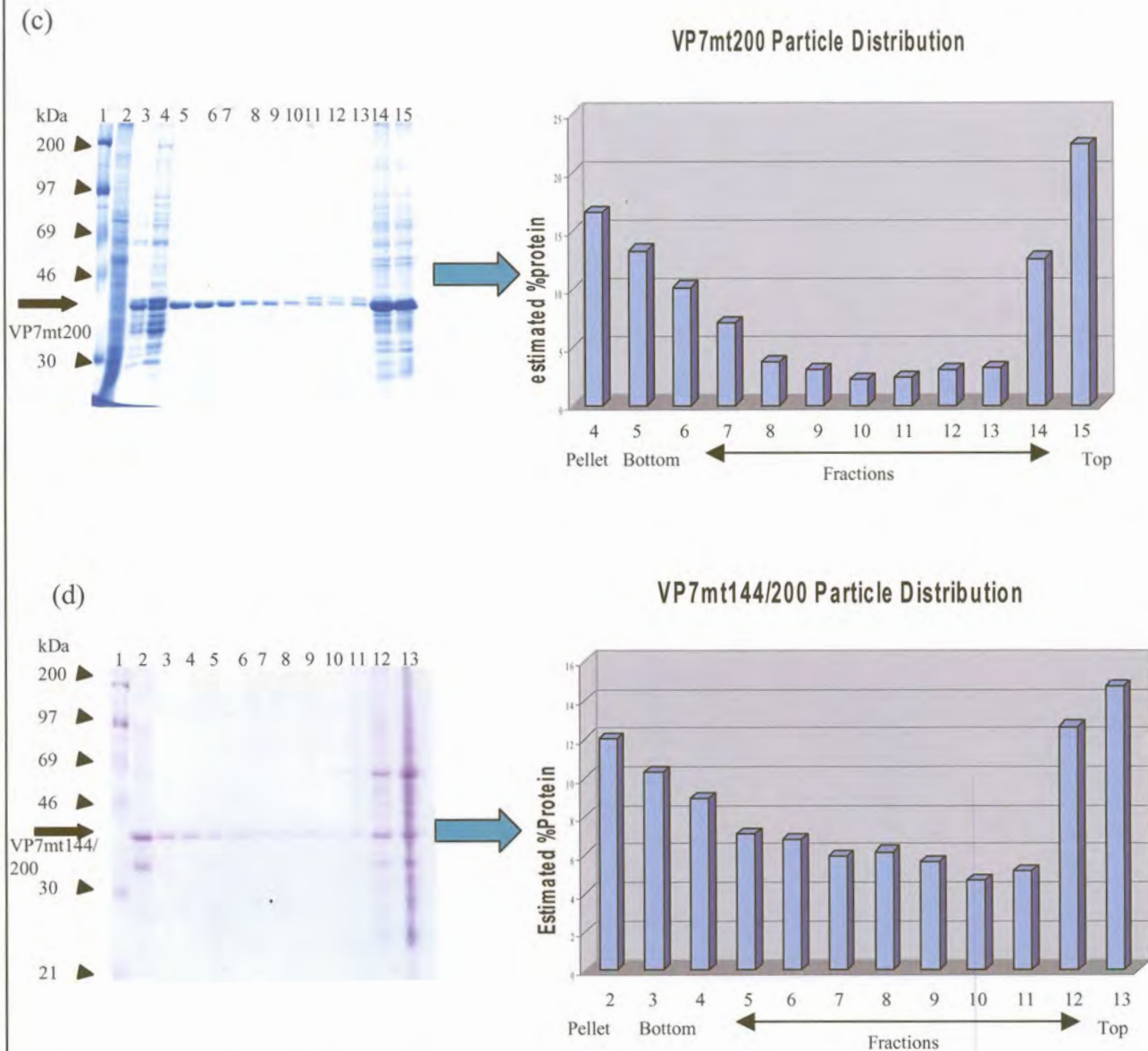


Figure 2.8 (c), (d). Distribution of VP7mt200 (c) and VP7mt144/200(d) in 30 –50% Sucrose Gradient (centrifugation conditions of 14 000rpm 1hr 15min) shown by SDS-PAGE analysis and graphic representation. Similarly to fig2.8(a), (b) the band intensities on SDS-PAGE gels of VP7mt200 or VP7mt144/200 in each fraction were quantitatively analyzed by the Sigma Gel™ analysis program and relative quantities were converted into the graphic form shown.

In figure (c) on the SDS-PAGE gel, lanes 1 and 2 respectively represent a protein size marker and the cell lysate of uninfected cells providing control. Lane 3 shows protein from a successful BacVP7mt200 infection showing VP7mt200 as a marker Lane 4 represents the pellet of the gradient and lanes 5 to 15 represent the sequential fractions of the gradient from bottom to top. In figure (d) on the SDS-PAGE gel, lane 1 represents a protein marker, lane 2 represents the pellet of the gradient and lanes 3 to 13 represent the sequential fractions of the gradient. As in figure 2.8(a) and (b), the graphs shows fractions containing an estimated percentage of the total protein.

To clarify these results, more specifically with respect to the soluble top fractions of the gradients, the centrifugation conditions were increased to 40 000rpm for 20 hours. Under these increased conditions, it was possible to increase the size separation of the previous top fractions of the gradient and thereby distinguish VP7 trimers and monomers. As can be seen in figure 2.9, the distribution of the bottom fractions of protein is similar to that seen under the slower centrifugation conditions. However, the change in centrifugation conditions showed the peak seen previously in the top fractions shifting to lower in the gradient. This is seen for both VP7mt144 and VP7mt144/200. It can be seen from the SDS-PAGE gel that this portion of the modified VP7 sediments to a position in the gradient where proteins larger than itself also sediment. This observation indicates that the modified protein must occur in an aggregation greater than its individual monomer form. Therefore, the protein found in the peak occurring at the top of the gradient is the trimer form of the protein.

One would expect that the protein occurring toward the bottom of the gradient where larger particles separate would conform to some particulate structure, thus bottom fractions were pooled and collected for investigation under the scanning electron microscope.

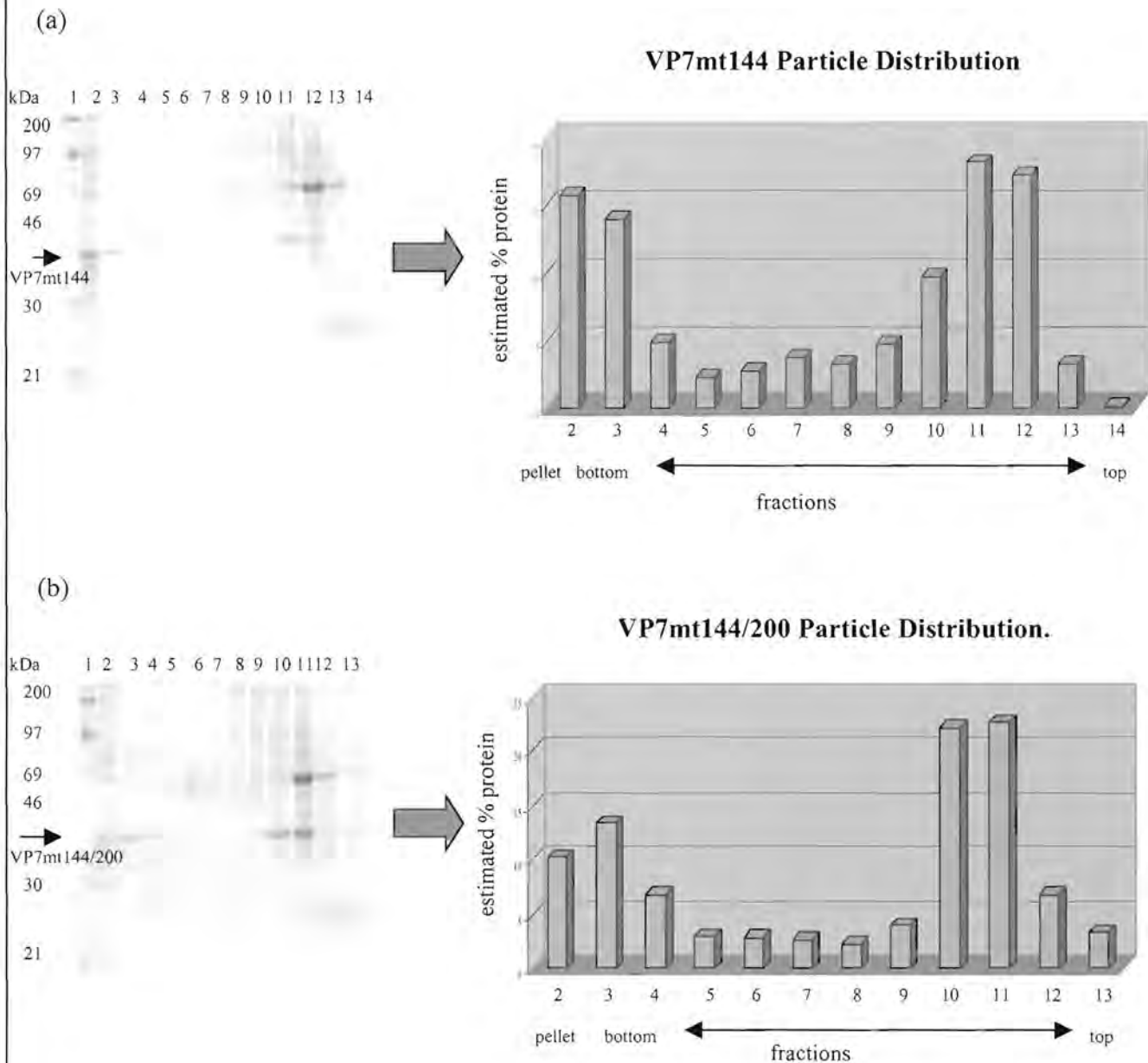


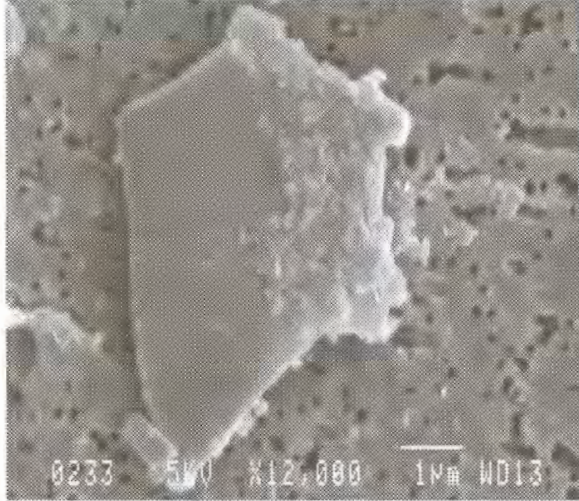
Figure 2.9 (a), (b). Distribution of VP7mt144 (a) and VP7mt144/200(b) in 30 –50% Sucrose Gradient (centrifugation conditions of 40 000rpm 20 hours) shown by SDS-PAGE analysis and graphic representation. As in fig 2.8, in (a) and (b) the band intensities on SDS-PAGE gels of VP7mt144 or VP7mt144/200 in each fraction were quantitatively analyzed by the Sigma Gel™ analysis program and relative quantities were converted into graphic form as the estimated % of the total protein present across all fractions. In figures (a) and (b) on the SDS-PAGE gel, lane 1 represent a protein size marker. Lane 2 represents the pellet of the gradient and lanes 3 to 14 (a) or lanes 3 to 13 (b) represent the sequential fractions of the gradient from bottom to top.

2.3.7. Scanning Electron Microscopy (S.E.M.).

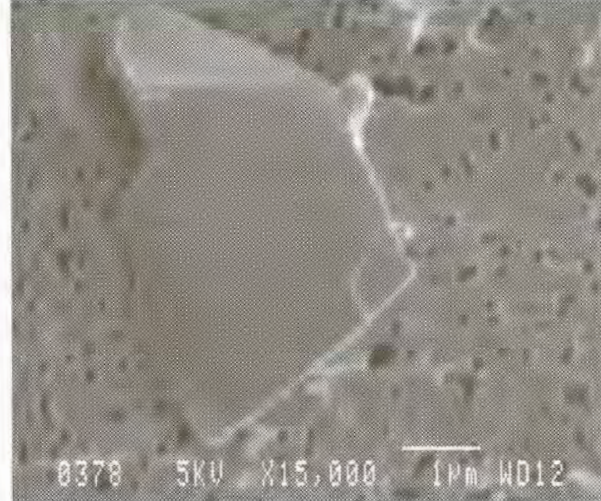
Samples of the putative modified protein structures were fixed, mounted and sputter coated with gold particles for investigation under the S. E. M. The structures found under the S.E.M. varied in form and size but showed a definite crystalline structure. Size fell into the range previously described by Chuma *et al.*, 1992, with the mean size being approximately 6µm in diameter. No distinct hexagonal crystals as those found in wild-type VP7 and VP7mt200 were observed (Maree, 2000). In figure 2.10(a), the structure formed by VP7mt144 could conceivably be a fragment of a hexagonal crystal. The structures are angular, with regular straight sides. It is possible that hexagonal crystals are formed but fragment during the preparation process. This may give some indication of a reduced stability of the structures. Unlike structures formed by VP7mt144, those formed by VP7mt144/200 (figure 2.10(c) and (d)) do not have regular sides, with distinct angles. A more ruffled structure is found. However, the layered structure also characteristic of structures formed by VP7, VP7mt200 and VP7mt144 is evident, being particularly noticeable in figure 2.10(d). It is clear that large particulate structures are formed by both VP7mt144 and VP7mt144/200 protein.

VP7mt144:

(a)

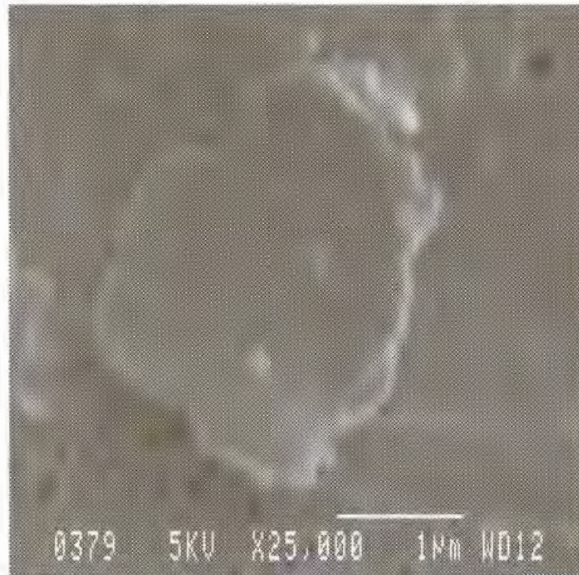


(b)



VP7mt144/200:

(c)



(d)

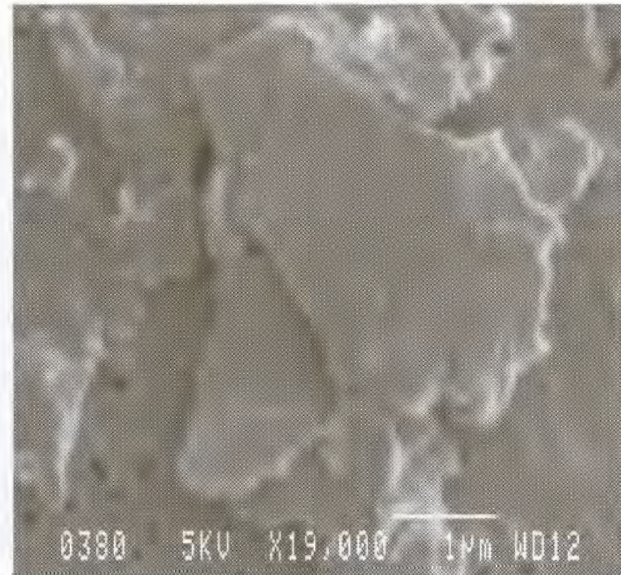


Figure 2.10 Scanning Electron Micrograph Photographs showing the crystalline structures formed by modified proteins VP7mt144 (a) and (b) and VP7mt144/200 (c) and (d).

2.4. DISCUSSION.

Wild-type AHSV VP7 is a highly hydrophobic, insoluble protein (Roy *et al.*, 1991; Maree *et al.*, 1998). When expressed in baculovirus-infected cells, it forms large particulate crystal structures with an average diameter of 6µm (Chuma *et al.*, 1992; Burroughs *et al.*, 1994; Maree *et al.*, 1998a and b). These crystal structures of VP7 are constituted from VP7 trimer aggregations. BTV VP7, which is more soluble than AHSV VP7, does not form crystals and remains as trimers in the cytosol of infected cells. The trimers are freely available for incorporation into the viral core. It has been deduced that the aggregation of trimers into VP7 crystals must be a factor of the solubility of the protein. Therefore, any modifications, which affect the solubility of VP7, will have some influence on the particulate structures formed.

The creation of a cloning site at position 144/145 of VP7, by the insertion of restriction enzyme sites *Sma*I, *Eco*R1 and *Xho*I, created a six amino acid insert of pro-gly-glu-phe-leu-glu. The effect of this insert was studied in the context of occurring as a single modification (VP7mt144) and as one part of a double modification (VP7mt144/200). The effect of the insertion was firstly investigated in terms of the individual VP7 protein, using predictive modelling to suggest any major changes in structure or properties. The change effected by the insert on the hydrophilicity profile of VP7 gives no indication on its own of any effect on protein solubility or structure, and should be interpreted in conjunction with the results of other studies. Structural protein modelling shows the six amino acid insert occurring as a loop on the surface of the protein. This would be expected as the site of the insertion is exposed on the surface in the wild-type protein. Modification at this site would not be expected to affect the internal folding of the protein.

In terms of the use of VP7 as a vaccine delivery system, the more informative results are those showing the effect of the insert on the VP7 aggregations into trimers and further into crystal structures. The primary indications of its effect on VP7 structures come from the light microscope observations. The reduction in relative quantities produced, as well as size of the crystals, is evident when the modified proteins are compared to wild-type VP7. It is clear that the ability to form crystals has not been abolished by the modification at site 144/145. However, crystal formation has been affected in terms of the size and distribution of the

crystals. This indicates some instability in crystal formation, causing an increased tendency of trimers to aggregate into and maintain smaller particulate structures, or increasing the tendency of VP7 to remain in its trimer form. The sucrose gradient centrifugation confirms this observation. The single mutant, VP7mt144, and the double mutant, VP7mt144/200, both show a similar distribution of protein in the gradient. There is a definite shift in the distribution of particulate structures and trimers compared to wild-type VP7. The shift away from the larger particulate structures in favour of increased proportions of smaller particulate structures (figure 2.8.(b) and (d)) and trimers (best shown in figure 2.9.) suggests an increase in solubility of VP7mt144 and VP7mt144/200 compared to wild-type VP7. An overall increase in the proportion of trimers is perhaps less evident in figure 2.8., when considering estimated percentages of protein in the two peaks. However, figure 2.9. shows a more definite increase in proportions of trimers, with the strongest peaks representing the trimer form of the protein. This increase in trimer proportion at the expense of larger particulate structures can be explained by the equilibrium between trimers and crystals described by Maree, 2000. The insolubility of wild-type VP7 means the equilibrium lies very much to the crystal form of VP7 with a minority of protein occurring in trimer form. Modification bringing about an increase in solubility of VP7 will shift the equilibrium to the trimer form, the extent of which would depend on the modification and its effect.

Various modifications have been made to AHSV VP7 with varying effects on the protein solubility. The effect of the replacement of selected amino acids in the top domain of AHSV VP7, showing differences to the more soluble BTV VP7, have been investigated in terms of the influence on solubility. The replacement of A167 by the more hydrophilic arginine and F209 by tyrosine did not significantly improve the solubility of VP7 (Monastyrskaya *et al.*, 1997). The replacement of L345 by the more hydrophilic arginine caused an estimated increase of 37% in the solubility of AHSV VP7 (Meyer, personal communication). The insertion of six amino acids at site 177 caused an estimated 40% increase in solubility (Maree, 2000). Maree, 2000, also reported no significant increase in solubility when the same amino acids were inserted at site 200. This was based on results from a simple differential centrifugation analysis. However, the distribution of VP7mt200 in the comparative sedimentation analysis (figure 2.8(c)) indicates some influence on solubility, with a shift away from the large particulate structures that pellet at the bottom of the gradient in favour of smaller particulate structures. Changes in solubility that were observed

in these previous studies, similarly to VP7mt144 and VP7mt144/200, influenced the formation of the larger crystalline structures without notably influencing the formation of trimers. The mutant VP7L345R produced an increased proportion of smaller crystalline structures (Meyer, personal communication) and the mutant VP7mt177 produced particulate structures of a distorted, more rounded appearance than the characteristic hexagonal shape (Maree, 2000). Another modification shown to influence VP7 crystal formation is that of the modified protein VP7mt200-NS3. This mutant contains an insert of 12 amino acids of NS3 protein at site 200 of VP7mt200, and while no influence on solubility was observed from sedimentation profiles, the crystal structures it produced had a more “ruffled” appearance. This may be due to a weakening of trimer-trimer interactions, disrupting trimer layers that make up the crystal (Meiring, 2001). Changes in solubility have thus been shown to manifest at the level of trimer-trimer interactions.

The increase in solubility and reduction in crystal formation can be explained by the disruption of hydrophobic interactions between trimers, which are thought to be responsible for crystal formation. This would explain the increase in solubility observed in VP7L345R where leucine has been substituted by the strongly hydrophilic amino acid arginine. The area of possible contact between trimers is limited, making trimer interactions relatively weak (Grimes *et al.*, 1998; Limn *et al.*, 2000). Thus, although the modification neither abolishes the formation of the trimers nor the interactions between trimers to form crystals, it does affect the strength of these interactions and therefore also affects the stability of the crystals that do form. This would account for the increase in the proportion of smaller particulate structures formed by both VP7mt144 and VP7mt144/200 as well as VP7L345R (Meyer, personal communication), where cumulative hydrophobic interactions are no longer strong enough to maintain the larger structures prevalent in the wild-type VP7. When one looks at the hydrophilicity profiles of VP7mt144 and VP7mt144/200, the insert at site 144/145 has created a prominent hydrophilic peak. It is feasible that it is this increase in hydrophilicity that is responsible for disturbing the hydrophobic interactions between trimers.

Both particulate structures as well as the individual trimers have potential as a vaccine delivery system. Particulate structures have a large surface area for the display of multiple epitopes, whereas trimers are more soluble and may be more practical for administration.

Therefore, the shift in equilibrium of large particulate structures to trimers may not diminish the feasibility of using VP7 as a vaccine delivery system. The maintenance of the trimer, and the crystalline composite structure, by the creation of cloning site 144 supports its potential for an epitope display vehicle. The double mutant VP7mt144/200 has two cloning sites for the insertion of multiple epitopes on the surface of VP7, which may enhance an immune response. The accessibility of epitopes at site 144/145 should be investigated as well as the immune response generated.

CHAPTER 3

Insertion of AHSV VP2 Neutralising Epitope in the Modified VP7, VP7mt144, its Effect on VP7 Structural Features and Immunogenicity.

3.1. INTRODUCTION.

The use of VP7 particulate structures or trimers as a vaccine delivery system would depend on its ability to accommodate and efficiently present peptide or epitope inserts as well as the ability of these inserts to elicit an immune response. As shown in chapter 2, the insertion of six amino acids between amino acids 144 and 145 of AHSV-9 VP7 did not abolish the formation of crystals. The solubility was affected to some extent, with the size distribution of crystalline structures tending towards the smaller particulate structure. A greater proportion of protein also remained in the trimer form, not aggregating into particulate structures of any significant size. These observations, however, should not detract from the potential utility of VP7 as a presentation system for epitopes. Smaller particles as well as the trimers themselves may be more or equally efficient for peptide display.

VP7 crystals have been shown to generate a protective immune response in mice (Wade-Evans *et al*, 1997; Wade-Evans *et al.*, 1998). The modification of VP7 to create VP7mt144 and VP7mt144/200 would not be expected to affect this ability. The protective immune response should be enhanced by the insertion of identified neutralising epitopes at the cloning sites created in the modified proteins. The ability of the chosen epitope to generate an immune response would depend on various factors. Firstly, the insertion of the epitope into VP7 must not affect the structure or folding of VP7 such that the formation of trimers or crystal particulate structures is affected, depending on the choice of the presentation system. The epitope must be presented in such a way on the surface of the VP7 protein that it occurs in the native recognised form, therefore the epitopes must be sufficiently

exposed on the surface of the protein and the structure or presentation of the epitope must not be affected by the environment of and interactions with the VP7 protein.

With the aim of developing an improved vaccine against AHSV, an identified neutralising epitope of the VP2 protein was chosen to insert in the cloning site created at position 144 of VP7mt144. The major antigenic domain of VP2 contains many smaller fragments that elicit neutralising antibodies. A strong linear epitope was identified by Venter *et al.*, 2000, between amino acids 369 and 407 of AHSV-9 VP2. This was supported by the separate identification of a strong neutralising area between amino acids 379 and 413 of AHSV-3 VP2 (Bentley *et al.*, 2000) and amino acids 377 and 400 of AHSV-4 VP2 (Martinez-Torrecuadrada *et al.*, 2001). Based on this evidence, a sequence of 25 amino acids from amino acid 377 to 401 of AHSV-9 VP2 was chosen to insert at cloning site 144 of VP7mt144. The choice of a linear neutralising epitope should eliminate the possibility of the protein environment of VP7 influencing the natural presentation of the epitope, in comparison to a more structurally dependent epitope. The 25 amino acid sequence would provide a significant size insert into the VP7 protein to give some further indication to the size of peptide insertions that could be accommodated at site 144/145. If this insert abolishes the ability of the protein to associate into trimers and, in turn, to form crystals, a possible size limitation of inserts which could be accommodated at this particular site will have been established. If the insert does not abolish the ability of the protein to associate into trimers, the possibility that it may be used as an epitope display vehicle is retained despite possible influences on solubility and/or crystal formation.

The insertion of 25 amino acids at site 144/145 was studied, similarly to the modifications creating VP7mt144 and VP7mt144/200, in terms of its effect on VP7 structure, trimer formation and crystal formation, as this would affect the presentation of the inserted epitope to an immune system. Secondly, the immune response generated by the modified VP7 protein containing the chosen epitope was also investigated, as the intended aim of the study is to investigate the potential of the system to elicit a protective immune response.

3.2. MATERIALS AND METHODS.

3.2.1. Materials.

AHSV-9 L2 cDNA in pBS was obtained from Dr F. F. Maree. Primers used were supplied by GIBCO BRL. β -agarase was obtained from FMC BioProducts. The pMOS Blue cloning kit was obtained from Amersham Pharmacia Biotech. Other reagents used were obtained from suppliers described in section 2.2.1.

3.2.2. PCR Amplification of a Small Antigenic Region of VP2.

A primer pair was designed to amplify the region of amino acids 377–401 (nucleotides 1141-1215) of AHSV-9 VP2 protein. The forward primer (jv2f) contained an overhang of an *EcoRI* site with an additional GC tag and the reverse primer (jv2r) contained an overhang of a *XhoI* site with an additional GC tag. The sequence of the primers is indicated in the table 3.1. Two T_m values were calculated according to the formula applicable to primers greater than 18 nucleotides in length: $T_m = 81.5 + 16.6\log[Na^+] + 0.41(\%G+C) - 675/n$, where n is the number of nucleotides in the primer. T_{m1} applied to the first five cycles of amplification and T_{m2} applied to the second phase of amplification. The average of the T_m values of the two primers was calculated and adjusted appropriately. The annealing temperature was taken as 5°C lower than the appropriate T_m value.

Table 3.1. Primers used in PCR Amplification of VP2 Epitope.

<u>Primer name.</u>	<u>Directed position on VP2.</u>	<u>Sequence.</u>	<u>T_m values (°C)</u>
jv2f	Nucleotide 1141-1161	5' GCGAATTCGATCCAAATCATGATACATGG 3' <i>EcoRI</i>	$T_{m1} = 43.38$ $T_{m2} = 53.6$
jv2r	Nucleotide 1195-1215	5' GCCTCGAGATTCGCGCTCTGTTCTTTCTG 3' <i>XhoI</i>	$T_{m1} = 47.03$ $T_{m2} = 59.25$

Reactions were prepared as described in section 2.2, including a negative control of an identical reaction lacking pBS-L2 cDNA template. The PCR program used included:

- A 2 minute denaturation step at 94°C
- 5 cycles of denaturation at 94°C for 30 seconds, annealing at 45°C for 3 seconds, elongation at 72°C for 30 seconds
- 15 cycles of denaturation at 94°C for 30 seconds, annealing at 51°C for 30 seconds and elongation at 72°C for 30 seconds.

- 15 cycles of denaturation at 94°C for 30 seconds, annealing at 51°C for 30 seconds with an increase in temperature of 0.5°C per cycle and elongation at 72°C for 30 seconds.
- A cycle of 7 minutes elongation at 72°C
- Hold at 4°C indefinitely.

The PCR products of the reaction and negative control were analysed by electrophoresis on a 2% agarose gel (1XTAE), as described by methods in chapter 2 (2.2.3.2.), using Φ X174 as a marker.

3.2.3. Cloning of VP2 epitope into the Modified VP7mt144 Gene.

3.2.3.1. General.

Cloning of the VP2 epitope was achieved by methods described in chapter 2, with minor additions and variations. Where necessary, analysis of the VP2 epitope by agarose gel electrophoresis was carried out on a 2% agarose gel (1XTAE) as opposed to the standard 1% agarose gel. In ligation reactions (chapter 2, section 2.2.3.4) for the insertion of the VP2 epitope, the standard insert:vector ratio of 3:1 was increased to approximately 5:1.

3.2.3.2. pMOS Blue Cloning.

The TA method cloning using the pMOS Blue cloning kit was carried out according to instructions provided by the manufacturer, involving ligation and transformation steps. Competent MOSBlue cells provided by the manufacturer were used, as well as *E. coli* XL1Blue cells, which were made competent according to the CaCl₂ method described in section 2.2.3.4. Blue/white selection on ampicillin (100µg/ml) and tetracycline hydrochloride (12.5µg/ml) plates, supplemented with 10µl 2% IPTG and 50µl 2% X-gal, was used to distinguish recombinants. Recombinants were selected by methods described in chapter 2.

3.2.3.3. Isolation of VP2 Epitope by β -Agarase Digestion of Agarose.

The digestion products containing the VP2 epitope were separated by electrophoresis on a 1% Low Melting Point (LMP) agarose gel at a low voltage of 65V to prevent melting of the gel. Also, a short time of 15 minutes was used to run the small 80 base pair fragment a short distance so that it could be easily viewed for excision. The DNA was excised from the gel and agarose was digested by β -agarase according to the manufacturer's instructions (FMC BioProducts): the gel slice was equilibrated for 1 hour with 10X the volume of 1X β -agarase buffer (supplied by the manufacturer at a 50X concentration). The gel was melted at 70°C then cooled to 45°C for digestion by 1U β -

agarase. The solution was centrifuged in a microfuge for 5 minutes to remove any undigested agarose, which collected in the pellet. The DNA was precipitated by the addition of 0.5 X the existing volume of 7.5M AmAc and 2.5 X the volume of 100% ethanol with incubation at -20°C overnight. The DNA was pelleted by centrifugation and washed with 70% ethanol before resuspending in 15µl ddH₂O. Electrophoresis of a small sample on a 2% agarose gel was used to confirm the presence of DNA of the appropriate size.

3.2.4. Immune Response Investigations.

3.2.4.1. Preparation of Protein for Inoculation into Mice.

Protein was expressed on large-scale (chapter 2, 2.2.7.4) and processed by sucrose gradient centrifugation at 40000rpm for 20 hours (chapter 2, section 2.2.11). Gradients were performed in triplicate to ensure sufficient quantities of protein could be recovered. Fractions of all three gradients containing the trimer form of VP7mt144-VP2 were pooled. The total volume was diluted to 5ml with 100mM Tris-HCl pH=8, 50mM NaCl. The protein was collected by centrifugation in the SW50.1 rotor at 20 000rpm for 15hrs. The pelleted protein was resuspended in 100µl of sterile 1XPBS (pH=7.4). A 10µl sample of the collected protein was analysed by SDS-PAGE and the concentration was estimated by comparison to the size marker of known concentration. The concentration of sample was then adjusted to 400ng/µl with sterile 1XPBS.

3.2.4.2. Inoculation of Mice with VP7mt144-VP2.

Five Balb/c mice were inoculated with prepared samples of VP7mt144-VP2 trimers. At each time, each mouse was inoculated with 10µg of prepared protein, equivalent to a volume of 25µl. Three inoculations were given two weeks apart. At day 0, 25µl of protein (10µg) was inoculated with an equal volume of Freund's Complete Adjuvant (FCA). At day 14, 25µl of protein was inoculated with an equal volume of Freund's Incomplete Adjuvant (FIA). At day 28, 25µl of protein sample was again inoculated with an equal volume of Freund's Incomplete Adjuvant (FIA). Before each inoculation, fresh protein samples were prepared. Inoculations were administered to the mice subcutaneously.

Mice were bled on day 42 by cardiac puncture, recovering approximately 1ml from each mouse. Antiserum was prepared by low speed centrifugation (3000rpm) of the blood collected from each mouse. This separated red blood cells as a pellet from the plasma. The plasma was collected and aliquoted into smaller quantities of 200µl and stored at -70°C.

3.2.4.3. Western Blot Analysis of Immune Response.

3.2.4.3.1. Sample Preparation.

Samples of AHSV serotype 9-infected BHK (baby hamster kidney) cells were provided by Dr M. van Niekerk. Also provided were mock-infected BHK cells. Cells were provided on monolayers in 75cm³ tissue culture flasks and were harvested in the following ways. AHSV-9 infected cells were easily dislodged from the flask surface by gentle agitation. Uninfected cells were removed from the flask by trypsin digestion. The monolayer was rinsed with 1XPBS solution. 10ml of trypsin/versene solution (Highveld Biological) at 37°C was added to the monolayer and left at room temperature for 1 minute. The trypsin solution was discarded and the monolayer was incubated for a further 3 minutes at 37°C. Cells were then dislodged by gentle agitation in 5ml 1XPBS. Both infected and uninfected cells were collected by low speed centrifugation at 3000 rpm for 5 minutes. Cells were washed twice in 1XPBS and finally resuspended in a total volume of 200µl 1XPBS. Samples were stored at -20°C.

3.2.4.3.2. Western Blot.

Samples were prepared for and separated on a 12% polyacrylamide minigel (section 2.2.9.) run at 120V for 2 hours. Samples were blotted onto a nitrocellulose membrane (Hybond C) using the Biorad E.C. 140 Mini Blot Module in a glycine, Tris-based buffer (14.4g glycine; 3.03g Tris in 1 litre; pH=8.3). Blotting was run at 0.12Amp for 60 to 90 minutes. The membrane was rinsed in 1XPBS pH=7.4 for 5 minutes, before blocking with blocking solution (1XPBS; 1% milk powder) for 30 minutes. Primary antibody was diluted in blocking solution to a dilution of 1/100. The membrane was incubated overnight in primary antibody solution, at room temperature and with agitation. The membrane was then rinsed three times for 5 minutes in washing solution (1XPBS, 0.05% Tween 20) before incubation for 1 hour in secondary antibody. The secondary antibody, peroxidase-conjugated protein A (ICN), was diluted to a 1 in 1000 dilution with blocking solution. The membrane was then rinsed 3 times for 5 minutes in washing solution, followed by a single wash with 1XPBS for 5 minutes. The membrane was then incubated at room temperature in substrate for 30 minutes to 1 hour. The substrate for development was prepared in the following way: 60ng 4-chloro-1-naphthol was dissolved in 20ml ice-cold methanol, and 60µl hydrogen peroxide was added to 100ml 1XPBS. The two solutions were mixed just prior to use. The detection reaction was stopped by rinsing the membrane in dH₂O.

3.3. RESULTS.

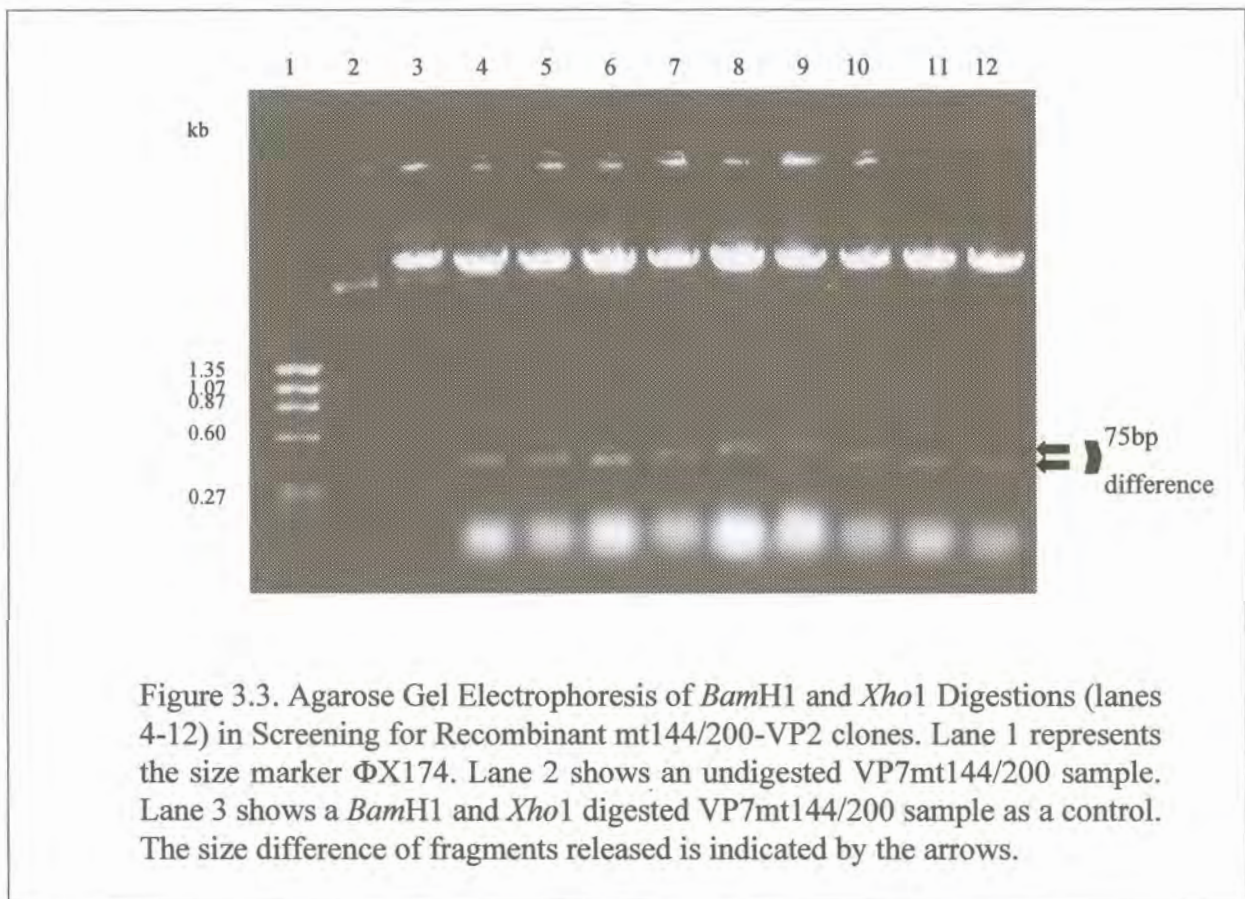
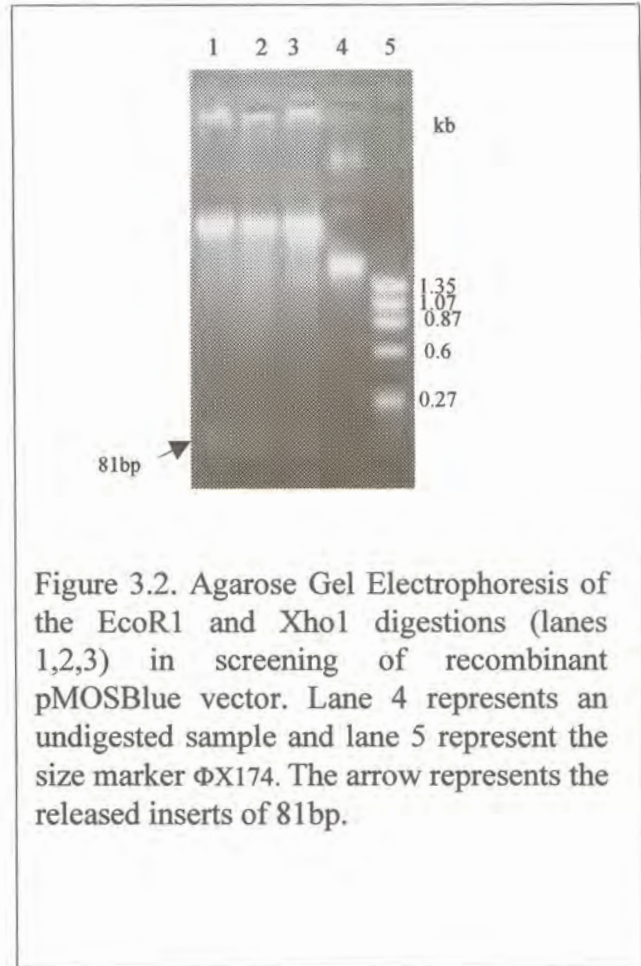
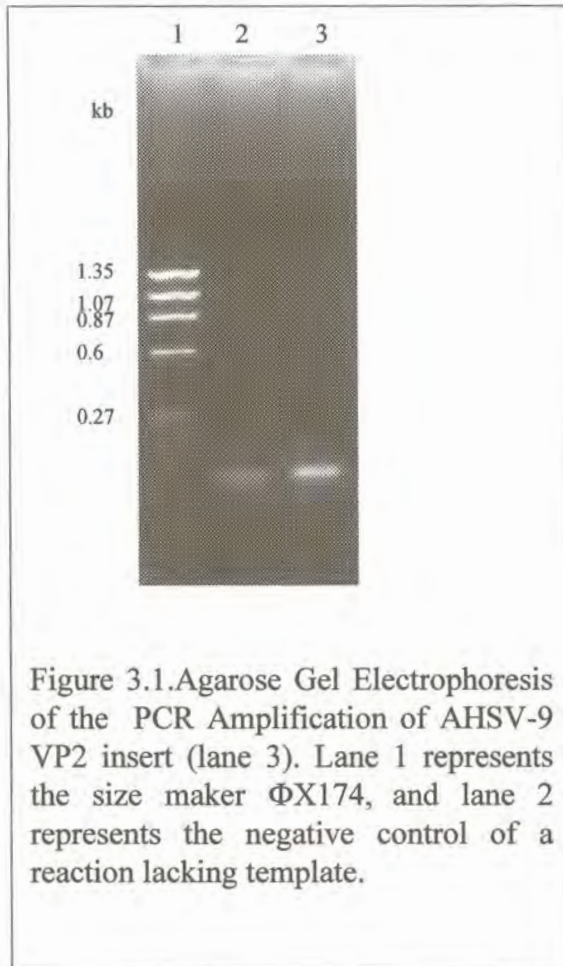
3.3.1. Construction of VP7mt144-VP2.

A sequence of 25 amino acids containing a suspected neutralising epitope of AHSV-9 VP2 was inserted into the cloning site created at position 144/145 of VP7mt144. PCR, using primers with restriction enzyme site overhangs, was used to amplify the segment of nucleotides 1141- 1215 (amino acids 377-401) of the cDNA clone of VP2 gene of AHSV-9. The forward primer was designed with an *EcoR1* overhang and the reverse with a *Xho1* overhang such that the amplified VP2 gene segment could be inserted between restriction enzyme sites *EcoR1* and *Xho1* at the 144/145 cloning site (section 3.2.2.; table 3.1.). The amplified DNA segment obtained was of the expected size of 81 base pairs. Figure 3.1 shows the PCR amplification of the AHSV-9 VP2 insert. The negative control shows a “fuzzy”, indistinct band of primer residues. The lane containing the amplified fragment shows a more intense band larger than the primer residues and which corresponds in size to the amplified segment.

Due to the small size of the amplified VP2 segment, and the corresponding difficulty in manipulation of this fragment, it was decided to first clone this segment into the pMOSBlue vector. This vector is specifically designed for the direct ligation of PCR-amplified products. Thus various problems associated with direct cloning of the segment into pFastBac-VP7mt144 could be avoided. These problems include the difficulty of digestion by restriction enzymes close to the ends of the PCR-amplified product, as well as the difficulty in purification of such a small fragment of DNA. The PCR-amplified VP2 segment was therefore directly ligated into pMOSBlue vector, after its retrieval by ethanol precipitation. *EcoR1* and *Xho1* digestion released a fragment corresponding to the expected size of 81 nucleotides, as can be seen in figure 3.2. The band appeared faint and fuzzy due to the particularly small size of the DNA fragment. Without the control of undigested sample, this band could be confused with contaminating RNA by virtue of its location and appearance in the gel. However, the uncut sample clearly indicated the absence of RNA and thus it could confidently be concluded to be the required fragment. This fragment then contained the appropriate sticky ends for cloning into VP7mt144 and VP7mt144/200.

Because of the small size of the fragment, the simple, commonly used methods for purification of DNA from a gel, including GENECLAN™ and the standard High Pure columns (Roche Diagnostics), could not be used to isolate and purify the fragment. The band of DNA was therefore excised from the gel and β -agarase (FMC Bioproducts) was used to dissolve the agarose of the gel (described in section 3.2.3.3). The fragment was then recovered by precipitation and cloned between the *EcoR1* and *Xho1* sites of VP7mt144 and VP7mt144/200. In screening, no recombinant VP7mt144-VP2 colonies were recovered on the first attempt. However, a double digestion by *BamH1* and *Xho1* showed a difference between the non-recombinant VP7mt144/200 and the recombinant VP7mt144/200-VP2. Non-recombinant VP7mt144/200 released a fragment of 375bp whereas the recombinant VP7mt144/200-VP2 released a fragment of 450bp. This difference of 75 base pairs could be distinguished on a 1% agarose gel, as shown in figure 3.3. Appropriate colonies were selected for further screening. A *Xho1* and *EcoR1* two-step double digest (not shown) confirmed the presence of the insert in selected colonies.

Due to the difficulties associated with the manipulation of the small fragment, it was decided not to repeat the failed attempt at the VP7mt144-VP2 cloning in the same way. The two modified genes, VP7mt144 and VP7mt144/200 are identical except for the presence of the cloning site at position 200/201 of VP7mt144/200. Therefore a recombinant VP7mt144-VP2 could be obtained by simply replacing a segment of VP7mt144, containing the cloning site but lacking the VP2 insert, with the corresponding segment of VP7mt144/200-VP2 containing the insert. This was achieved by *BamH1* and *Xho1* digestion of both VP7mt144 and VP7mt144/200-VP2. A two-step double digest was performed. Digestion was first carried out by *Xho1*, followed by *BamH1* with adjustment of the reaction volume and appropriate buffer. The smaller 5' segment released from VP7mt144/200-VP2 was cloned into the larger pFastBacVP7mt144 vector. Recombinant colonies were screened by the same *BamH1/Xho1* digestions used in their construction. Selected colonies of VP7mt144-VP2 were then screened for the correct insert by automated DNA sequencing.



3.3.2. Sequence Verification of VP7mt144-VP2.

Automated DNA sequencing of the selected clones confirmed the insertion of the 75 nucleotide segment of VP2 at site 144/145 of VP7mt144. PCR did not introduce any mutations in the VP2 sequence. The insertion also did not cause any shift in the reading frame and thus will be translated as a 25 amino acid insert of the VP7mt144 fusion protein. The sequence alignment of VP7mt144-VP2 to VP7mt144 is shown in figure 3.4. The insertion of the VP2 sequence is highlighted in red.

3.3.3. Physicochemical Properties and Structural Modeling of VP7mt144-VP2.

The effect of the insertion on the hydrophilicity profile of VP7mt144 was investigated (methods described in chapter 2, section 2.2.6). This is shown in figure 3.5. The VP2 insert was specifically chosen for the evidence of its role as a neutralising epitope (Venter *et al.*, 2000; Bentley *et al.*, 2000; Martínez-Torrecedrada *et al.*, 2001). In accordance with this property, it is a particularly hydrophilic sequence (Venter *et al.*, 2000). As can be seen in figure 3.5, the insert created a large hydrophilic area in the protein. With the rest of the protein being largely hydrophobic, the insertion of a relatively large, highly hydrophilic sequence may effect the folding of the protein from its original form. The folding of the protein was investigated by structural modelling, using the complete VP7 sequence of BTV-10 as a template (also refer to section 2.2.6). Figure 3.6. shows the results of the structural modelling. The green area is the bottom domain of α -helices and the blue area is the top domain of the β -sheets. The insert of VP2 sequence is indicated in yellow. It appears to loop out of the surface of the protein and does not appear to interfere with the folding of the protein into the α -helices and β -sheets. Thus, it is expected that the VP2 epitope will appear as a loop on the surface of the protein.

Figure 3.4. CLUSTAL X (1.81) Sequence Alignment of VP7mt144-VP2 to VP7mt144.

```

mt144          GTTTAAATTCGGTTAGGATGGACGCGATAGCAGCAAGAGCCTTGTCCGTTGTACGGGCAT 60
mt144vp2      GTTTAAATTCGGTTAGGATGGACGCGATAGCAGCAAGAGCCTTGTCCGTTGTACGGGCAT
*****

mt144          GTGTCACAGTGACAGATGCGAGAGTTAGTTTGGATCCAGGAGTGATGGAGACGTTAGGGA 120
mt144vp2      GTGTCACAGTGACAGATGCGAGAGTTAGTTTGGATCCAGGAGTGATGGAGACGTTAGGGA
*****

mt144          TTGCAATCAATAGGTATAATGGTTTAAACAAATCATTTCGGTATCGATGAGGCCACAAACCC 180
mt144vp2      TTGCAATCAATAGGTATAATGGTTTAAACAAATCATTTCGGTATCGATGAGGCCACAAACCC
*****

mt144          AAGCAGAACGAAATGAAATGTTTTTATGTGTA CTGATATGGTTTTAGCGGCGCTGAAACG 240
mt144vp2      AAGCAGAACGAAATGAAATGTTTTTATGTGTA CTGATATGGTTTTAGCGGCGCTGAAACG
*****

mt144          TCCAAATGGGAATATTTACCAGATTATGATCAAGCGTTGGCAACTGTGGGAGCTCTCG 300
mt144vp2      TCCAAATGGGAATATTTACCAGATTATGATCAAGCGTTGGCAACTGTGGGAGCTCTCG
*****

mt144          CAACGACTGAAATCCATATAATGTTTCAGGCCATGAATGACATCGTTAGAATAACGGGTC 360
mt144vp2      CAACGACTGAAATCCATATAATGTTTCAGGCCATGAATGACATCGTTAGAATAACGGGTC
*****

mt144          AGATGCAAACATTCGGACCAAGCAAAGTGCAAACGGGGCCTTATGCAGGAGCGGTTGAGG 420
mt144vp2      AGATGCAAACATTCGGACCAAGCAAAGTGCAAACGGGGCCTTATGCAGGAGCGGTTGAGG
*****

mt144          TGCAACAATCTGGCAGATATTACGTACCGCCCGGGGAATTC-----
mt144vp2      TGCAACAATCTGGCAGATATTACGTACCGCCCGGGGAATTCGATCCAAATCATGATACAT 480
*****

mt144          -----CTCG
mt144vp2      GGAAAAACCATGTCAAAGAAATCAGAGAGAGGATGCAGAAAGAACAGAGCGCGAATCTCG 540
*****

mt144          AGCAAGGTCGAACGCGTGGTGGGTACATCAATTCAAATATTCGAGAAGTGTGTATGGATG 600
mt144vp2      AGCAAGGTCGAACGCGTGGTGGGTACATCAATTCAAATATTCGAGAAGTGTGTATGGATG
*****

mt144          CAGGTGCTGCGGGACAGGTCAATGCGCTGCTAGCCCCAAGGAGGGGGGACGCAGTCATGA 660
mt144vp2      CAGGTGCTGCGGGACAGGTCAATGCGCTGCTAGCCCCAAGGAGGGGGGACGCAGTCATGA
*****

mt144          TCTATTTGTTTGGAGACCGTTGCGTATATTTTGTGATCCTCAAGGTGCGTCACTTGAGA 720
mt144vp2      TCTATTTGTTTGGAGACCGTTGCGTATATTTTGTGATCCTCAAGGTGCGTCACTTGAGA
*****

mt144          GCGCTCCAGGAACTTTTGTCACCGTTGATGGAGTAAATGTTGCAGCTGGAGATGTCGTCCG 780
mt144vp2      GCGCTCCAGGAACTTTTGTCACCGTTGATGGAGTAAATGTTGCAGCTGGAGATGTCGTCCG
*****

mt144          CATGGAATACTATTGCACCAGTGAATGTTGGAAATCCTGGGGCACGCAGATCAATTTTAC 840
mt144vp2      CATGGAATACTATTGCACCAGTGAATGTTGGAAATCCTGGGGCACGCAGATCAATTTTAC
*****

```

```

mt144      AGTTTGAAGTGTTATGGTATACGTCCTTGGATAGATCGCTAGACACGGTTCGGGAATTGG
mt144vp2   AGTTTGAAGTGTTATGGTATACGTCCTTGGATAGATCGCTAGACACGGTTCGGGAATTGG 900
*****

mt144      CTCCAACGCTCACAAGATGTTATGCGTATGTCTCTCCCACTTGGCACGCATTACGCGCTG
mt144vp2   CTCCAACGCTCACAAGATGTTATGCGTATGTCTCTCCCACTTGGCACGCATTACGCGCTG 960
*****

mt144      TCATTTTTCAGCAGATGAATATGCAGCCTATTAATCCGCCGATTTTCCACCGACTGAAA
mt144vp2   TCATTTTTCAGCAGATGAATATGCAGCCTATTAATCCGCCGATTTTCCACCGACTGAAA1020
*****

mt144      GGAATGAAATTGTTGCGTATCTATTAGTAGCTTCTTTAGCTGATGTGTATGCGGCTTTGA
mt144vp2   GGAATGAAATTGTTGCGTATCTATTAGTAGCTTCTTTAGCTGATGTGTATGCGGCTTTGA1080
*****

mt144      GACCAGATTTCAGAATGAATGGTGTGTCGCGCCAGTAGGCCAGATTAACAGAGCTCTTG
mt144vp2   GACCAGATTTCAGAATGAATGGTGTGTCGCGCCAGTAGGCCAGATTAACAGAGCTCTTG1140
*****

mt144      TGCTAGCAGCCTACCACTAGTGGCTGCGGTGTTGCACGGTCACCGCTTTCATTAGTGTGCG
mt144vp2   TGCTAGCAGCCTACCACTAGTGGCTGCGGTGTTGCACGGTCACCGCTTTCATTAGTGTGCG1200
*****

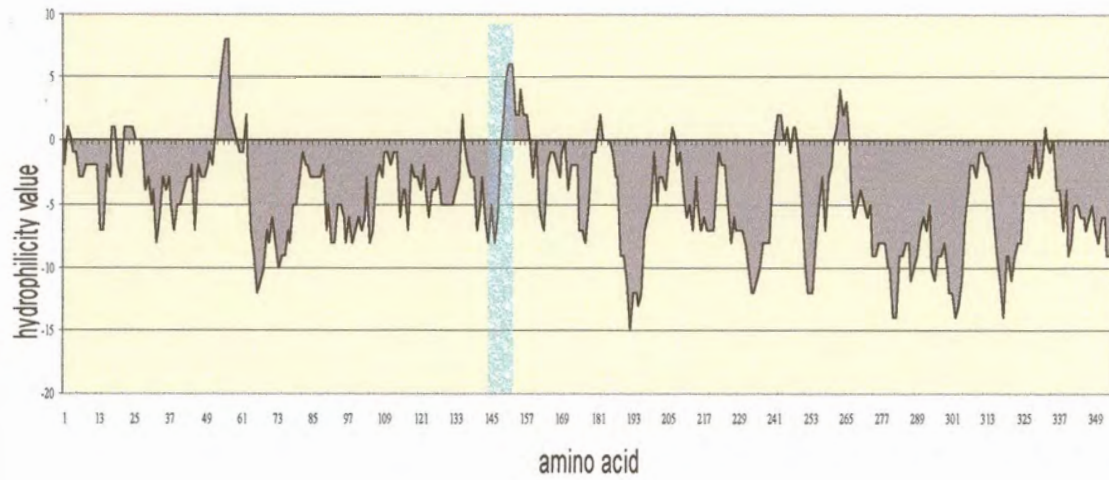
mt144      CGTCGGTTCTTATGCTGATAAAGTACGCATAAGTAATACGTCAATACCGAATACACTTAC
mt144vp2   CGTCGGTTCTTATGCTGATAAAGTACGCATAAGTAATACGTCAATACCGAATACACTTAC1260
*****

mt144      AGA
mt144vp2   AGA 1263
***

```

(a)

VP7mt144 Hydrophilicity Plot



(b)

VP7mt144-VP2 Hydrophilicity Plot

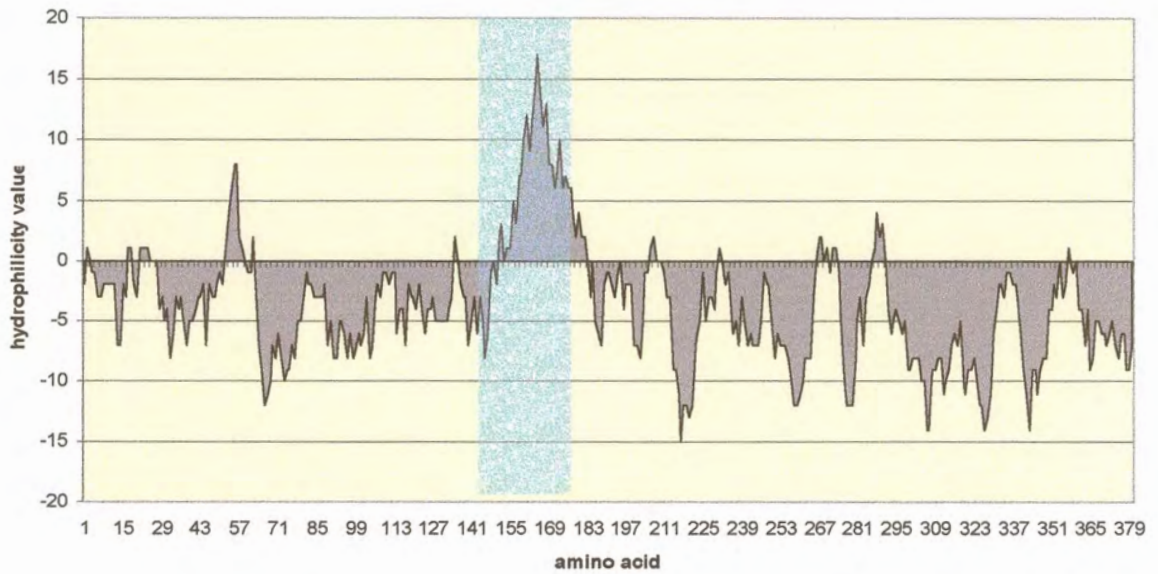


Figure 3.5. Hydrophilicity Plots of VP7mt144 (a) and VP7mt144-VP2 (b) according to the Hopp and Woods Predictive Method (Hopp and Woods, 1981; Hopp and Woods, 1983).

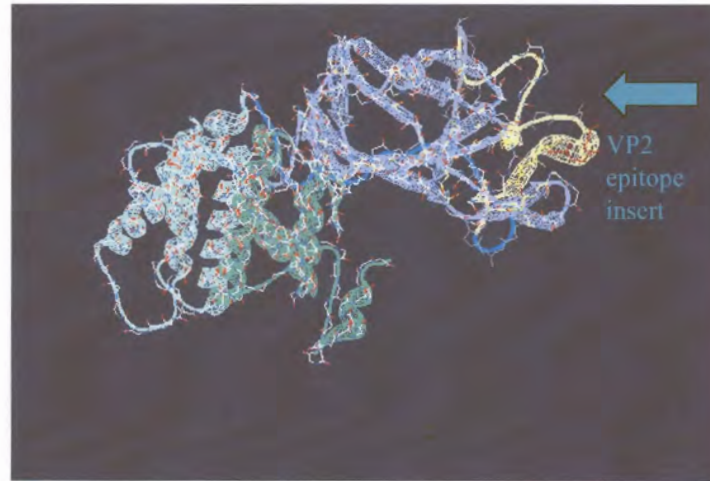


Figure 3.6. Structural Modelling of VP7mt144VP2. The bottom domain of α -helices is indicated in green. The top domain of β -sheets are indicated in blue. The VP2 insert is indicated in yellow.

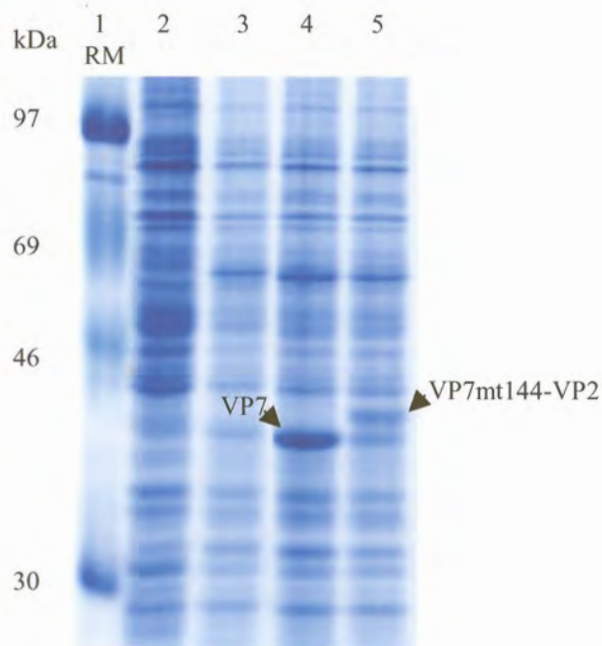


Figure 3.7 SDS-PAGE Analysis of Expression of VP7mt144-VP2. Lane 1 represents the protein size marker, lanes 2 and 3 show mock- and wild-type baculovirus-infected cell extract respectively. Lane 4 shows Bacmt144-infected cell extract. An arrow indicates the position of VP7mt144. Lane 5 shows Bacmt144-VP2-infected cell extract. An arrow indicates the position of VP7mt144-VP2.

3.3.4. Expression of VP7mt144-VP2.

The sequence analysis confirmed that the reading frame of VP7mt144-VP2 is intact and thus translation and expression of a full-length fusion protein is expected. The baculovirus expression system was used to express the modified protein, as described in chapter 2 (section 2.2.7). The recombinant baculovirus containing the modified gene was designated Bacmt144-VP2. Expression of the protein was analysed by SDS-PAGE (described in 2.2.8). The size difference of 25 amino acids in VP7mt144-VP2 compared to VP7mt144 would increase the size of the protein by approximately 3 kDa, which is clearly visible on an SDS-PAGE gel. As can be seen from figure 3.7, there is a significant size increase in VP7mt144-VP2 compared to VP7mt144. The level of expression of the protein is high, although does not appear to be as high as that of VP7mt144.

3.3.5. Light Microscope Observations.

The first indications of any particulate structures formed by the modified proteins can be seen in the recombinant baculovirus-infected cells under the light microscope. Similarly to VP7mt144 (section 2.3.5), cells infected with recombinant Bacmt144-VP2 baculovirus show distinct structures appearing as needle-like shapes in the two-dimensional field of vision of the light microscope. These structures are widespread, with the distribution being similar to that of VP7mt144. Often more than one structure is visible per cell. As for VP7mt144, fewer structures are visible in Bacmt144-VP2-infected cells compared to wild-type VP7-baculovirus infected cells. Light microscope observations are shown in figure 3.9., with photographs being taken at a 63X magnification.

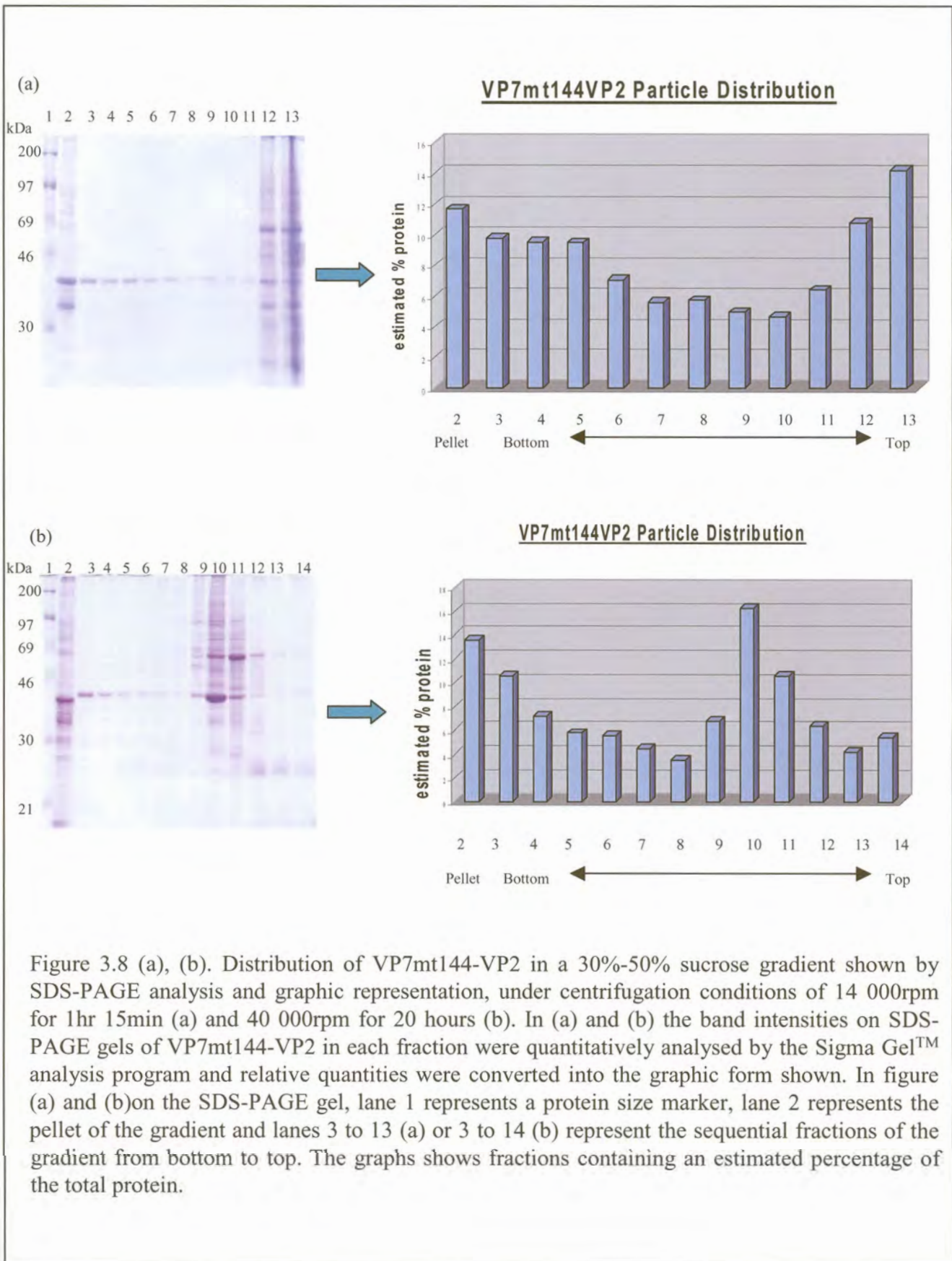
3.3.6. Solubility Studies of VP7mt144-VP2.

It was apparent under the light microscope that some form of particulate structure is still formed by the modified VP7mt144-VP2 proteins. The solubility study of VP7mt144-VP2 by sucrose gradient distribution gives more insight into the effect of the additional 25 amino acids on firstly trimer formation i.e. associations and interactions of individual proteins, and secondly on the particulate structure formation, involving interactions and associations of trimers.

The solubility and the particulate structure of VP7mt144-VP2 were investigated by its distribution in a discontinuous 30-50% sucrose gradient, as described by methods in chapter 2 (section 2.2.11). Figure 3.8. shows the distribution of VP7mt144-VP2 in the 30-50% sucrose gradient after centrifugation at 14000rpm for 1 hour 15 min (a) and increased conditions of 40000rpm for 20 hours (b). Both an SDS-PAGE analysis and a graphic representation of the distribution are shown. Under both centrifugation conditions, the distribution of VP7mt144-VP2 protein forms two peaks, clearly identified in the graphical representation. For the initial centrifugation conditions, at a lower speed and for a shorter time period, the peak occurring at the bottom of the gradient is shallow, with a significant proportion of protein found in the middle fractions. When one compares this to the distribution of VP7mt144 under the same conditions (figure 2.8.(b)), it appears that a slightly more uniform distribution of VP7mt144-VP2 protein occurs in fractions in the middle and towards the bottom of the gradient. This would indicate a greater distribution of varying sizes of particulate structures. The greatest proportion of particulate structures is still found in the pellet. Like VP7mt144, when centrifugation conditions were increased, the peak occurring in the top fractions shifted to lower down in the gradient. Similarly to VP7mt144, VP7mt144-VP2 sediments to a position in the gradient equivalent to proteins larger than itself, indicating that VP7mt144-VP2 occurring in this peak most likely exists in the form of trimers rather than a monomer of the protein.

3.3.7. Scanning Electron Microscopy Studies.

Samples of the VP7mt144-VP2 particulate structures were prepared in the same way as that of VP7mt144 and VP7mt144/200, described in chapter 2 (section 2.2.13). Structures observed under the S. E. M. varied in size and shape. The average length of structures was observed to be approximately 6 μ m. No distinct hexagonal structures characteristic of wild-type VP7 crystals were observed. Structures were distinctly angular but appeared more needle-shaped rather than the characteristic hexagonal-shape of wild-type VP7 crystals. Figure 3.10 shows structures observed under the S. E. M.



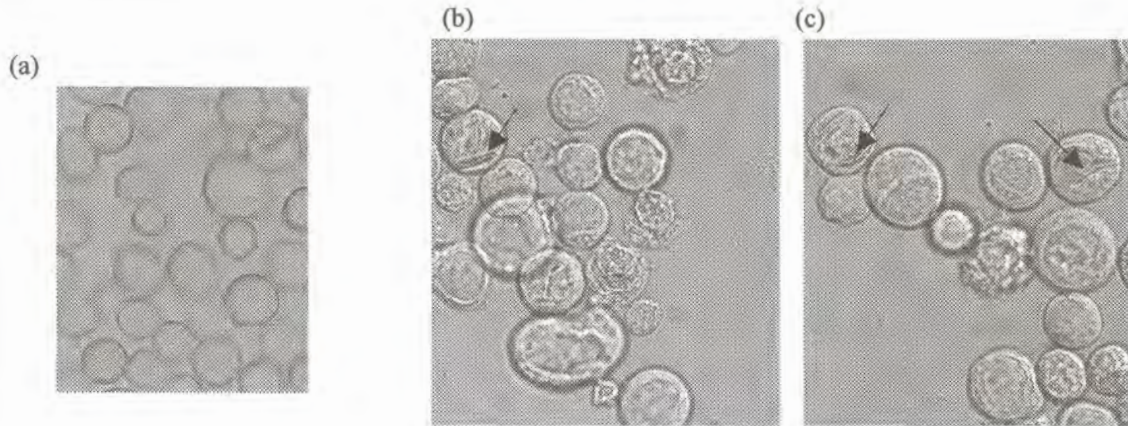


Figure 3.9 Light Microscope Observations of Recombinant VP7mt144VP2 baculovirus infected sf9 cells (b) and (c). The arrows indicate particulate structures visible within the cells, which are not visible in wild-type baculovirus infected cells (a). Photographs were taken at a 63X magnification.

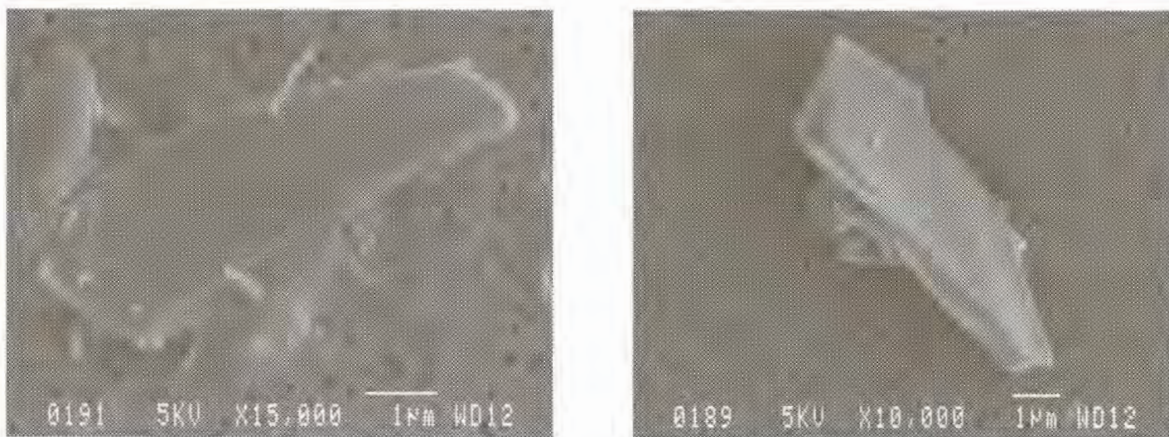


Figure 3.10. Scanning Electron Microscope Observations of VP7mt144VP2 Crystal Structures.

3.3.8. Immune Study of VP7mt144-VP2.

The ability of VP7mt144-VP2 to present the VP2 epitope to the immune system was studied by the ability of antiserum generated against the recombinant protein to detect and recognise native AHSV protein. As discussed previously, the particulate crystal structures as well as the constitutive trimers themselves may be suitable vehicles for the presentation of epitopes. Crystal particles of VP7 containing a different epitope were to be tested for their ability to generate an immune response by another colleague (Meyer, personal communication), and thus it was decided to test the constitutive trimers of VP7mt144-VP2 in this regard. This would provide a broader perspective on the whole in terms of the use of VP7 as an epitope delivery system.

The protein was prepared for inoculation as discussed in section 3.2.4.1. VP7mt144-VP2 was expressed on large-scale and harvested accordingly. Sucrose gradient centrifugation of cell lysate was used to separate trimers from the larger particulate structures of VP7mt144-VP2. Conditions chosen were those of a 30-50% sucrose gradient, spun at 40 000rpm for 20 hours. Fractions of the gradient identified to contain trimers were pooled. This would correspond to fractions 8, 9, and 10 shown in figure 3.8(b). The protein was collected from the sucrose solution by dilution of the sucrose and centrifugation to pellet the protein. The pellet was resuspended in sterile 1XPBS and adjusted to the appropriate concentration for inoculation into mice. This method of preparation of VP7mt144-VP2 produced a heterogenous mix of proteins and included significant proportions of baculovirus as well as sf9 cell proteins. If one looks at figure 3.8(b), one can see that the fractions of the gradient containing the VP7mt144-VP2 trimers also contain significant quantities of other proteins in comparison to other fractions containing the particulate structures of VP7mt144-VP2. This heterogenous mix might be expected to influence the presentation of the VP7mt144-VP2 trimers to the immune system of the mice.

The program for inoculation of mice is described in section 3.2.4.2. Three inoculations of 10µg of protein were given two weeks apart. The protein was prepared fresh each time to ensure minimal breakdown of the trimer structure in the sample. Serum was collected at day 42. The red blood cells were removed by centrifugation and the antiserum was stored at -70°C. The antiserum was tested for its ability to recognise native AHSV-9 proteins. This would give some indication to the antibodies generated against the protein used in

inoculation. With VP7 and VP2 sequences present in VP7mt144-VP2, the antiserum would be expected to recognise native VP7 in a Western blot, with the possibility of also recognising VP2 depending on how successfully the VP2 epitope is presented to the immune system.

AHSV-9- infected BHK cell extract (3.2.4.3.1) was separated on a 12% SDS-PAGE gel. Also included were an uninfected BHK cell extract as a negative control and a purified sample of VP7mt144-VP2 from Bacmt144-VP2-infected sf9 cells as a positive control. A western blot was performed as described in section 3.2.4.3.2. The prepared antiserum from the five mice was pooled and was used as the primary antibody at the higher end of the recommended concentration, at a dilution of 1/100. The result is shown in figure 3.11(a). No bands were visible in either mock-infected or AHSV-9 infected cell extracts. A single band was visible in the baculovirus-expressed VP7mt144-VP2 sample. This band corresponded to the size of VP7mt144-VP2. The response to the positive control indicated then that the antiserum was able to recognise the purified form of VP7mt144-VP2 but not the native AHSV-9 proteins expressed in BHK cells. The expression of these proteins in BHK cells was controlled by SDS-PAGE analysis of cell extract of AHSV-9-infected cells in comparison to that of uninfected BHK cells. A clear difference was visible in protein patterns on an SDS-PAGE gel. For confirmation of expression, a western blot analysis of the two samples was performed in which α -AHSV-6 antiserum was used as the primary antibody. VP7 of AHSV-6 shows cross-reactivity to VP7 of AHSV-9. The expression of AHSV-9 VP7 was confirmed by the appearance of a band corresponding to the expected size of VP7 (results not shown).

It was considered that the band detected by the antiserum might not be representative of VP7mt144-VP2, but rather another protein of similar size expressed in the baculovirus expression system. This would explain the presence of this band in cell extract of baculovirus origin and not the AHSV-9 infected BHK cells. A western blot analysis was thus performed directing the prepared antiserum to Bacmt144-VP2, Bacmt144, wild-type baculovirus and mock-infected sf9 cell extract. The result is shown in figure 3.11(b). Various proteins are detected in the Bacmt144-VP2-infected sample, which are also present in mock- or wild-type baculovirus-infected samples. A very faint band is visible in both Bacmt144-VP2- and Bacmt144-infected samples. It corresponds to the size of proteins VP7mt144-VP2 and the smaller VP7mt144 in the respective samples. Thus the antibodies

generated in the mice only weakly recognised the primary protein intended to be presented to the immune system in mice. The more dominant antibodies in the antiserum recognise wild-type baculovirus and sf9 insect cell proteins. This would affect a positive outcome of a western blot analysis.

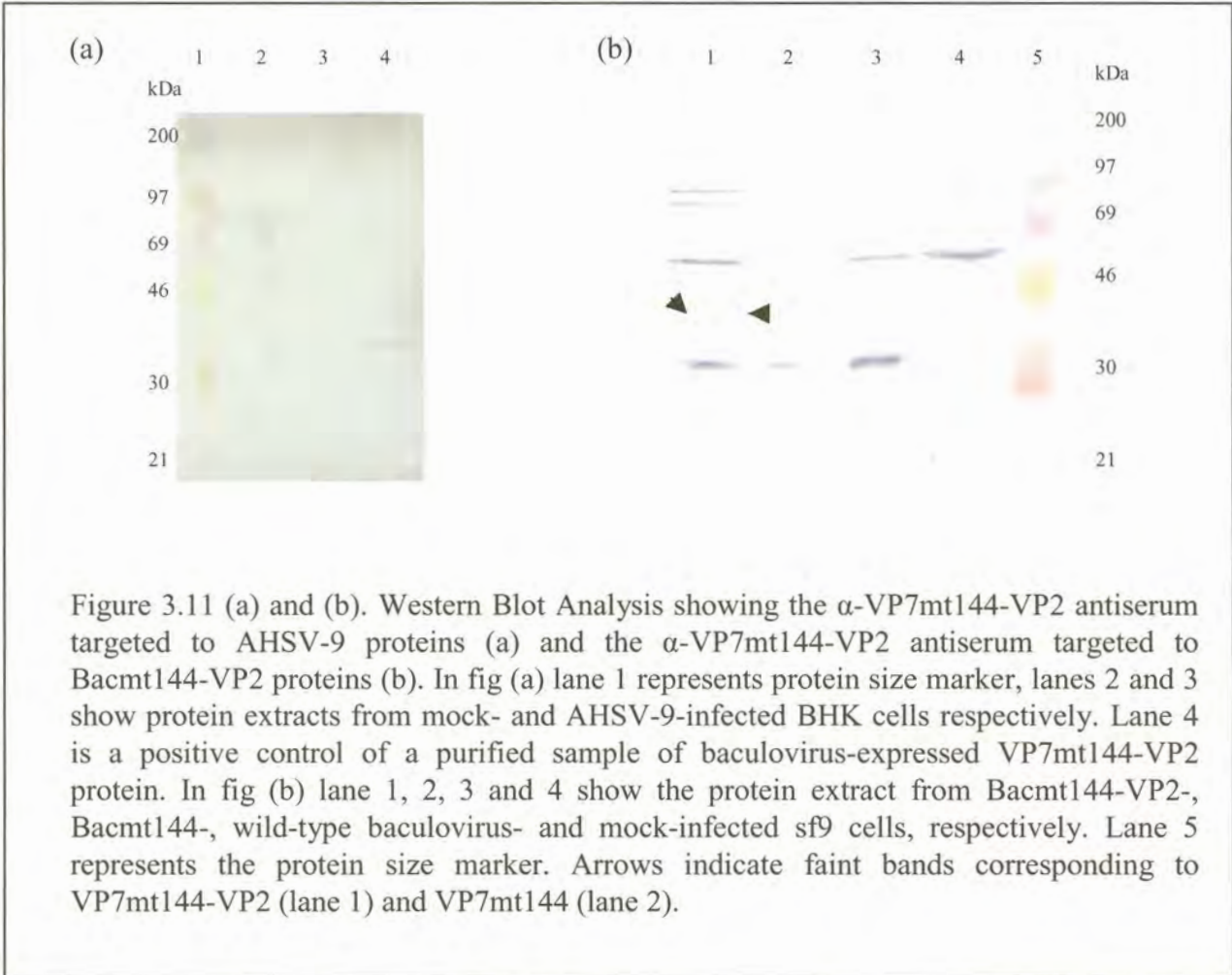
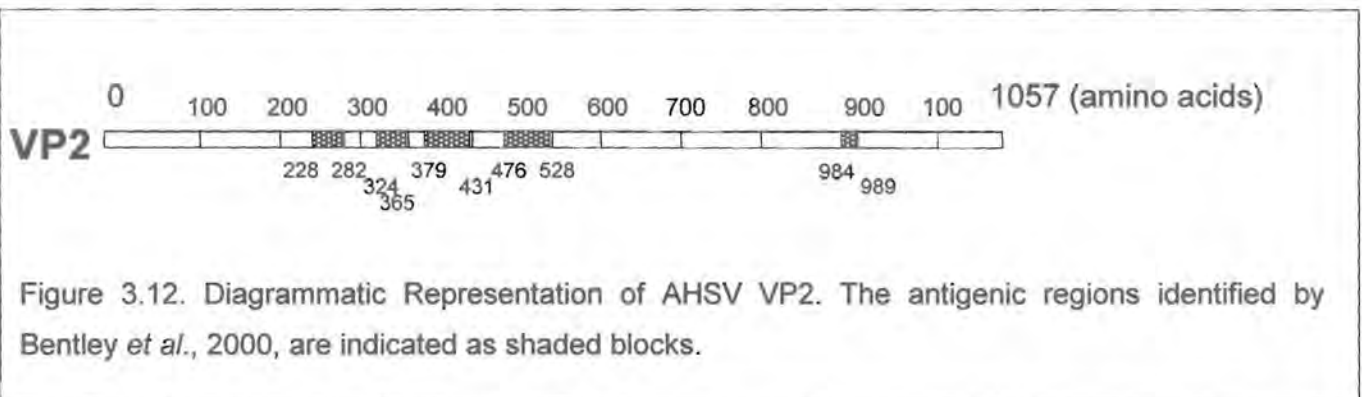


Figure 3.11 (a) and (b). Western Blot Analysis showing the α -VP7mt144-VP2 antiserum targeted to AHSV-9 proteins (a) and the α -VP7mt144-VP2 antiserum targeted to Bacmt144-VP2 proteins (b). In fig (a) lane 1 represents protein size marker, lanes 2 and 3 show protein extracts from mock- and AHSV-9-infected BHK cells respectively. Lane 4 is a positive control of a purified sample of baculovirus-expressed VP7mt144-VP2 protein. In fig (b) lane 1, 2, 3 and 4 show the protein extract from Bacmt144-VP2-, Bacmt144-, wild-type baculovirus- and mock-infected sf9 cells, respectively. Lane 5 represents the protein size marker. Arrows indicate faint bands corresponding to VP7mt144-VP2 (lane 1) and VP7mt144 (lane 2).

3.4. DISCUSSION.

In chapter 2, it was shown that the insertion of 6 amino acids at site 144/145 of VP7 did not abolish the formation of large particulate structures when expressed in insect cells. This supported the requirement for a robust nature of VP7 structures in the display of foreign epitopes. The direction of the investigation as described in this chapter was two-fold. Firstly, the extension of the size of possible inserts at this site, which would similarly not abolish the formation of particulate structures, was investigated. Secondly, the presentation of such an insert to an immune system to generate specific antibodies was investigated. Venter *et al.*, 2000, identified a strong linear epitope between amino acids 369 and 407 of AHSV-9 VP2. Bentley *et al.*, 2000, supported this region as having strong neutralising activity by the identification of residues 379-413 of AHSV-3 VP2 as containing neutralisation epitopes. Figure 3.12. shows antigenic regions of AHSV-3 VP2 identified by Bentley *et al.*, 2000. Furthermore, Martínez-Torrecuadrada *et al.*, 2001, identified a region of amino acids 377-400 of AHSV-4 VP2 which has the capability of inducing neutralising antibodies. A sequence of 25 amino acids from amino acids 377-401 of AHSV-9 VP2 was chosen for insertion into VP7mt144, and VP7mt144-VP2 was created. Similarly to chapter 2, the insertion was firstly investigated in terms of its effect on VP7 solubility and structure.



Structural modelling of VP7mt144-VP2 predicts the large hydrophilic insert of VP2 to occur as a large loop on the surface of the top domain of VP7. It does not appear to interfere greatly with the folding of VP7 and the top and bottom domains are distinctly intact. The structural modelling provides no indication to the effect of the insert on VP7 intermolecular interactions to form trimers and larger particulate structures, nor does it provide any

indication to how the VP2 epitope is presented in such associations. Light microscope observations show the presence of particulate structures of VP7mt144-VP2 in Bacmt144-VP2-infected cells. This indicates that the insert did not abolish the interactions of individual VP7 to form trimers and subsequently associate into larger particulate structures.

Smaller influences affecting the structural features of VP7 were studied by sedimentation analysis. This showed similar results to VP7mt144 in terms of its effect on redistribution of the size and proportion of particulate structures in comparison to VP7. Similarly to VP7mt144, a significant proportion of protein does not associate and accumulate into particulate structures, but rather remains associated in the trimer form. This is shown in figure 3.8 (b), with the strongest band of VP7mt144-VP2 occurring in fraction 9, a position in the gradient representing the sedimentation position of trimers. There is an observed difference in the size distribution of protein that does associate into particulate structures, with a more uniform distribution of particulate sizes occurring for VP7mt144-VP2 (figure 3.8(a)) compared to VP7mt144 (figure 2.8 (b)). The greater proportion of smaller particulate structures of VP7mt144-VP2 compared to VP7mt144 indicates, as described in chapter 2, weaker hydrophobic associations between the constitutive trimers in forming and stabilising larger particulate structures. The insertion of the 25 amino acid sequence therefore does not appear to influence the association of VP7mt144-VP2 into trimers, but does appear to influence the association of trimers into stable larger particulate crystal structures.

Sequences longer than 25 amino acids have been inserted into VP7 with similar conclusions being drawn. A 48 amino acid epitope of Hepatitis B virus (HBV) was incorporated into the amino terminus of BTV VP7. This did not abolish the trimer structure as the chimeric VP7 was incorporated into CLP's when co-expressed with VP3 and wild-type VP7. The insertion did, however, influence the interaction between trimers and VP3 in the core, indicated by the necessity for the presence of wild-type VP7 to stabilise interactions required for core formation (Belyaev and Roy, 1992). Larger inserts of 105 amino acids have been introduced to sites 177 and 200 of AHSV VP7, as reported by Maree (2000). Similarly, insertions did not affect the formation of trimers, as particulate structures were formed. However, trimer-trimer interactions were affected, as the structures were not of the characteristic shape and size of wild-type VP7 particles. A size limitation on inserts that do not disturb the formation of trimers has not been established.

As discussed previously, the observed changes in the size distribution of particulate structures does not detract from the potential of VP7 crystals to be used as an epitope display vehicle. Smaller particulate structures would provide a sufficient surface area for the display of multiple epitopes to the immune system. Larger particulate structures carrying epitopes may not be a viable option. The reduced stability of the larger structures due to weakened hydrophobic interactions between trimers may not permit the maintenance of the larger structure during the various stages of preparation and administration of a vaccine.

The results of the S.E.M. showed the particulate structures formed by VP7mt144-VP2 as not having the distinct hexagonal structure apparent for that of wild-type VP7, as well as VP7mt200 (Maree, 2000). This may be due to breakdown of the hexagonal shape during preparation of the samples for S.E.M. This is a feasible explanation, particularly when the stability of the larger particulate structures of VP7mt144-VP2 is questioned. When BTV VP7 crystals were grown by Basak *et al.*, 1992, different forms of crystal were obtained by trimeric associations. These included the hexagonal rod-shapes, rectangular plate-like shapes and diamond-shaped plates. Thus, it is possible for VP7 to associate into larger particulate structures taking different forms. It may be possible that the more needle-shaped structures observed for VP7mt144-VP2 are not a result of degradation of hexagonal crystals, but rather the primary form taken by the association of trimers of VP7mt144-VP2.

The structural studies of the effect of the 25 amino acid insert on VP7mt144 supported its potential as a scaffold for epitope presentation in terms of the physical structures it forms. The second important aspect for consideration is how inserted epitopes would be presented in these structures. Other particulate structures, such as the hepatitis B core antigen, have been successful in the presentation of epitopes to the immune system, inducing protective immune responses (Yon *et al.*, 1992; Schodel *et al.*, 1994; Milich *et al.*, 1995; Schodel *et al.*, 1996; Fehr *et al.*, 1998; Milich *et al.*, 2001). Whole virus particles have also shown potential as vaccine carrier systems, such as Japanese encephalitis virus (Konishi *et al.*, 1997; Hunt *et al.*, 2001), the murine leukemia virus (Kayman *et al.*, 1999) and the cowpea mosaic virus (Brennan *et al.*, 2001). Little is known of the potential of smaller composite structures such the VP7 trimer for use as an epitope display system.

The trimer structure of the VP7mt144-VP2 construct was specifically chosen to present to the immune system of mice. As discussed previously, in a similar investigation by a

colleague (Meyer, personal communication), particulate crystal structures were chosen as the vehicle for presentation of an epitope. Thus, the choice of trimers sought to provide a broader indication as to the potential of the various possible presentation systems of modified VP7. With indications of a reduced stability of particulate structures of VP7mt144-VP2, the trimers may provide an alternative system for epitope delivery. To investigate this, antibodies were generated against VP7mt144-VP2 trimers. Unfortunately, results were inconclusive. The western blot analysis of the prepared antiserum directed toward Bacmt144-VP2-infected cell extract showed only a faint detection of VP7mt144-VP2. When one considers the high level of expression of VP7mt144-VP2 in recombinant baculovirus-infected cells, the faint detection found in the western blot indicates a very poor immune response in the mice to VP7mt144-VP2. This may be due to the lack of purity of the sample used in inoculations. As described in section 3.3.8., when isolating the trimer form of the protein, a large proportion of the baculovirus and sf9 cell protein is simultaneously recovered. This contaminating protein must influence the effective presentation of the VP7mt144-VP2 protein as a whole to the immune system. The dominant antibodies in the antiserum are directed toward wild-type baculovirus and sf9 cell proteins (shown in figure 3.11.(b)). The fact that antiserum from five mice was pooled may also account to some extent for the poor detection of protein on the western blot. The variable immune responses from the five mice may have diluted α -VP7mt144-VP2 antibodies from better immune responses when the antiserum was pooled.

Another explanation for the weak immune response to VP7mt144-VP2 may be the form of the protein used in inoculation i.e. the trimer. The trimer may be a less effective form for exposure of the protein to the immune system, in comparison perhaps to larger crystal structures. Wade-Evans *et al.*, 1998, suggested that the conformation and assembly of VP7 into crystals was an important factor in the mechanism of the protection induced in mice, protecting against a heterologous serotype challenge. Results of a similar investigation, using modified VP7 crystals as the vehicle to present epitopes to the immune system (Meyer, personal communication), showed the antiserum to strongly detect VP7 constructs. Also, antiserum generated against VP7-NS3 crystals in rabbits was able to detect VP7 epitopes by western blot analysis (Meiring, 2001). Thus, the trimer structure may have been a significant factor in the weak response shown by the antiserum to VP7mt144-VP2.

Due to the poor immune response, the conditions used to test the ability of the antiserum to detect native AHSV-9 proteins produced by BHK cell infection did not produce a conclusive result. It cannot be deduced that the antiserum does not recognise VP7 or VP2 produced by AHSV-9 infection. The western blot analysis used was not of sufficient sensitivity to show informative, conclusive results. Another shortcoming of the western blot, which may be considered, is that it inherently involves a denaturing process. The conformation of the AHSV VP7 or VP2 protein is not preserved and thus antibodies would be required to recognise denatured epitopes in the SDS-PAGE gel. This may have been a factor in the negative result observed, although this has not played a role in the detection of α -VP7 antibody in previous experiments (Meyer, personal communication; Meiring, 2001).

More sensitive methods for the investigation of the antiserum would be required to determine if the VP2 epitope was efficiently presented in such a way to generate antibodies to the VP2 insert. Two methods with a greater sensitivity used in antibody detection are the ELISA and the virus neutralisation assay. In many cases the ELISA has been shown to be more sensitive and less cumbersome than a virus neutralisation assay which uses whole virus particles to detect the presence of neutralising antibodies (Paweska *et al.*, 1997; Wilson and Morgan, 1998; Pratelli *et al.*, 2002). However, in some cases ELISA does not detect antibodies in antiserum that tested positive by a virus neutralisation assay (Dixon and De Groot, 1992). This may be due to the fact that antibodies against different viral epitopes will react in the two different methods. With this in mind, and also considering the problem of insolubility of baculovirus-expressed VP2 (Du Plessis *et al.*, 1998) that would affect its preparation for use in an ELISA, the next approach for testing the neutralising immune response generated by the VP2 epitope would be the virus neutralisation assay. This is a more conclusive approach as it tests the ability of antiserum to recognise the native virus and would ultimately test the success of the trimeric construct in generating neutralising antibodies. The virus neutralisation assay will thus be a focus of future investigations.

CHAPTER 4

CONCLUDING REMARKS

VP7 particulate structures have shown potential as a vaccine delivery system. They are easily synthesised in large quantities by expression in recombinant baculovirus-infected cells (Chuma *et al.*, 1992; Maree *et al.*, 1998a; Maree *et al.*, 1998b). The crystal structure has been shown to be robust, with the insertion of foreign sequences at sites 177 and 200 not affecting the formation of crystals (Maree, 2000; Meiring, 2001). Furthermore, VP7 crystals have shown an inherent ability to generate a protective immune response in mice (Wade-Evans *et al.*, 1997; Wade-Evans *et al.*, 1998). These findings justified further investigation into the capacity of VP7 to display foreign peptides on its surface. To expand the range of sites available for the insertion of peptides from sites 177 and 200 (Maree, 2000), a cloning site between amino acid positions 144 and 145 was created. This was investigated in terms of its potential as a site for epitope display.

In summary of the findings of this study, the creation of a cloning site and resulting introduction of six amino acids at site 144/145 of VP7 did not abolish either the formation of crystal particulate structures or the trimer unit. The modification did affect the solubility of the protein. A relatively small increase in trimers, in proportion to the larger particulate structures, was noted. The change in solubility saw a more pronounced increase in proportion of smaller particulate structures in comparison to the relatively larger structures of wild-type VP7. The insertion of a larger sequence of 25 amino acids at this site similarly did not abolish the formation of crystal particulate structures or trimer associations. The observation of a wider distribution of smaller particulate structures of VP7mt144-VP2 presents indications that the insert may affect the stability of interactions in the formation of larger particulate structures. This may be a factor for consideration in the utility of the large crystal structure of VP7 as an antigen delivery system. In terms of addressing the size limits of epitopes able to be accommodated in VP7, the 25 amino acid insert does not significantly affect the structural features of VP7 to reject its potential function as an epitope delivery system.

The efficiency of the presentation of the chosen neutralising epitope of VP2 to the immune system at site 144/145 could not be determined in this study. Various factors may have influenced this outcome. The poor nature of the immune response to VP7mt144-VP2 as a whole, generating relatively low proportions of anti-VP7mt144-VP2 specific antibodies in the antiserum, was a strong contributing factor. This may be due to the inherent inefficiency of the individual trimer units of the protein to generate an immune response in comparison to the larger particulate structures. Also, the presence of relatively large proportions of contaminating baculovirus and sf9 cellular protein may have strongly influenced the effective presentation of VP7mt144-VP2 to the immune system. A second consideration regarding the inconclusive result is the analysis used for the detection of antibodies in the antiserum. The nature of the western blot method uses denatured protein for the capture of antibody in the antiserum. Although the VP2 insert was identified as a linear epitope (Venter *et al.*, 2000, Bentley *et al.*, 2000; Martinez-Torrecuadrada *et al.*, 2001), and thus its recognition should not be affected by the denaturation of the protein, recognition of VP7 may have been affected by its denaturation. A more sensitive and more accurate approach would be required to test the presence of neutralising antibodies in the antiserum. A virus neutralisation assay is a more conclusive approach as it tests the ability of antiserum to recognise the native virus, and would ultimately test the success of the trimeric construct in generating neutralising antibodies against the VP2 epitope. A positive result would indicate the efficient exposure of the VP2 epitope on the surface of VP7mt144-VP2. This is an essential criterion if site 144/145 is to be used as a site for the display of epitopes in the VP7 particulate structure vaccine system. Future study should be targeted at this aim.

Other future investigations should be directed down three main avenues:

- The flexibility of VP7 in accommodation of different size epitopes should be investigated. A size limit of epitopes, larger than 25 amino acids, should be established. Also the minimum size of epitopes for efficient recognition by the immune system should be established. This will depend on how well various sites present the epitopes to the immune system.
- The varying capabilities of the different cloning sites in modified VP7 in terms of accommodation and display of epitopes should be investigated. It would be expected that different sites would not have the same limitations in terms of size of inserts. The efficiency of the display of epitopes within the composite structures of VP7 would vary at different sites.

- Another relevant area of investigation would be to consider the efficiency in the generation of a suitable protective immune response by trimer units in comparison to the larger particulate crystal structures.

Further investigation in these areas will provide a strong foundation for the development of the potential of the VP7 vaccine delivery system.

PAPERS AND CONGRESS CONTRIBUTIONS

Publications in Journals.

Maree, F. F.; Meiring, T.; Riley, J. Meyer, Q. C. and Huisman, H. Effects of Site-Directed Insertion Mutagenesis on the Crystal Formation, Solubility and CLP Formation of African Horsesickness Virus VP7. (*In Preparation*).

International Congress Participation.

Posters.

Meyer, Q. C.; van Rensburg, R.; Riley, J. and Huisman, H. 2001. The Effect of a Variety of Small Amino Acid Insertions in the Top Domain of African Horsesickness Virus Core Protein VP7 on Crystal Formation, and Solubility. *XVII Biennial Conference on Phage/Virus Assembly*. Espoo, Finland. June 30- July 5, 2001.

Maree, F. F.; Riley, J.; Meyer, Q. C. and Huisman, H. 2000. Effects of Site-Directed Insertion Mutagenesis on the Crystal Formation, Solubility and CLP Formation of African Horsesickness Virus VP7. *7th Conference on Double Stranded RNA Viruses*. Aruba, December 2-7, 2000.

Local Congress Participation.

Posters.

Riley, J. Maree, F. F. and Huisman, H. 2000. The Construction of Two Mutant AHSV-9 VP7 Clones and Their Effect on Crystal Structure Formation. *Seventeenth Congress of the South African Genetics Society*. Pretoria, South Africa. June 2000.

REFERENCES

- Adler, S. Reay, P.; Roy, P. and Klenk, H. D. (1998). Induction of T Cell Response by Bluetongue Virus Core-like Particles Expressing a T Cell Epitope of the M1 Protein of Influenza A Virus. *Medical and Microbiological Immunology* **187**: 91-96.
- Alexander, K. A.; Kat, P. W.; House, J.; House, C.; O'Brien, S. J.; Laurenson, M. K.; McNutt, J. W. and Osburn, B. I. (1995). African Horsesickness and African Carnivores. *Veterinary Microbiology* **47(1-2)**: 133-140.
- Attoui, H.; Stirling, J. M.; Munderloh, U. G.; Billoir, F.; Brookes, S. M.; Burroughs, J. N.; de Micco, P.; Mertens, P. P. and de Lamballerie, X. (2001). Complete Sequence Characterisation of the genome of the St. Croix River virus, a New Orbivirus Isolated from the Cells of *Ixodes scapularis*. *Journal of General Virology* **82(4)**: 795-804.
- Basak, A. K.; Stuart, D. I. And Roy, P. (1992). Preliminary Crystallographic Study of the Bluetongue Virus Capsid Protein, VP7. *Journal of Molecular Biology* **228**: 687-689.
- Basak, A. K.; Gouet, P.; Grimes, J.; Roy, P. and Stuart, D. (1996). Crystal Structure of the Top Domain of African Horse Sickness Virus VP7: Comparisons with Bluetongue Virus VP7. *Journal of Virology* **70 (6)**: 3797-3806.
- Basak, A. K.; Grimes, J. M.; Gouet, P.; Roy, P. and Stuart, D. (1997). Structures of Orbivirus VP7: Implications for the Role of This Protein in the Viral Lifecycle. *Structure* **5(7)**: 871-883.
- Belyaev, A. S. and Roy, P. (1992). Presentation of Hepatitis B Virus PreS₂ Epitope on Bluetongue Virus Core-Like Particles. *Virology* **190**: 840-844.
- Bentley, L.; Fehrsen, J.; Jordaan, F.; Huismans, H. and Du Plessis, D. H. (2000). Identification of Antigenic Regions on VP2 of African Horsesickness Virus Serotype 3 by Using Phage-Displayed Epitope Libraries. *Journal of General Virology* **81**: 993-1000.
- Birnboim, H. C. and Doly, J. (1979). A Rapid Alkaline Extraction Procedure for Screening Recombinant Plasmid DNA. *Nucleic Acid Research* **7(6)**: 1513-1523.
- Borden, E. C.; Shope, R. E. and Murphy, F. A. (1971). Physicochemical and Morphological Relationships of Some of the Arthropod-Borne Viruses to Bluetongue Virus- a New Taxonomic Group. Physicochemical and Serological Studies. *Journal of General Virology* **13**:261-271.
- Braverman, Y. and Chizov-Ginsburg. (1996). Role of Dogs (*Canis domesticus*) as hosts for African Horsesickness Virus. *Veterinary Microbiology* **51**: 19-25.
- Bremer, C. W. (1976). A Gel Electrophoretic Study of the Protein and Nucleic Acid Components of African Horsesickness Virus. *Onderstepoort Journal of Veterinary Research* **43**: 193-200.

- Bremer, C. W.; Huismans, H. and Van Dijk, A. A. (1990). Characterization and Cloning of African Horsesickness Virus Genome. *Journal of General Virology* **71**: 793-799.
- Bremer, C. W.; Du Plessis, D. H. and Van Dijk, A. A. (1994). Baculovirus Expression of Non-Structural Protein NS2 and Core Protein VP7 of African Horsesickness Virus Serotype 3 and their Use as Antigens in an Indirect ELISA. *Journal of Virological Methods* **48**: 245-256.
- Brennan, F. R.; Jones, T. D.; *et al.* (2001). Cowpea Mosaic Virus as a Vaccine Carrier of Heterologous Antigens. *Molecular Biotechnology* **17(1)**: 15-26.
- Burrage, T. G.; Trevejo, R.; Stone-Marschat, M. and Laegried, W. W. (1993). Neutralizing Epitopes of African Horsesickness Virus Serotype 4 are Located on VP2. *Virology* **196**: 799-803.
- Burrage, T. G. and Laegried, W. W. (1994). African Horsesickness: Pathogenesis and Immunity. *Comparative Immunology, Microbiology and Infectious Diseases*. **17 (3/4)**: 275-285.
- Burroughs, J. N.; O'Hara, R. S.; Smale, C. J.; Hamblin, C.; Walton, A.; Armstrong, R. and Mertens, P. P. C. (1994). Purification and Properties of Virus Particles, Infectious Subviral Particles, Cores and VP7 Crystals of African Horsesickness Virus Serotype 9. *Journal of General Virology* **75**: 1849-1857.
- Calisher, R. H. and Mertens, P. P. C. (1998). Taxonomy of African Horsesickness Virus. In: Mellor, P. S.; Baylis, H.; Hamblin, C.; Calisher, C. M.; Mertens, P. P. C. (eds). African Horsesickness Virus. *Archives of Virology Supplement* **14**: 3-11.
- Chuma, T.; Le Blois, H.; Sánchez-Vizcaíno, J. M.; Diaz-Laviada, M. and Roy, P. (1992). Expression of the Major Core Antigen VP7 of African Horsesickness Virus by a Recombinant Baculovirus and its Use as a Group-Specific Diagnostic Reagent. *Journal of General Virology* **73**: 925-931.
- Chung, T. and Miller, R. H. (1988). A Rapid and Convenient Method for the Preparation and Storage of Competent Cells. *Nucleic Acid Research* **16**: 3580.
- Cloete, M.; Du Plessis, D. H.; Van Dijk, A. A.; Huismans, H. and Viljoen, G. J. (1994). Vaccinia Virus Expression of the VP7 Protein of South African Bluetongue Virus Serotype 4 and Its Use as an Antigen in Capture ELISA. *Archives of Virology* **135**: 405-418.
- Cowley, J. A. and Gorman, B. M. (1987). Genetic Reassortment for the Identification of the Genome Segment Coding for the Bluetongue Virus Hemagglutinin. *Journal of Virology* **61**: 2304-2306.
- Cowley, J. A. and Gorman, B. M. (1989). Cross-Neutralisation of Genetic Reassortants of Bluetongue Virus Serotype 20 and 21. *Veterinary Microbiology* **19**: 37-51.
- De Maula, C. D.; Bonneau, K. R. and MacLachlan, N. J. (2000). Changes in the Outer Capsid Proteins of Bluetongue Virus Serotype Ten that Abrogate Neutralization by Monoclonal Antibodies. *Virus Research* **67(1)**: 59-66.

- Dixon, P. F. and De Groot, J. (1992). Detection of Rainbow Trout Antibodies to Infectious Pancreatic Necrosis Virus by an Immunoassay. *Diseases of Aquatic Organisms* **26(2)**: 125-132.
- Du Plessis, M.; Cloete, M.; Aitchison, H. and Van Dijk, A. A. (1998). Protein Aggregation Complicates the Development of Baculovirus-Expressed African Horsesickness Virus Serotype 5 VP2 Subunit Vaccines. *Onderstepoort Journal of Veterinary Research* **65**: 321-329.
- Eaton, B. T. and Hyatt, A. D. (1989). Association of Bluetongue Virus with the Cytoskeleton. *Subcellular Biochemistry* **15**:229-269.
- Eaton, B. T.; Gould, A. R.; Hyale, A. D.; Coupar, B. E. H.; Martyn, J. C. and White, J. R. (1991). A Bluetongue Serogroup-Reactive Epitope in the Amino Terminal Half of the Major Core Protein VP7 is Accessible on the Surface of Bluetongue Virus Particles. *Virology* **180**: 687-696.
- Fassi-Fihri, O.; El Harrak, M. and Fassi-Fehri, M. M. (1998). Clinical, Virological and Immune Responses of Normal and Immunosuppressed Donkeys (*Equus asinus africanus*) after inoculation with African Horsesickness Virus. *Archives of Virology Supplement* **14**: 49-56.
- Fehr, T.; Skrastina, D.; *et al.* (1998). T Cell-Independent Type 1 Antibody Response Against B Cell Epitopes Expressed Repetitively on Recombinant Virus Particle. *Proceedings of the National Academy of Sciences USA* **95(16)**: 9477-9481.
- French, T. J. and Roy, P. (1990). Synthesis of Bluetongue Virus (BTV) Core-Like Particles by a Recombinant Baculovirus Expressing the Two Major Structural Core Proteins of BTV. *Journal of Virology* **64 (4)**: 1530-1536.
- French, T. J.; Marshall, J. J. A. and Roy, P. (1990). Assembly of Double-Shelled, Virus-like Particles of Bluetongue Virus by the Simultaneous Expression of Four Structural Proteins. *Journal of Virology* **64 (12)**: 5695-5700.
- Fukusho, A.; Ritter, G. D. and Roy, P. (1987). Variation in the Bluetongue Virus Neutralization Protein VP2. *Journal of General Virology* **68**: 2967-2973.
- Fukusho, A.; Yu, Y.; Yamaguchi, S. and Roy, P. (1989). Completion of the Sequence of Bluetongue Virus Serotype 10 by the Characterisation of a Structural Protein, VP6, and a Non-Structural Protein NS2. *Journal of General Virology* **70(7)**: 1677-1689.
- Geourjon, C.; Deleage, G. and Roux, B. (1991). ANTHEPROT: An Interactive Graphics Software for Analysing Protein Structures from Sequences. *Journal of Molecular Graphics* **9(3)**: 188-190, 167.
- Geourjon, C. and Deleage, G. (1995). ANTHEPROT 2.0: A Three-dimensional Module Fully Coupled with Protein Sequence Analysis Methods. *Journal of Molecular Graphics* **13(3)**: 209-212, 199-200.

Ghosh, M. K.; Deriaud, E.; Saron, M. F.; Lo-Man, R.; Henry, T.; Jiao, X.; Roy, P. and Leclerc, C. (2002). Induction of Protective Antiviral Cytotoxic T Cells by a Tubular Structure Capable of Carrying Large Foreign Sequences. *Vaccine* **20(9-10)**: 1369-1377.

Gorman, B. M. and Taylor, J. (1985). Orbiviruses. In: *Virology*: 275-278, B. N. Fields *et al.* (eds). Raven Press, New York.

Gould, A. R.; Hyatt, A. D. and Eaton, B. T. (1988). Morphogenesis of a Bluetongue Virus Variant with an Amino Acid Alteration at a Neutralization Site in the Outer Coat Protein, VP2. *Virology* **165**: 23-32.

Grabowska, A. M.; Jennings, R.; *et al.* (2000). Immunization with Phage Displaying Peptides Representing Single Epitopes of the Glycoprotein G Can Give Rise to Partial Protective Immunity to HSV-2. *Virology* **269(1)**: 47-53.

Grimes, J.; Basak, A. K.; Roy, P. and Stuart, D. (1995). The Crystal Structure of Bluetongue Virus VP7. *Nature* **373**: 161-170.

Grimes, J. M.; Jakana, J.; Ghosh, M.; Basak, A. K.; Roy, P.; Chui, W.; Stuart, D. I. and Prasad, B. V. (1997). An Atomic Model of the Outer Layer of the Bluetongue Virus Core Derived from the X-Ray Crystallography and Electron Cryomicroscopy. *Structure* **5(7)**: 885-893.

Grimes, J. M.; Burroughs, J. N.; Gouet, P.; Diprose, J. M.; Malby, R.; Zientaras, S.; Mertens, P. P. C. and Stuart, D. I. (1998). The Atomic Structure of the Bluetongue Virus Core. *Nature* **373**: 167-170.

Guan, H. H.; Budzinsky, W.; *et al.* (1998). Liposomal Formulations of Synthetic MUC1 Peptides: Effects of Encapsulation Versus Surface Display of Peptides on Immune Responses. *Bioconjugate Chemistry* **9(4)**: 451-458.

Guex, N. and Peitsch, M. C. (1997). SWISS-MODEL and the Swiss-Pdb Viewer: An Environment for Comparative Protein Modelling. *Electrophoresis* **18**: 2714-2723.

Guex, N.; Diemand, A. and Pietsch, M. C. (1999). Protein Modelling For All. *TIBS* **24**: 364-367.

Hamblin, C; Salt, J. S.; Mellor, P. S.; Graham, S.D.; Smith, P.R. and Wohlsein, P. (1998). Donkeys as Reservoirs of African Horsesickness Virus. *Archives of Virology Supplement* **14**: 37-47.

Hassan, S. S. and Roy, P. (1999). Expression and Functional Characterisation of Bluetongue Virus VP2 Protein: Role in Cell Entry. *Journal of Virology* **73(12)**: 9832-9842.

Hassan, S. H.; Wirblich, C.; Forzan, M. and Roy, P. (2001). Expression and Functional Characterization of Bluetongue Virus VP5 Protein: Role in Cellular Permeabilisation. *Journal of Virology* **75(18)**: 8356-8367.

Higgins, D. G. and Sharp, P. M. (1988). CLUSTAL- a Package for Performing Multiple Sequence Alignments on a Microcomputer. *Gene* **73**: 237-244.

Huismans, H. (1979). Protein Synthesis in Bluetongue Virus-Infected Cells. *Virology* **92**: 385-396.

Huismans, H. and Erasmus, B. J. (1981). Identification of the Serotype-Specific and Group-Specific Antigens of Bluetongue Virus. *Onderstepoort Journal of Veterinary Research* **48**: 51-58.

Huismans, H.; Van Dijk, A. A. and Bauskin, A. R. (1987a). In Vitro Phosphorylation and Purification of a Non-Structural Protein of Bluetongue Virus Protein With an Affinity for Single-Stranded RNA. *Journal of Virology* **61**: 3589-3595.

Huismans, H.; Van Dijk, A. A. and Els, H. J. (1987b). Uncoating of Parental Bluetongue Virus to Core and Subcore Particles in Infected L Cells. *Virology* **157**: 180-188.

- Iwata, H.; Yamagawa, M. and Roy, P. (1992). Evolutionary Relationships Among the Gnat-Transmitted Orbiviruses that Cause African Horsesickness, Bluetongue and Epizootic Hemorrhagic Disease So Evidenced by Their Capsid Protein Sequences. *Virology* **191**: 251-261.
- Jennings, R.; Simms, J. R. and Heath, A. W. (1998). Adjuvants and Delivery Systems for Viral Vaccines- Mechanisms and Potential. *Developments Biological Standards* **92**: 19-28.
- Kahlon, J.; Sugiyama, K. and Roy, P. (1983). Molecular Basis of Bluetongue Virus Neutralization. *Journal of Virology* **48 (3)**: 627-632.
- Kayman, S. C.; Park, H.; Saxon, M. and Pinter, A. (1999). The Hypervariable Domain of the Murine Leukemia Virus Surface Protein Tolerates Large Insertions and Deletion, Enabling Development of a Retroviral Particle Display System. *Journal of Virology* **73(3)**: 1802-1808.
- Konishi, E.; Win, K. S.; Kurane, I.; Mason, P. W.; Shope, R. E. and Ennis, F. A. (1997). Particulate Vaccine Candidate for Japanese Encephalitis Induces Long-lasting Virus-Specific Memory T Lymphocytes in Mice. *Vaccine* **15(3)**: 281-286.
- Laegried, W. W. (1994). Diagnosis of African Horsesickness. *Comparative Immunology, Microbiology and Infectious Diseases*. **17 (3/4)**: 297-303.
- Laviada, M. D.; Roy, P. Sanchez-Vizcaíno, J. M. and Casal, J. I. (1995). The Use of African Horsesickness Virus NS3 Protein, Expressed in Bacteria, as a Marker to Differentiate Infected from Vaccinated Horses. *Virus Research* **38**: 205-218.
- Le Blois, H. and Roy, P. (1993). A Single Point Mutation in the VP7 Major Core Protein of Bluetongue Virus Prevents the Formation of Core-Like Particles. *Journal of Virology* **67 (1)**: 353-359.
- Lewis, S. A. and Grubman, M. J. (1990). Bluetongue Virus: Surface Exposure of VP7. *Virus Research* **16**: 7-26.
- Limn, C.; Staueber, N.; Monastyrskaya, K.; Gouet, P. and Roy, P. (2000). Functional Dissection of the Major Structural Protein of Bluetongue Virus: Identification of Key Residues within VP7 Essential for Capsid Assembly. *Journal of Virology* **74(18)**: 8658-8669.
- Lobato, Z. I.; Coupar, B. E.; Gray, C. P.; Lunt, R. and Andrew, M. E. (1997). Antibody Responses and Protective Immunity to Recombinant Vaccinia Virus-Expressed Bluetongue Antigens. *Veterinary Immunology and Immunopathology* **59(3-4)**: 293-309.
- Lord, C. C.; Venter, G. J.; Mellor, P. S.; Paweska, J. T. and Woolhouse, M. E. (2002). Transmission Patterns of African Horsesickness and Equine Encephalosis Viruses in South African Donkeys. *Epidemiology and Infection* **128(2)**: 265-275.
- Luckow, V. A.; Lee, S. C.; Barry, G. F. and Olins, P. O. (1993). Efficient Generation of Infectious Recombinant Baculoviruses by Site-specific Transposon Mediated Insertion of Foreign Genes into a Baculovirus Genome Propagated in *Escherichia coli*. *Journal of Virology* **67**: 4566-4579.

- Mandell, M. and Higa, A. (1970). Calcium-dependent DNA infection. *Journal of Molecular Biology* **53**: 159-162.
- Maree, F.F. and Huismans, H. (1997). Characterisation of Tubular Structures Composed of Non-Structural Protein NS1 of African Horsesickness Virus Expressed in Insect Cells. *Journal of General Virology* **78(5)**: 1077-1082.
- Maree, S.; Durbach, S. and Huismans, H. (1998a). Intracellular Production of African Horsesickness Virus Core-Like Particles by Expression of the Two Major Core Proteins, VP3 and VP7, in Insect Cells. *Journal of General Virology* **79**: 333-337.
- Maree, S.; Durbach, S.; Maree, F. F.; Vreede, F. and Huismans, H. (1998b). Expression of the Major Core Structural Proteins VP3 and VP7 of African Horsesickness Virus and Production of Core-Like Particles. *Archives of Virology [Supplement]* **14**: 203-209.
- Maree, F. F. (2000). Multimeric Protein Structures of African Horse Sickness Virus and their Use as Antigen Delivery Systems. *Thesis Submitted in the Fulfilment of the Requirements for the Degree Philosophy Doctorales (University of Pretoria)*.
- Martin, L. A.; Meyer, A. J.; O'Hara, R. S.; Fu, H.; Mellor, P. S., Knowles, N. J. and Mertens, P. P. (1998). Phylogenetic Analysis of African Horsesickness Segment 10: Sequence Variation, Virulence Characteristics and Cell Exit. *Archives of Virology Supplement* **14**: 281-293.
- Martinez-Costas, J.; Sutton, G.; Ramadevi, N. and Roy, P. (1998). Guanylyltransferase and RNA 5'-triphosphatase Activities of the Purified Expressed VP4 Protein of Bluetongue Virus. *Journal of Molecular Biology* **280(2)**: 391-399.
- Martínez-Torrecuadrada, J. L. and Casal, J. I. (1995). Identification of a Linear Neutralization Domain in the Protein VP2 of African Horsesickness Virus. *Virology* **220**: 391-399.
- Martínez-Torrecuadrada, J. L.; Díaz-Laviada, M.; Roy, P.; Sanchez, C.; Vela, C. Sanchez-Vizcaíno, J. M. and Casal, J. I. (1996). Full Protection Against African Horsesickness AHS in Horses Induced by Baculovirus-Derived AHS Virus Serotype 4 VP2, VP5 and VP7. *Journal of General Virology* **77**: 1211-1221.
- Martínez-Torrecuadrada, J. L.; Langeveld, J. P. M.; Venteo, A.; Sanz, A.; Dalsgaard, K.; Hamilton, W. D. O. ; Meleon , R. H. and Casal, J. I. (1999). Antigenic Profile of African Horsesickness Virus Serotype 4 VP5 and Identification of a Neutralizing Epitope Shared with Bluetongue Virus and Epizootic Hemorrhagic Disease Virus. *Virology* **257**: 449-459.
- Martínez-Torrecuadrada, J. L.; Langeveld, J. P.; Meloen, R. H. and Casal, J. I. (2001). Definition of Neutralizing Sites on African Horsesickness Virus Serotype 4 VP2 at the Level of Peptides. *Journal of General Virology* **82(10)**: 2415-2424.
- McIntosh, B. M. (1958). Immunological types of Horsesickness Virus and their Significance in Immunisation. *Onderstepoort Journal of Veterinary Research* **27**: 465-538.
- Mellor, P. S. (1993). African Horsesickness: Transmission and Epidemiology. *Veterinary Research* **24**: 199-212.

- Mellor, P. S. (1994). Epizootiology and Vectors of African Horsesickness Virus. *Comparative Immunology, Microbiology and Infectious Diseases* **17** (3/4): 287-296.
- Meiring, T. L. (2001). An Investigation into Non-Structural Proteins NS3 and NS3A of African Horsesickness. *Thesis Submitted in the Fulfilment of the Requirements for the Degree MSc (University of Pretoria)*.
- Mertens, P. P. C.; Brown, F. and Sanger, D. V. (1984). Assignment of the Genome Segments of Bluetongue Virus Type 1 to the Proteins Which they encode. *Virology* **135**: 207.
- Mertens, P. P. C.; Burroughs, J. N.; Walton, A.; Welby M. P.; Fu, H.; O'Hara, R. S.; Brookes, S. M. and Mellor, P. (1996). Enhanced Infectivity of Modified Bluetongue Virus Particles for Two Insect Cell Lines and for Two *Culicoides* Vector Species. *Virology* **217**: 582-593.
- Mikhailov, M.; Monastyrskaya, K.; Bakker, T. and Roy, P. (1996). A New Form of Particulate Single and Multiple Immunogen Delivery System Based on Recombinant Bluetongue Virus-Derived Tubules. *Virology* **217**(1): 323-331.
- Milich, D. R.; Peterson, D. L.; Zheng, J.; Hughes, J. L.; Wirtz, R. and Schodel, F. (1995). The Hepatitis Nucleocapsid as a Vaccine Carrier Moiety. *Annals of the New York Academy of Sciences* **754**: 187-201.
- Milich, D. R.; Schodel, F.; Hughes, J. L.; Jones, J. E. and Peterson, D. L. (1997). The Hepatitis B Core and e Antigens Elicit Different Th Cell Subsets: Antigen Structure Can Affect Th Cell Phenotype. *Journal of Virology* **71**(3): 2192-2201.
- Milich, D. R.; Hughes, J.; Jones, J.; Sallberg, M. and Phillips, T. R. (2001). Conversion of Poorly Immunogenic Malaria Repeat Sequences into a Highly Immunogenic Candidate Vaccine. *Vaccine* **20**(5-6): 771-788.
- Monastyrskaya, K.; Staeuber, N.; Sutton, G. and Roy, P. (1997). Effects of Domain-Switching and Site-Directed Mutagenesis on the Properties and Functions of the VP7 Proteins of Two Orbiviruses. *Virology* **237**: 217-227.
- Murphy, F. A.; Borden, E. C.; Shope, R. E. and Harrison, A. (1971). Physicochemical and Morphological Relationships of some of the Arthropod-Borne Viruses to Bluetongue Virus- A New Taxonomic Group. *Electron Microscopic Studies. Journal of General Virology* **13**(2): 273-288.
- Murphy, F. A.; Fauquet, T. M.; Bishop, D. H. L.; Ghabrial, S. A.; Forvis, A. W., Mortelli, G. P.; Mayo, M. A. and Summers, M. D. (1995). Virus Taxonomy: The Classification and Nomenclature of Viruses. *The Sixth Report of the International Committee on Taxonomy of Viruses*. Springer-Verlag, Wien.
- Nuttall, P. A.; Jacobs, S. C.; Jones, L. D.; Carey, D. and Moss, S. R. (1992). Enhanced Neurovirulence of Tick-borne *Orbivirus* Resulting from Genetic Modulation. *Virology* **187**: 407-412.

- O'Hagan, D. T.; MacKiachan, M. L. (2001). Recent Developments in Adjuvants for Vaccines Against Infectious Diseases. *Biomolecular Engineering* **18(3)**: 69-85.
- O'Hara, R. S.; Meyer, A. J.; Burroughs, J. N.; Pullen, L.; Martin, L. A. and Mertens, P. P. (1998). Development of a Mouse Model System, Coding Assignments and Identification of the Genome Segments Controlling Virulence of African Horsesickness Virus Serotypes 3 and 8. *Archives of Virology* **14**: 259-279.
- Oldfield, S.; Adachi, A.; Urakawa, T.; Hirasawa, T. and Roy, P. (1990). Purification and Characterisation of the Major Group-Specific Core Antigen VP7 of Bluetongue Virus Synthesised by a Recombinant Baculovirus. *Journal of General Virology* **71**: 2649-2656.
- Paweska, J. T.; Binus, M. M.; Woods, P. S. A. and Chimside, E. D. (1997). A Survey for Antibodies to Equine Arteritis Virus in Donkeys, Mules and Zebra Using Virus Neutralisation (VN) and Enzyme Linked Immunosorbent Assay. *Equine Veterinary Journal* **29(1)**: 40-43.
- Peitsch, M. C. (1995). Protein Modelling by E-mail. *Bio/Technology* **13**: 658-660.
- Prasad, B. V. V.; Yamaguchi, S. and Roy, P. (1992). Three-dimensional Structure of Single-Shelled Bluetongue Virus. *Journal of Virology* **66**: 2135-2142.
- Pratelli, A.; Elia, G.; Martella, V.; Palmieri, A.; Cirone, F.; Tinelli, A.; Corrente, M. and Buonavoglia, C. (2002). Prevalence of Canine Coronavirus Antibodies by an Enzyme-Linked Immunosorbent Assay in Dogs in the South of Italy. *Journal of Virological Methods* **102(1-2)**: 67-71.
- Ramadevi, N.; Burroughs, N. J.; Mertens, P. P.; Jones, I. M. and Roy, P. (1998). Capping and Methylation of mRNA by Purified Recombinant VP4 Protein of Bluetongue Virus. *Proceedings of the National Academy of Sciences USA* **95(23)**: 13537-13542.
- Romito, M.; Du Plessis, D. H. and Viljoen, G. J. (1999). Immune Responses in a Horse Inoculated with the VP2 Gene of African Horsesickness Virus. *Onderstepoort Journal of Veterinary Research* **66**: 139-144.
- Roy, P.; Fukusho, A.; Ritter, D. G. and Lyons, D. (1988). Evidence for Genetic Relationship Between RNA and DNA Viruses from the Sequence Homology of a Putative Polymerase Gene of Bluetongue Virus With That of Vaccinia Virus: Conservation of RNA Polymerase Genes From Diverse Species. *Nucleic Acid Research* **16**: 11759-11767.
- Roy, P. (1989). Bluetongue Virus Genetics and Genome Structure. *Virus Research* **13**:179-206.
- Roy, P. Adachi, A.; Urakawa, T.; Booth, T. F. and Thomas, C. P. (1990). Identification of Bluetongue Virus VP6 Protein as a Nucleic Acid-Binding Protein and the Localisation of VP6 in Virus-Infected Vertebrate Cells. *Journal of Virology* **64**: 1-8.
- Roy, P.; Hirasawa, T.; Fernandez, M.; Blinov, V. N. and Sanchez-Vixcaino Rodrique, J. M. (1991). The Complete Sequence of the Group-Specific Antigen, VP7, of African Horsesickness disease Virus Serotype 4 Reveals a Close Relationship to Bluetongue Virus. *Journal of General Virology* **72**: 1237-1241.

- Roy, P. (1992). From Genes to Complex Structures of Bluetongue Virus and their Efficacy as Vaccines. *Veterinary Microbiology* **33(1-4)**: 223-234.
- Roy, P.; Mertens, P. C. and Casal, I. (1994). African Horse sickness Virus Structure. *Comparative Immunology, Microbiology and Infectious Diseases* **17 (3/4)**: 243-273.
- Roy, P. (1996). Genetically Engineered Particulate Virus-Like Structures and Their Use as Vaccine Delivery Systems. *Intervirology* **39**: 62-71.
- Roy, P.; Bishop, D. H. L.; Howard, S.; Aitchison, H. and Erasmus, B. (1996) Recombinant-Baculovirus-Synthesised African Horsesickness Virus (AHSV) Outer-Capsid Protein VP2 Provides Protection Against Virulent AHSV Challenge. *Journal of General Virology* **77**: 2053-2057.
- Roy, P. and Sutton, G. (1998). New Generation of African Horsesickness Virus Vaccines Based on Structural and Molecular Studies of the Virus Particles. *Archives of Virology [Supplement]* **14**: 177-202.
- Sambrook, J.; Fritsch, F. F. and Maniatis, T. (1989). Molecular Cloning: Laboratory Manual. Second Edition. *Cold Spring Harbor Laboratory Press, Cold Spring Harbor, USA*.
- Scanlen, M.; Paweska, J. T.; Verschoor, J. A. and Van Dijk, A. A. (2002). The Protective Efficacy of a Recombinant VP2-based African Horsesickness Subunit Vaccine Candidate is Determined by Adjuvant. *Vaccine* **20(7-8)**: 1079-1088.
- Schodel, F.; Wirtz, R.; Peterson, D.; Hughes, J.; Warren, R.; Sadiff, J. and Milich, D. (1994). Immunity to Malaria Elicited by Hybrid Hepatitis B Virus Core Particles Carrying Circumsporozite Protein Epitopes. *Journal of Experimental Medicine* **180(3)**: 1037-1046.
- Schodel, F.; Peterson, D. and Milich, D. (1996). Hepatitis B Virus Core and e Antigen: Immune Recognition and Use as a Vaccine Carrier Moiety. *Intervirology* **39(1-2)**: 104-110.
- Sjolander, A.; Lovgren Bengtsson, K.; Johansson, M. and Morein, B. (1996). Kinetics, Localisation and Isotype Profile of Antibody Responses to Immune Stimulating Complexes (iscoms) Containing Human Influenza Virus Envelope Glycoproteins. *Scandinavian Journal of Immunology* **43(2)**: 164-172.
- StClair, N.; Shenoy, B.; Jacob, L. D. and Margolin, A. L. (1999). Cross-Linked Protein Crystals for Vaccine Delivery. *Proceedings of the National Academy of Sciences of the United States of America* **96**: 9469-9474.
- Stone-Marschat, M. A.; Moss, S. R.; Burrage, T. G.; Barber, M. L.; Roy, P. and Laegried, W. W. (1996). Immunization with VP2 is Sufficient for Protection Against Lethal Challenge with African Horsesickness Virus Type 4. *Virology* **220**: 219-222.
- Suhrbier, A. (1997). Multi-Epitope DNA Vaccines. *Immunology and Cell Biology* **75**: 402-408.
- Summers, M. D. and Smith, G. E. (1987). A Manual of Methods for Baculovirus Vectors and Insect Cell Culture Procedures. *Texas Agricultural Experiment Station bulletin 1555, Texas Agricultural Experiment Station, College Station, Texas*.

Tan, B. H.; Nason, E.; Staueber, N; Jiang, W.; Monastyrskaya, K. and Roy, P. (2001). RGD Tripeptide of Bluetongue Virus VP7 Protein is Responsible for Core Attachment to Culicoides Cells. *Journal of Virology* **75(8)**: 3937-3947.

Tanaka, S.; Mikhailov, M. and Roy, P. (1995). Synthesis of Bluetongue Virus Chimeric VP3 Molecules and Their Interactions with VP7 Protein to Assemble into Virus Core-Like Particles. *Virology* **214**: 593-601.

Taraporewala, Z.F.; Chen, D. and Patton, J.T. (2001). Multimers of the Bluetongue Virus Non-Structural Proteins, NS2, Possess Nucleotidyl Phosphatase Activity: Similarities between NS2 and Rotavirus NSP2. *Virology* **280(2)**: 221-231.

Taylor, M. B.; Van Der Meyden, C. H.; Erasmus, B. J.; Reid, R.; Labuschagne, J. H.; Dreyer, L. and Prozesky, O. W. (1992). Encephalitis and Chorioretinitis Associated with Neurotropic African Horse Sickness Virus Infection in Laboratory Workers. IV. Experimental Infection of the Vervet Monkey *Cercopithecus pygerythrus*. *South African Medical Journal* **81**: 462-467.

Thomas, C. P.; Booth, T. F. and Roy, P. (1990). Synthesis of Bluetongue Viral-Coded Phosphoprotein and Formation of Inclusion Bodies by Recombinant Baculovirus in Insect Cells: It Binds the Single-Stranded RNA Species. *Journal of General Virology* **71**: 2073-2083.

Turnbull, P. J.; Cormack, S. B. and Huismans, H. (1996). Characterisation of the Gene Encoding Core Protein VP6 of two African Horsesickness Virus Serotypes. *Journal of General Virology* **77(7)**: 1421-1423.

Uitenweerde, J. M.; Theron, J.; Stoltz, M.A. and Huismans, H. (1995). The Multimeric Nonstructural NS2 Proteins of Bluetongue Virus, African Horsesickness Virus, and Epizootic Hemorrhagic Disease Virus Differ in their Single-Stranded RNA-Binding Ability. *Virology* **209(2)**: 624-632.

Urakawa, T. and Roy, P. (1988) Bluetongue Virus Tubules Made in Insect Cells by Recombinant Baculovirus: Expression of NS1 Gene of Bluetongue Virus Serotype 10. *Journal of Virology* **62**: 3919-3927.

Van Der Meyden, C. H.; Erasmus, B. J.; Swanepoel, R. and Prozesky, O. W. (1992). Encephalitis and Chorioretinitis Associated with Neurotropic African Horse Sickness Virus Infection in Laboratory Workers. I. Clinical and Neurological Observations. *South African Medical Journal* **81**: 451-454.

Van Niekerk, M.; Smit, C. C.; Fick, W. C.; Van Staden, V. and Huismans, H. (2001a). Membrane Association of African Horsesickness Virus Nonstructural Protein NS3 Determines its Cytotoxicity. *Virology* **279(2)**: 499-508.

Van Niekerk, M.; Van Staden, V., Van Dijk, A. A. and Huismans, H. (2001b). Variation of African Horsesickness Virus Non-Structural Protein NS3 in Southern Africa. *Journal of General Virology* **82(1)**: 149-158.

- Van Staden, V. and Huismans, H. (1991). A Comparison of Genes which Encode Non-Structural Protein NS3 of Different Orbiviruses. *Journal of General Virology* **72(5)**: 1073-1079.
- Van Staden, V.; Scholtz, M.A. and Huismans, H. (1995). Expression of Non-Structural Protein NS3 of African Horsesickness Virus (AHSV): Evidence for a Cytotoxic Effect of NS3 in Insect Cells, and Characterisation of the Gene Products in AHSV Infected Vero Cells. *Archives of Virology* **140(2)**: 289-306.
- Van Staden, V.; Smit, C.C.; Stoltz, M. A.; Maree, F.F. and Huismans, H. (1998). Characterisation of two African Horsesickness Virus proteins, NS1 and NS3. *Archives of Virology Supplement* **14**: 251-258.
- Venter, M.; Napier, G. and Huismans, H. (2000). Cloning, Sequencing and Expression of the Gene that Encodes the Major Neutralization-Specific Antigen of African Horsesickness Virus Serotype 9. *Journal of Virological Methods* **86**: 41-53.
- Verwoerd, D. W.; Louw, H. and Oellermann, R. A. (1970). Characterization of Bluetongue Virus Nucleic Acid. *Journal of Virology* **5**: 1-7.
- Verwoerd, D. W.; Els, H. J; De Villiers, E. M. and Huismans, H. (1972). Structure of the Bluetongue Virus Capsid. *Journal of Virology* **10**: 783-794.
- Verwoerd, D. W.; Huismans, H. and Erasmus, B. J. (1979). Orbiviruses. In: *Comprehensive Virology* 14:285-345. H. Fraenkel-Conrat and R. R. Wagner (eds). Plenum Press, New York.
- Vreede, F. T. and Huismans, H. (1994). Cloning, Characterisation and Expression of the Gene that Encodes the Major Neutralisation-Specific Antigen of African Horsesickness Virus Serotype 3. *Journal of General Virology* **75**: 3629-3633.
- Vreede, F.T. and Huismans, H. (1998). Sequence Analysis of the RNA Polymerase Gene of African Horsesickness Virus. *Archives of Virology* **143(2)**: 413-419.
- Wade-Evans, A. M.; Romero, C. H.; Mellor, P.; Takamatsu, H.; Anderson, J.; Thevasagayam, J.; Fleming, M. J.; Mertens, P. P. and Black, D. N. (1996). Expression of the Major Core Structural Protein (VP7) of Bluetongue Virus, by a Recombinant Capripox Virus, Provides Partial Protection of Sheep Against a Virulent Heterotypic Bluetongue Virus Challenge. *Virology* **220(1)**: 227-231.
- Wade-Evans, A. M.; Pullen, L.; Hamblin, C.; O'Hara, R.; Burroughs, J. N. and Mertens, P. P. C. (1997). African Horsesickness Virus VP7 Sub-Unit Vaccine Protects Mice Against a Lethal, Heterologous Serotype Challenge. *Journal of General Virology* **78**: 1611-1616.
- Wade-Evans, A. M.; Pullen, L.; Hamblin, C.; O'Hara, R.; Burroughs, J. N. and Mertens, P. P. C. (1998). VP7 from African Horsesickness virus Serotype 9 Protects Mice Against a Lethal, Heterologous Serotype Challenge. *Archives of Virology* **14**:211-219.
- Wang, L. F.; Hyatt, A. D.; Whiteley, P. C.; Andrew, M.; Li, J. K. K. and Eaton, B. T. (1996). Topography and Immunogenicity of Bluetongue Virus Epitopes. *Archives of Virology* **141**: 111-123.

- Westerlund-Wikstrom, B. (2000). Peptide Display on Bacterial Flagella: Principles and Applications. *International Journal of Medical Microbiology* **290(3)**: 223-230.
- Wilson, A. D. and Morgan, A. J. (1998). Indirect Measurement of Epstein-Barr Virus Neutralising Antibodies by ELISA. *Journal of Virological Methods* **73(1)**: 11-19.
- Wittmann, E. J. and Baylis, M. (2000). Climate Change: Effects on *Culicoides*-Transmitted Viruses and Implication for the U. K. *The Veterinary Journal* **160**: 107-117.
- Xu, G.; Wilson, W.; Mecham, J.; Murphy, K.; Zhou, E. M. and Tabachnick, W. (1997). VP7: An Attachment Protein of Bluetongue Virus for Cellular Receptors in *Culicoides variipennis*. *Journal of General Virology* **78(7)**: 1617-1623.
- Yip, Y. L.; Smith, G.; *et al.* (2001). Comparison of Phage pIII, pVIII and GST as Carrier Proteins for Peptide Immunisation in Balb/c Mice. *Immunology Letters* **79(3)**: 197-202.
- Yon, J.; Rud, E.; *et al.* (1992). Stimulation of Specific Immune Responses to Simian Immunodeficiency Virus using Chimeric Hepatitis B Core Antigen Particles. *Journal of General Virology* **73(10)**: 2569-2575.
- Zheng, Y. Z.; Hyatt, A.; Wang, L. F.; Eaton, B. T.; Greenfield, P. F. and Reid, S. (1999). Quantification of Recombinant Core-Like Particles of Bluetongue Virus Using Immunosorbent Electron Microscopy. *Journal of Virological Methods* **80(1)**: 1-9.